WEBER RIVER BASIN CLIMATE VULNERABILITY ASSESSMENT

January 2021

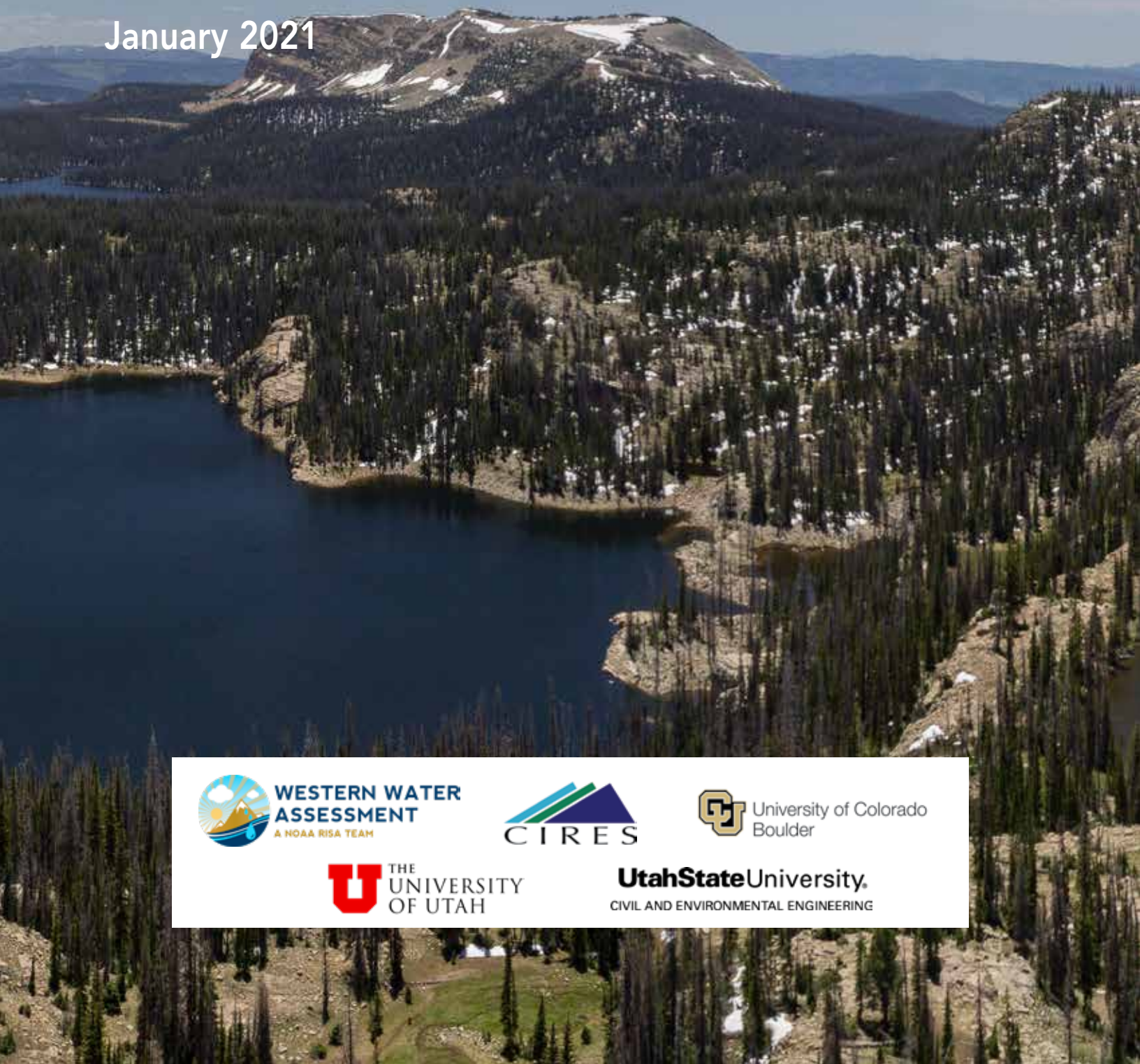

WESTERN WATER ASSESSMENT
A NOAA RISA TEAM

CIRES

University of Colorado Boulder

THE UNIVERSITY OF UTAH

UtahStateUniversity
CIVIL AND ENVIRONMENTAL ENGINEERING

WEBER RIVER BASIN
CLIMATE VULNERABILITY ASSESSMENT

January 2021

Submitted by

Seth Arens
Western Water Assessment, University of Colorado-Boulder
Global Change and Sustainability Center, University of Utah

Logan Jamison and Paul Brooks
Department of Geology and Geophysics, University of Utah

Alex Weech and Court Strong
Department of Atmospheric Science, University of Utah

Jacob Everitt and David E. Rosenberg
Utah Water Research Lab and Dept. of Civil and Environmental Engineering, Utah State University

Design and Layout

Ami Nacu-Schmidt, CIRES Center for Science and Technology Policy Research

Cover Photo

Hight Uinta's from Notch Peak. Credit: Ricky/Adobe Stock

EXECUTIVE SUMMARY

Photo: Sunset at the Great Salt Lake, Utah. Credit: Johnny/Adobe Stock.

This report, generated through a unique collaboration between climate scientists, hydrologists, modelers, and the Weber Basin Water Conservancy District (WBWCD), provides a detailed review of historical climate and hydrology, downscaled projections of future precipitation, temperature and hydrology, and a vulnerability analysis of the WBWCD water system to inform water supply planning in the Weber River basin. State of the art modeling techniques are used to provide site-specific climate projections for the entire Weber River basin and a suite of modeling approaches are used to translate climate projections into streamflow projections for the Weber River.

Use of multiple climate modeling techniques is an approach that uses a range of information to describe future climate scenarios and impacts to water supply. The primary goal of delivering multiple projections of future climate is to provide WBWCD the information necessary to evaluate and plan for multiple future climate scenarios based on the range of future climate projections. *There is no probability to each scenario and each scenario is considered equally likely.* Multiple, plausible scenarios of climate, streamflow, demand, reservoir sedimentation and reservoir evaporation are used in a vulnerability analysis of WBWCD's water system to determine how changing climate will stress the system.

HISTORICAL CLIMATE AND HYDROLOGY

Climate is changing in the Weber River basin. Historical temperatures have increased since the 1980s, but clear changes to precipitation, snowfall and streamflow in the Weber River basin were not observed. Globally, air temperature has increased by 1.8°F since 1850. Utah temperatures warmed by 2° to 3.5°F since 1850, with most of the warming occurring after 1970. Warming, since 1850, is attributed largely to increases in greenhouse gases in the atmosphere that trap heat near Earth's surface. Climate and hydrology are examined critically in five sub-basins of the Weber River basin: the headwaters of the Weber River, Lost Creek, South Fork of the Ogden River, Chalk Creek and East Canyon Creek. Analyses by sub-basin are designed to quantify current spatial variability in climate and streamflow, to identify mechanisms underlying this variability, and to inform spatially-explicit, future projections of streamflow. The analysis of historical climate and hydrology indicates:

- Every sub-basin in the watershed experienced a significant increase in temperature, with the rate of warming accelerating rapidly beginning in 1985.
- Temperatures in each sub-basin, post-1985, are on average 1.6° F warmer than pre-1985 temperatures.
- The highest sub-basin, which produced the most water (Weber above Oakley), exhibits much greater interannual variability in temperature than other sub-basins.
- There was no significant change in annual or seasonal precipitation over time in the Weber River basin.
- There was no significant change in streamflow in any sub-basin of the Weber River basin from 1920-2018.
- Water yield (runoff efficiency) varies across subcatchments ranging from 13% in Lost Creek to 48% in Weber River above Oakley.

- Water yield (runoff efficiency) increases and variability decreases as precipitation increases.
- Snowmelt is beginning earlier, but proceeding more slowly; if this trend continues, water yield is likely to decline in the future.

FUTURE CLIMATE

Scientists study future climate by using global climate models (GCMs), which are computer simulations of the state of the Earth's atmosphere, oceans, land surface, sea ice and land ice. Economic and policy scenarios are used to generate future atmospheric greenhouse gas concentrations which are incorporated into GCM's to simulate future climate. Future climate and hydrology projections will be presented for moderate and high emissions scenarios for mid-century (2050's) and end-of-century (2085). Several climate modeling techniques were used to provide future climate projections for the entire Weber River basin at a spatial resolution of 2.5 miles and at monthly or annual time scales. Projections of temperature, precipitation and potential evapotranspiration using statistically downscaled climate data are provided as the median result from climate models. Projections of temperature, precipitation, snow, extreme precipitation and evaporation are obtained using dynamically downscaled climate data from a single climate model that was selected for its accuracy in recreating northern Utah climate.

While probabilities cannot be applied to specific climate projections in this report, the degree of certainty in a specific climate projection is expressed qualitatively in terms of confidence level: *low confidence*, *medium confidence* and *high confidence*. Confidence level is determined by the underlying scientific understanding resulting from the type, amount, quality, consistency and agreement of evidence. In general there is higher confidence in projections that directly or indirectly involve temperature and lower confidence in projections relating to precipitation. The expression of scientific certainty in terms of confidence is modeled after the method used in the Intergovernmental Panel on Climate Change assessment reports. The following information is a summary of future climate projections for the Weber River basin. Table i summarizes future projections for temperature, precipitation, snow, water use and evaporation.

Temperature

- Moderate greenhouse gas emissions increase maximum temperatures by approximately 4°F by 2050 and 7°F by 2085. *High confidence*.
- High greenhouse gas emissions increase maximum temperatures by 6°F by 2050 and 12°F by 2085. *High confidence*.
- Interannual variability in warming is relatively small; there are many hot years in a row and fewer historically normal years. *Medium confidence*.
- The greatest warming will take place in the springtime as the snowpack melts sooner and bare ground is exposed which absorbs more solar radiation. *High confidence*.
- The strongest warming in the short-term will take place in valley locations such as Morgan and Ogden Valleys; valleys will warm more than the Uinta Mountains. *Medium confidence*.

Precipitation

- Most climate models project a slight increase in precipitation for the Weber River basin. *High confidence*.
- By mid-century, the greatest precipitation increases occur in January and February in the Wasatch and Uinta Mountains. *Medium confidence*.
- Precipitation is projected to decrease in May and June throughout the 21st century. *Medium confidence*.
- Mountain precipitation may increase in November and December throughout the century, but warmer temperatures mean early winter precipitation may fall as rain. *High confidence*.
- A large increase in September precipitation is due to an interaction of monsoon moisture and fall Pacific storms. *Low confidence*.

Snow

- By mid-century, annual snowfall is projected to decrease by 30% along the Wasatch Front and 10-15% in the lower elevations (below 7500 feet) of the Wasatch Back. *Medium confidence*.
- Elevations above 7500 feet in the Wasatch and Uinta Mountains are projected to see a 10% increase in snowfall by the end of the century. *Medium confidence*.
- High elevation (above 7500 feet) locations that historically receive the most snow will have a dramatic shift toward an earlier timing in peak snowpack. *High confidence*.

Extreme precipitation

- Extreme precipitation is an event where rain falls very intensely over a short period of time; these events often cause flash flooding.
- On the Wasatch Front, little change in extreme precipitation is projected for the next several decades. *Medium confidence*.
- By the end of the century, extreme once-per-decade storms will be 10% stronger than in the past. *Medium confidence*.

Table i. Summary of climate change projections. Temperature (T) is expressed as an average temperature increase compared to historical temperatures. Annual precipitation change (P) is expressed as a percent change compared to the historical period. Snow-level is expressed as an elevation in feet that mean snow level changes. Snow is expressed as a percent change in snow-water equivalent compared to the historical period. Potential evaporation (PET) is expressed as a percent change compared to the historical period. Water use is expressed as a percent increase in water use compared to average water use from 2010-2018. RCP4.5, RCP6.0, RCP8.5 are emissions scenarios; RCP4.5 and 6.0 use moderate levels of future emissions, RCP5.8 uses high levels of future emissions. Evaporation is expressed as an annual average increase in the amount of water evaporated from Willard Bay in acre-feet. Climate projections are derived from three datasets, LOCA statistically downscaled, MACA statistically downscaled and University of Utah dynamically downscaled.

PARAMETER	METHOD	LOCATION	RCP4.5		RCP6.0		RCP8.5	
			2050	2085	2040	2090	2050	2085
T	LOCA	Basin-wide	+4°	+7°	-	-	+6°	+12°
T	Dynamic	Ben Lomond	-	-	+2.7°	+5.3°	-	-
T	Dynamic	Thaynes Cyn	-	-	+2.3°	+4.6°	-	-
T	Dynamic	Trial Lake	-	-	+2.4°	+4.8°	-	-
P	LOCA	Basin-wide	0%	+5%	-	-	0%	+5%
P	Dynamic	Basin-wide	-	-	+5%	+10%	-	-
P	Dynamic	Ben Lomond	-	-	+4%	+7%	-	-
P	Dynamic	Thaynes Cyn	-	-	+8%	+13%	-	-
P	Dynamic	Trial Lake	-	-	+9%	+17%	-	-
Snow-level	LOCA	Basin-wide	+1200′	+1200′	-	-	+1800′	+3600′
Snow	Dynamic	Ben Lomond	-	-	-2%	-7%	-	-
Snow	Dynamic	Thaynes Cyn	-	-	+1%	-0.4%	-	-
Snow	Dynamic	Trial Lake	-	-	+2.3%	+3%	-	-
PET	MACA	Ogden	+5%	+9%	-	-	+8%	+16%
Water use	MACA	Ogden	+6%	-	-	-	+10%	-
Evaporation	Dynamic	Willard Bay	-	-	+1565	+3368	-	-

Evaporation

- Evaporation of water from Willard Bay increases in all months for mid-century and December through August in the late century projections. *High confidence*.
- The greatest increases in evaporation occur during the warm months; April – September for mid-century and March – July for end-of-century projections. *High confidence*.
- The mid-century increase in evaporation amounts to a loss of 1500 acre feet per year, and the late-century increase amounts to a loss of 3300 acre-feet per year. *Medium confidence*.

Potential evapotranspiration

- Potential evapotranspiration (PET) is a measure of the atmosphere's "thirst" from water through evaporation of water from soils and transpiration of water from plants.

- In 2050, PET is projected to increase by 5% given a moderate emissions scenario (RCP4.5) and by 8% under a high emissions scenario. *High confidence* that PET will increase. *Medium confidence* regarding level of increase.

FUTURE OUTDOOR WATER USE

Changes in climate are likely to impact the amount of water used to irrigate outdoor landscapes. As temperatures rise and other climate parameters change, potential evaporation (PET) is projected to increase. In general, when it is hotter, PET is higher and plants use more water. A linear regression model is constructed to relate water used in four Ogden neighbors to PET and then used as a tool to project future water use.

- Using water use data from the Ogden area and observations of PET, a model was created to relate PET to water use; PET explained 60% of the variability in water use.
- A low and high PET scenario was used to project water use.
- By 2050, water use in four Ogden-area neighborhoods is projected to increase by 6% for a low PET scenario and by 10% for a high PET scenario.
- The greatest increases in water use are expected to occur in April through June which is validated by predictions of significantly warmer and drier future spring by mid-century. Water use is projected to decrease slightly in August and September.

FUTURE WEBER RIVER STREAMFLOW

Three techniques were used to provide projections of Weber River streamflow for mid- and end-of-century. The three techniques are: a statistical streamflow model informed by historical hydroclimate, a Variable Infiltration Capacity (VIC) model, and a temperature and precipitation sensitivity analysis. Projections of streamflow were developed for the headwaters of the most productive sub-basin of the Weber River basin (the Weber River above Oakley). The three techniques will provide slightly different projections in some cases and similar projections in others. When two different techniques to project streamflow converge on a single projection, there is greater certainty in that projection. As with future climate, certainty in a specific streamflow projection will be expressed by confidence level. Due to disagreement amongst modeling techniques, specific projections of total streamflow were generally assigned low confidence, while streamflow projections related to temperature, like timing of peak flow, were assigned higher confidence. Projections from the three streamflow models should be used as the basis to develop scenarios describing the range of future water availability and not as a tool to determine a most likely future availability of water. Table ii compares the results of all streamflow projection techniques.

Statistical streamflow model

- The importance of a multi-year climate impact on groundwater differentiates the statistical streamflow model from the other two approaches.
- Three climate scenarios (low, medium, and high precipitation) are used.
- Under the medium precipitation scenario with moderate emissions, annual streamflow increases by 5% (*medium confidence*); peak streamflow is 20% higher (*medium confidence*), occurs 10-days earlier and returns to base flow conditions sooner (*medium confidence*). Note that moderate the emissions scenario assumes a 2°F increase in temperature and we are currently at 1.6°F warmer for these catchments.
- Under the medium precipitation scenario with high emissions, there is a 16% decrease in annual streamflow (*medium confidence*), a 32% decrease in peak streamflow (*low confidence*) and melt-induced flow occurs 2 to 3-week earlier (*high confidence*).
- The high precipitation scenario highlights the possibility of severe early-season flooding, with continuous melt-induced flow starting as early as February. *Low confidence*.
- The low precipitation scenario suggests the possibility of severe drought, with annual streamflow 30%

lower than the lowest year on record, or 25% of annual average streamflow. The site-specific statistical model of streamflow indicates a multi-year sensitivity to climate mediated through groundwater recharge which can either buffer or exacerbate the effects of a dry year. *High confidence*.

- Mean daily discharge in January is a function of multi-year climate; deviations from long-term mean January discharge are strong predictors of runoff efficiency for the coming year. *High confidence*.

VIC model

- Four climate scenarios were selected based on a climate model's temperature or precipitation projection relative to the mean of all climate models: warm/dry, hot/dry, warm/wet and hot/wet.
- For a moderate emissions scenario, annual streamflow decreases by 7% in 2055 for a hot/dry scenario, but increases for all other scenarios with the greatest increase (11.2%) for a warm/wet scenario. *Low confidence*.
- In the high emissions scenario, annual streamflow is projected to increase for all scenarios by 2055 with an increase of nearly 13% for a warm/wet scenario. *Low confidence*.
- Streamflow in winter and early spring is likely to increase while late summer and fall streamflow (baseflow) decreases. *High confidence*.

Table ii. Summary of annual streamflow volume projections. Streamflow projections were developed using three techniques: a statistical streamflow model (statistical), a variable infiltration capacity model (VIC) and a temperature and precipitation sensitivity analysis (sensitivity). For each method several different scenarios were used that considers different levels of temperature increase and future changes to precipitation (see section 4 of the report for scenario descriptions). Low P, medium P and high P abbreviates, low, medium and high precipitation. Future projections of streamflow are expressed as a percentage change compared to the historical period. Streamflow projections are provided for two time periods (2050 and 2085) and a moderate (RCP4.5) or high (RCP8.5) emissions scenario.

STREAMFLOW SCENARIO	METHOD	RCP4.5		RCP8.5	
		2050	2085	2050	2085
Low P	Statistical	0%	-	-30%	-
Medium P	Statistical	+5%	-	-16%	-
High P	Statistical	+5%	-	-13%	-
WarmdDry	VIC	+2%	+6%	+1%	+2%
Hot/dry	VIC	-7%	-4%	+0.1%	+8%
Warm/wet	VIC	+11%	+15%	+13%	+26%
Hot/wet	VIC	+8%	+18%	+23%	+14%
Warm/dry	Sensitivity	-16%	-12%	-	-
Hot/dry	Sensitivity	-20%	-37%	-	-
Warm/wet	Sensitivity	+29%	+25%	-	-
Hot/wet	Sensitivity	+12%	-1%	-	-

- In one scenario (hot/wet scenario for 2055), peak streamflow occurred nearly two months earlier and the peak's magnitude is greatly reduced. *Low confidence*.

Temperature and precipitation sensitivity analysis

- Four climate scenarios were used: warm/dry, hot/dry, warm/wet and hot/wet.
- Streamflow projections using this technique were lower than VIC model projections; most scenarios project a decrease streamflow and greater scenario variability.
- Projections for 2055 show the greatest decrease in streamflow for the hot/dry scenario (-20.2%) and the greatest increase in streamflow for the hot/wet scenario (+29%). *Low confidence*.
- In 2055, peak monthly streamflow is projected to occur one month earlier. *Medium confidence*.

BOTTOM-UP SYSTEM VULNERABILITY ANALYSIS

Utah State University conducted a climate vulnerability study for the Weber Basin, Utah. The study used a bottom-up approach (Brown et al., 2019; Brown and Wilby, 2012) wherein we showed how changes to combinations of future uncertain streamflow, demand, reservoir sedimentation, and reservoir evaporation conditions would affect total basin reservoir storage and deliveries to users. Six scenarios of future streamflow—each 30-years in length at a monthly timestep—varied total basin annual flow from approximately 800,000 to 975,000 acre-feet per year. The scenarios were drawn from three periods in the paleo record, two periods in the most recent century of

gaged records, and a Western Water Assessment scenario for 2030 to 2060 streamflow under hot and dry climate. Six scenarios of future annual demands ranged from 362,000 to 846,000 acre-feet per year and represented select combinations of a wider set of 63 scenarios of uncertain future population growth, total per capita water use, agricultural to urban water transfers, and increased landscape evapotranspiration. Data for future reservoir sedimentation was scarce so we constructed three scenarios of 0%, 10%, and 30% filling of total storage that represent the current assumption of no buildup, gradual filling over time, and more severe filling. Three scenarios of future evaporation from Willard Bay reservoir had rates of 3.2, 3.7, and 4.0 feet per year. These rates represented the current value used by the Utah Division of Water Resources (UDWRe) and historical and late 21st century values estimated by the University of Utah in the earlier part of this report. *Each streamflow, demand, reservoir sedimentation, and reservoir evaporation scenario is possible in the future. These scenarios cannot be assigned probabilities or likelihoods. These scenarios represent current engineering best practice to describe, quantify, and manage in the face of future conditions that are deeply uncertain*. Together, 324 runs comprising combinations of six streamflow, six demand, three reservoir sedimentation, and three reservoir evaporation rate scenarios were simulated using the prior-existing UDWRe RiverWare model for the Weber basin and the RiverSmart plugin to automate the large number of model runs. The main results and findings are:

System Strengths

- The current modeled historical conditions with about 960,000 acre-feet per year of inflow, 550,000 acre-feet of demand, no sedimentation, and 3.2 feet per year of evaporation from Willard Bay is able to consistently maintain total reservoir storage above the 380,000 acre-feet moderate (yellow) target defined in the drought contingency plan.
- Demands would need to increase by about 160,000 acre-feet per year and/or inflow decrease by about 80,000 acre-feet per year from the modeled historical conditions for total reservoir storage to drop below the 380,000 acre-feet target in 10 to 20% of modeled years.
- For the 10% reservoir sedimentation rate, the yellow, orange, and red reservoir storage targets of 380,000, 320,000, and 280,000 acre-feet are met the same fraction of years for the same inflows and demands as with 0% sedimentation.
- During the modeled historical conditions, delivery requests are met nearly all the time with few shortages. Deliveries are met and shortages are small across all three reservoir sedimentation rates.
- The Weber Basin system storage is insensitive to Willard Bay evaporation rates between 3.2 and 4.0 feet per year. *Despite uncertainty about the future reservoir evaporation rate, this climate factor did not affect system storage in the stream flow, demand, or reservoir sedimentation scenarios tested*.

System Vulnerabilities

- When reservoir sedimentation rates increase to 30%, the yellow, orange, and red reservoir storage targets are violated much more frequently. A unit volume reduction in inflow leads to more violations in storage targets than the same unit volume increase in demand.
- In the hot-dry future climate scenario that has average inflows of 800,000 acre-feet per year, total reservoir storage will fall below the 380,000 acre-feet moderate target in 50% or more of simulated years regardless of the annual demand.
- Several droughts within the tested scenarios last four years and longer. During these droughts, total reservoir storage stays below the red 280,000 acre-feet threshold for multiple years. However, during these droughts, the reservoir sedimentation rate does not affect storage level.
- The historical system is very close to seeing a total basin shortage of 40,000 acre-feet per year or more in at least 1 of 30 years. If demand increases by 100,000 acre-feet per year, the worst shortage would increase to about 160,000 acre-feet per year and some shortage would occur in 50% of years.
- As expected, shortages increase substantially as inflows decrease and demands increase.

INTRODUCTION

Weber Basin Water Conservancy District (WBWCD) is a regional water supplier that provides water to cities, districts and companies in five northern Utah counties, serving approximately 675,000 residents. In 1942, the US Bureau of Reclamation (BOR) began to plan for the construction of the Weber Basin Project (WBP), a series of reservoirs, aqueducts and canals in the Weber River basin to provide water for residents of the northern Wasatch Front. On June 26, 1950, by decree of the Second District Court of Utah, WBWCD was created to operate and manage the WBP. By 1969, through the efforts of BOR and WBWCD, seven reservoirs and a series of aqueducts and canals were built to provide water to residents of David, Weber, Morgan, Summit and parts of Box Elder Counties. In 1988, construction of an eighth reservoir, Smith and Morehouse, was completed by WBWCD and in 2017, a project to increase the capacity of Willard Bay Reservoir was completed (WBWCD 2018). In total, the seven upstream reservoirs and one downstream reservoir (Willard Bay) store 583,443 acre-feet (af) of water at full capacity (NRCS National Water and Climate Center 2019). WBP developed approximately 207,000 af of water rights in the Weber River basin. The WBWCD acquired an additional 62,000 af of water rights for a total of approximately 258,000 af of water annually considering all sources (WBWCD 2017). In 2018, WBWCD distributed 227,000 af of water with 52,000 af treated for municipal use, 136,000 af for irrigation and 22,000 af for groundwater replacement deliveries (WBWCD 2018a).

The complex geography of the Weber River basin includes eight smaller basins, or sub-basins, two mountain ranges and four valleys. The basin is divided into two major sub-basins (Figure 1). The headwaters of the Ogden River in the Wasatch Mountains reach an elevation of over 9,000 feet. The headwaters of the Weber River in the Uinta Mountains reach an elevation of over 11,000 feet in the Uinta Mountains and drain a total area of 2,500 square miles encompassing the western Uinta Mountains, northern Wasatch Mountains and eastern shore of the Great Salt Lake. The Ogden River joins the Weber River in the Great Salt Lake Valley before the Weber River meanders its way to Ogden Bay of the Great Salt Lake. Several mountain valleys punctuate the Weber River basin: Ogden Valley, Morgan Valley and Snyderville Basin.

The climate of the Weber River basin varies due to elevation and location relative to mountain ranges. In populated regions of the basin, average annual temperatures range from 52°F in Ogden to 43°F in Park City. Historically, temperatures range between 108°F in Ogden to -40°F in Coalville. At 9000 feet in the Uinta Mountains, annual average temperature is 37°F and temperatures range from -15°F to 80°F (NRCS National Water and Climate Center 2019b) Averaged basin-wide, the Weber River basin is the wettest in Utah, receiving approximately 26 inches annually, twice the statewide average. The Wasatch and the Uinta Mountains are subject to slightly different climates and weather patterns that bring precipitation. In general, the Uinta Mountains are slightly drier and cooler compared to the Wasatch Mountains. Annual precipitation in the northern Wasatch Mountains near Ben Lomond Peak reaches nearly 70 inches, while precipitation in the headwater of the Weber River range from 35-40 inches (Utah Division of Water Resources 2009). Annual precipitation tends to be more variable in the Wasatch Mountains compared to the Uinta Mountains (NRCS National Water and Climate Center 2019b). After the Bear River, the Weber River basin has the highest average water yield in Utah with 1.2 million acre-feet and produces the most water relative to the basin's area. In contrast with precipitation, which varies by a factor of 2-3 annually, annual streamflow can vary by a factor of more than ten.

Photo: Pineview Reservoir from Sardine Peak Trailhead, Utah. Credit: Ladanifer/Adobe Stock.

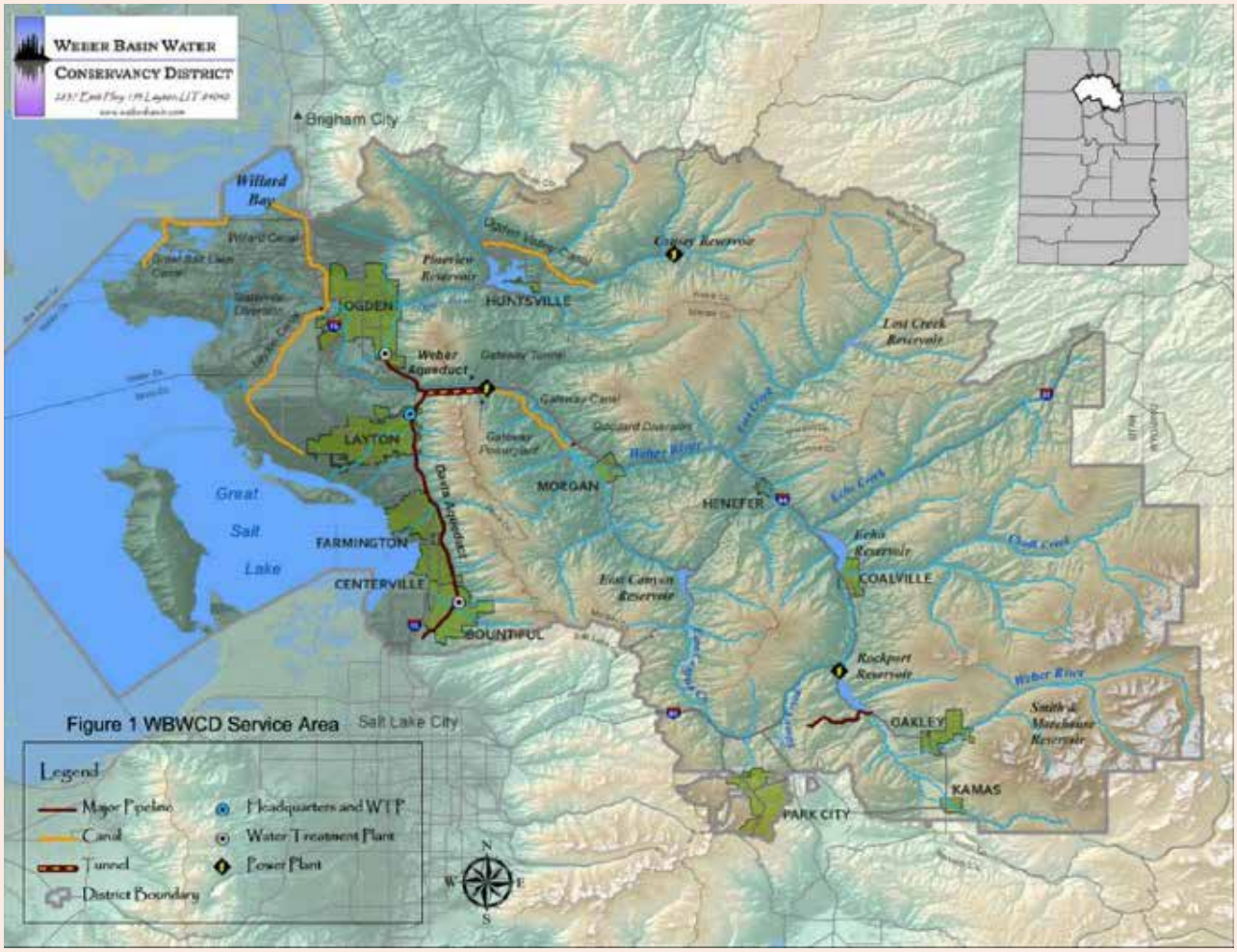

Figure 1. The Weber River basin including reservoirs, canals, pipelines, tunnels and district service area boundaries (WBWCD 2018).

Drought is a major concern of WBWCD. Despite ample upstream and downstream reservoir storage and its mission to provide municipal and industrial water to 675,000 Utah residents, WBWCD owns relatively junior water rights in the basin, making its supply vulnerable to shortages in periods of drought. Since 1971, total water storage in the Weber River basin varied from near-full capacity in 28 of 47 years, to a low of approximately 130,000 af in 1992 (22% full capacity). Total storage dipped below 200,000 af in seven years since 1971. Most droughts were short in duration, but the multi-year droughts in 2001-2004 and 2013-2016 triggered a mandatory 20% reduction in secondary water delivery for irrigation (WBWCD 2018). Three consecutive years of drought and record low snow conditions in spring of 2015 coming on the heels of two prior years of drought spurred WBWCD to more quantitatively consider drought in long-term planning.

In 2019, WBWCD completed work on a collaborative effort to develop a drought contingency plan for their water system. WBWCD's Drought Contingency Plan was with first plan of its kind by a Utah water provider. Various drought information sources were used to test the impact of drought on water supply in the Weber River basin: historical records, paleo-tree ring records (dating back to 1400) and projections of future drought (WBWCD 2018). Most droughts in the historical record were short and none lasted longer than 4-5 years; the most recent droughts in the early 2000s each lasted three years. Examination of a record of drought dating back to 1400 and projections of 21st century drought showed past droughts were more severe and longer than those experienced since WBWCD began providing water in the 1950s. Climate change is expected to increase the

probability of severe multi-year drought (Ault et al. 2014). Climate change was only a small part of the analysis of drought in the Drought Contingency Plan, but the plan was a starting point for WBWCD's consideration of climate change in its long-term planning.

Long-term water resource planning requires balancing the expected future demand for water with the future supply. Over the past several years WBWCD has worked to understand its future supply and demand through the development of both the "Supply and Demand Study" and the "Drought Contingency Plan." Assessing future water demand involves estimating both future population and future per capita use of water. A detailed understanding of past climate and water supply has historically informed water managers about future water supply. However, to fully understand future water supply in the context of climate change, WBWCD decided to pursue a more detailed study of future climate change and its impacts on Weber River basin water supply.

To address questions about future climate and its impact on the Weber River basin water supply, WBWCD partnered with Western Water Assessment, the University of Utah and Utah State University to develop a climate vulnerability assessment. The Weber Basin Climate Vulnerability Assessment provides a historical context to climate and water supply, basin-specific projections of climate and hydrology and a vulnerability analysis of WBWCD's water system. To do this, the Weber Basin Climate Vulnerability Assessment will include:

1. Regional trends in climate, overview of principles and causes of climate change and its impacts on water resources (Section 1).
2. Observed changes in climate and hydrology in five subcatchments of the Weber River basin (Section 2a-d).
3. Downscaled projections of future climate (Section 3a-c).
4. Projections of future Weber River flow using three methods (Section 4a-c).
5. Specific impacts of climate change: outdoor water use, extreme precipitation, snow and evaporation (Section 5a-d).
6. Vulnerability analysis of WBWCD water system considering climate, drought, demography, and other factors.

1. OVERVIEW OF CLIMATE CHANGE

Key Points

- The Earth's atmosphere and oceans are warming. Measurements of air temperature show a 1.8°F increase globally since 1850 and a 2 to 3.5°F increase in Utah since 1970.
- Observations of warming and other changes to climate are attributed mainly to an increase in concentrations of greenhouse gases in the atmosphere, particularly carbon dioxide.
- Atmospheric carbon dioxide increased by 46% since 1850.
- Climate change will likely cause changes to water quantity, water quality, the timing of water availability and demand for water.

Observations of air temperature at local, regional, continental and global scales all show a warming of Earth's climate. As of 2017, global air temperatures increased by 1.8°F since 1850 (Masson-Delmotte et al. 2018). As global temperatures increase, Earth warms unevenly; air temperatures over oceans warm more slowly than over land. Interior, continental locations warm faster than locations near coasts and the greatest warming has occurred in northern latitudes of North America and Asia. The contiguous United States has also warmed by 1.8°F since 1850, but most of that warming has occurred since 1970. Alaska has warmed at twice the rate of the contiguous United States with approximately 3.5°F of warming since 1970. The Intermountain West has also experienced warming at rates greater than the United States as a whole. Air temperatures in much of Utah have warmed by 2 to 3°F while eastern Utah has warmed by more than 3°F from 1901-2016 (USGCRP 2018).

It is important to make the distinction between *weather* and *climate*. Weather is the condition of the atmosphere (temperature, wind, precipitation, etc.) that occurs at a specific time in a specific location. For example, at 9 am on October 15th, 2019 in Ogden, the air temperature is 44°F and a south wind is blowing at 6 miles per hour. *Climate* is the average weather that occurs at a specific location over a long period of time. Climate is typically considered as an average over 30 years and can be expressed at many time scales such as daily, monthly or annually. For example, over the last 30 years, the average daily high and low temperatures on October 15th in Ogden are 65°F and 43°F, respectively. *Climate change* can be defined as a persistent and lasting change in the average or range of climate conditions (Lukas et al. 2014).

The long-term trend of increasing global temperatures is an example of climate change. However, warming is only one aspect of climate change. *Global warming* is often used as an interchangeable term with climate change, however global warming and climate change are not synonymous. *Global warming* describes the observation that Earth's air temperature is warming. Climate change refers to not only changes in temperature, but to any change climate parameters such as precipitation, evaporation, wind speed, typical weather patterns, intensity of storms, prevalence of drought, snowfall and many others. Many key impacts of climate change begin with increases in air temperature. Warmer temperatures are associated with increased evaporation rates, which increases the total amount of water vapor in the atmosphere and can cause more frequent and severe

Photo: Satellite photo of the Great Salt Lake from August 2018 after years of drought, reaching near-record lows. The difference in colors between the northern and southern portions of the lake is the result of a railroad causeway. Credit: Copernicus Sentinel-2, ESA/Creative Commons.

precipitation events (USGCRP 2017). The increase in air temperature and evaporation can cause weather patterns to shift; this shift in weather patterns means changes in precipitation are not expressed uniformly around the world; precipitation has increased in some regions and decreased in others. For example, much of the northern United States and Canada is expected to see an increase in precipitation with climate change while the southeastern and southwestern United States and northern Mexico are expected to experience a decrease in precipitation (USGCRP 2018).

Before discussing the causes of climate change, a brief explanation of an important physical process in our atmosphere is necessary. The *greenhouse effect* is the process by which gases in the atmosphere absorb radiation (heat) emitted from the Earth's surface. The energy absorbed by "greenhouse" gases is then re-radiated back to Earth which warms the planet. Greenhouse gases in the atmosphere (water vapor, carbon dioxide, methane and nitrous oxide) act as a blanket trapping heat in the lower portions of the atmosphere.

Without the presence of greenhouse gases, particularly water vapor and carbon dioxide, air temperatures on Earth would be 60°F colder, likely leaving the planet uninhabitable (USGCRP 2018). For the at least the last 800,000 years, the concentration of carbon dioxide in the atmosphere fluctuated between 180 parts per million (ppm) and 280 ppm (Luthi et al. 2008). These fluctuations in atmospheric carbon dioxide closely follow global temperatures over tens of thousands of years in transitions between glacial cycles ("ice ages"). Atmospheric carbon dioxide of 180 ppm coincided with periods of glaciation where much of the northern hemisphere was covered in massive ice sheets. Interglacial periods were characterized by higher atmospheric carbon dioxide concentrations, warmer temperatures, ice-free landscapes and higher sea levels. Variations in Earth's tilt and orbit (the Milankovitch cycles) are a key triggering mechanism in the transition into and out of ice ages (NOAA National Centers for Environmental Information 2019).

Climate change is occurring because of a large and rapid increase of greenhouse gases in the atmosphere, especially carbon dioxide. In 1850, atmospheric carbon dioxide concentration was 280 ppm, the typical maximum concentration in the cycle of glacial and interglacial cycles of the last 800,000 years. By September 2019, atmospheric carbon dioxide concentration rose to 408.5 ppm, a 46% increase since 1850 (NOAA Earth Systems Research 2019). The increase in carbon dioxide in the atmosphere increases the strength of the greenhouse effect. Using the analogy of a blanket trapping heat near the Earth's surface, higher concentrations of carbon dioxide in the atmosphere create a thicker blanket and trap more heat, leading to further increases in temperature. Climate variations can occur through a variety of processes, but the cumulative changes to Earth's climate since 1850 is almost entirely attributed to the rapid increase in atmospheric greenhouse gases, particularly carbon dioxide (IPCC 2018; USGCRP 2017). Many factors affect how much energy from the sun enters and exits Earth's atmosphere (variation in incoming solar radiation, volcanic eruptions, atmospheric greenhouse gas concentration and natural climate variability) and cycles in climate at different timescales influence both regional and global climate. Considering all factors that affect climate, except the concentration of greenhouse gases in the atmosphere, the Earth's climate would have experienced a slight cooling trend over the last 50 years (USGCRP 2018).

On the scale of a watershed, climate change will likely impact hydrology and the availability of water in several ways. First, climate change is expected to change long-term patterns and amounts of annual precipitation for a watershed. On the continental scale, annual precipitation in the United States has increased by about 4% since the beginning of the 20th century. In the Southwest, precipitation has generally decreased, but most locations in northern Utah, including the Weber River basin, have not experienced any significant trend in precipitation (USGCRP 2017). Climate change will likely increase the incidence of extreme precipitation events where rainfall falls in greater amounts over short periods of time and can cause flooding. Increases in the incidence of extreme precipitation events will likely be paired with increased periods of drought. Climate change is also expected to cause longer periods of drought between rainfall events (Prein et al. 2016). It is also likely that droughts of greater severity and longer duration will occur in the future. In the Southwest, there is a

much greater future risk of a multi-year, decadal and multi-decadal droughts than in the past (Ault et al. 2014). Increased drought, higher temperatures and lengthening of the wildfire season all increase the risk of wildfire in the western United States (Westerling 2016). Wildfire, especially large catastrophic wildfire, causes reductions to water quality, increased sedimentation and potentially changes in the quantity and timing of water supply (Smith et al. 2011; Reneau et al. 2007; Westerling 2016; Maxwell et al. 2019).

Regardless of the amount of precipitation falling, warming temperatures are associated with an increase in the amount of winter precipitation falling as rain, especially at low and mid-elevation locations. Although snowfall may increase at high elevations in the western United States, seasonal accumulation of snow at low and mid-elevations is expected to decline (Rhoades, Ullrich, and Zarzycki 2018). Reductions in low elevation winter snowpack at lower elevations and warmer spring temperatures are associated with an earlier onset of snowmelt and a shift of peak runoff of rivers and streams to earlier in the spring (Ault et al. 2015; Bardsley et al. 2013; US National Climate Assessment 2014). Finally, higher temperatures will drive increases in evaporation and plant transpiration which will increase water demand by plants in agricultural, urban and natural ecosystems.

2. HISTORICAL HYDROLOGY AND CLIMATE OF THE WEBER RIVER BASIN

A. INTRODUCTION

Predicting how streamflow will respond to a changing climate across the complex terrain of WBWCD's service area requires detailed knowledge of how climate has varied in the past, how this variability has resulted in spatial and temporal heterogeneity in streamflow, and a modeling framework capable of representing both historical and future hydrological response. Previous analyses of streamflow in the Weber River basin using tree ring data suggests that streamflow has been much more variable in the past than during the modern era (Bekker et al. 2014). Predicting streamflow under future climate scenarios is extremely difficult as hydrological models developed and calibrated under current temperature and precipitation may not capture streamflow responses under future climate (Milly et al. 2008). A comprehensive and spatially-explicit analysis of historical data is useful both for the identification of new variables, beyond temperature and precipitation, that may add predictability to streamflow and the quantifying of spatial variability in the response to climate. Here, we develop high-resolution spatial data sets of past climate, sub-basin hydrological response, and statistical models of streamflow. Our new analyses of historical climate and statistical streamflow prediction under future climate complement the physical approach of a Variable Infiltration Capacity (VIC) model projections of streamflow (Wood and Bardsley 2015) and projections of streamflow determined through a temperature and precipitation sensitivity analysis (Bardsley et al. 2013).

A common assumption in streamflow prediction under future climate scenarios is that changes in precipitation and temperature will have similar effects on streamflow across a region. However, the fraction of precipitation exiting a basin as streamflow (water yield) can vary tremendously within sub-basin (a smaller watershed within the larger Weber River basin) due to variation in geography and geology. Recent work in the Wasatch demonstrated that water yield can vary by a factor of three or more in neighboring basins that experience similar climate (Gelderloos 2018). These unique hydrologic responses functions result from interactions between weather and climate on multiple scales and the topography, geology, and vegetation characteristics of individual sub-basins. For example, water yield in Big Cottonwood Canyon is lower than in neighboring Little Cottonwood Canyon due to differences in the underlying geology that influence groundwater storage (Gelderloos 2018). These observations are consistent with related research throughout the world and highlight the need for both empirical analyses and models that capture these variable hydrologic responses at the sub-basin scale (J.W. Kirchner 2006; P. D. Brooks et al. 2015; Fan et al. 2019).

The analysis presented in this section quantifies how temperature, precipitation, streamflow volume, and water yield, vary within the eight sub-basins within the Weber River Basin and how they have changed over time. These analyses allow us to quantify how these factors interact and provides the basis for developing statistical models of streamflow in Section 4. The time frame for analysis is the period of streamflow record for each location with a stream gage. Of the eight sub-basins originally identified, the flow regime in three is heavily modified by management decisions (East Canyon Creek near Morgan, Ogden River below Pineview and Weber River at Gateway) which preclude a direct evaluation of how climate variability influences streamflow. In these three sub-basins the individual effects of river diversions, reservoir storage, and reservoir releases mask climatic controls on streamflow generation. Results focus on the five basins that are not as strongly affected by management decisions: the Weber River above Oakley (WO), Lost Creek (LC), South Fork of the Ogden River (OSF), Chalk Creek (CC) and East Canyon Creek above Jeremy Ranch (ECJ).

Photo: Devil's Slide, a geological formation located near the border of Wyoming in northern Utah's Weber Canyon. Credit: Jenny Thompson/Adobe Stock.

B. STUDY DOMAIN

Key Points

- Analyses focus on areas minimally affected by management decisions to clearly identify climate-landscape interactions that control annual surface water supply.
- Sub-basins delineated based on contributing land area above USGS stream gauges.
- Five watersheds within the Weber River basin chosen for sub-basin scale analyses: the Weber River above Oakley (WO), Lost Creek (LC), South Fork of the Ogden River (OSF), Chalk Creek (CC) and East Canyon Creek above Jeremy Ranch (ECJ).
- Daily streamflow data from USGS stream gauges dates back to 1905 in WO, 1922 in LC and OSF, 1928 in CC, and 2001 in ECJ.
- Monthly climate data compiled via PRISM (a model that provides gridded historical climate data) for water years 1896-2018 at 4km grid cell resolution.

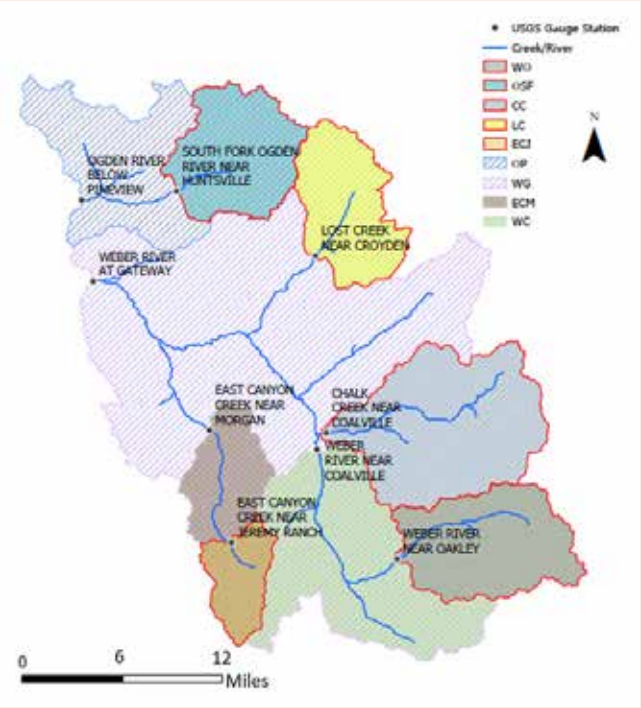

Figure 2. Weber and Ogden River basins. Five individual headwater catchments used in hydroclimate analyses and streamflow modeling are outlined in red. Minimal direct management allows for direct evaluation of hydrologic response to climate.

This analysis focuses on the hydroclimate response of five headwater sub-basins with relatively minimal direct management (Figure 2). These five locations are associated with existing stream gauges and span the range in geography, geology, and vegetation of the Weber basin.

C. VARIABILITY IN CLIMATE FROM THE INSTRUMENTAL RECORD

Key Points

- Every sub-basin in the watershed experienced a significant increase in temperature, with the rate of warming accelerating rapidly beginning in 1985. *Very high confidence*.
- Temperatures post-1985 are on average 1.6°F warmer than pre-1985 temperatures. *Very high confidence*.
- Variability of mean annual temperature is similar in all sub-basins except Weber above Oakley where variability was roughly twice as large as other catchments. *Very high confidence*.
- There has been no significant change in annual or seasonal precipitation over time.
- Variability of annual precipitation is similar in all sub-basins. *Very high confidence*.

Historical climate data were calculated using the Parameter-elevation Regression on Independent Slopes Model (PRISM) ("http://www.prism.oregonstate.edu," 2017) from 1981 – 2010. PRISM uses climate-elevation regressions to interpolate historical climate station precipitation and temperature date across the land surface using climate-elevation regressions and historic climate station data (Daly et al. 2008). In interpolation, mathematical equations (regressions) are used to estimate the temperature and precipitation values at locations between

observation points. Interpolation is an important technique for estimating these values at locations where historical observations do not exist. PRISM datasets include monthly precipitation, temperature, dew point temperature, and potential evapotranspiration (PET) at 2.5 mile horizontal resolution. Evaluation of PRISM-derived climate was performed by comparing PRISM-derived values to local instrumental records from SNOTEL locations. Although SNOTEL data are incorporated into PRISM calculations, this screening was used to check for artifacts arising from interpolation algorithms in steep, complex terrain were not biasing data. The data value of each 2.5 mile grid box is weighted by the fractional area of the box that is contained within the given watershed. The summation of all watershed grid values weighted by the fractional area results in the total value for the entire watershed. This allowed us to compile temperature and precipitation data for the entire basin at 2.5 mile resolution.

Mean annual temperature and precipitation in the Weber River basin vary from 36°F in high elevations of the Uinta Mountains to 52°F along the eastern shore of the Great Salt Lake (Figure 3). High elevations of Wasatch Mountains receive nearly 70 inches of precipitation annually and precipitation in the Uinta Mountains ranges from 37-52 inches. Valley locations within the Weber basin receive less than 20 inches of annual precipitation. Figure 4 provides mean annual temperature and precipitation and measures of variability for each sub-basin.

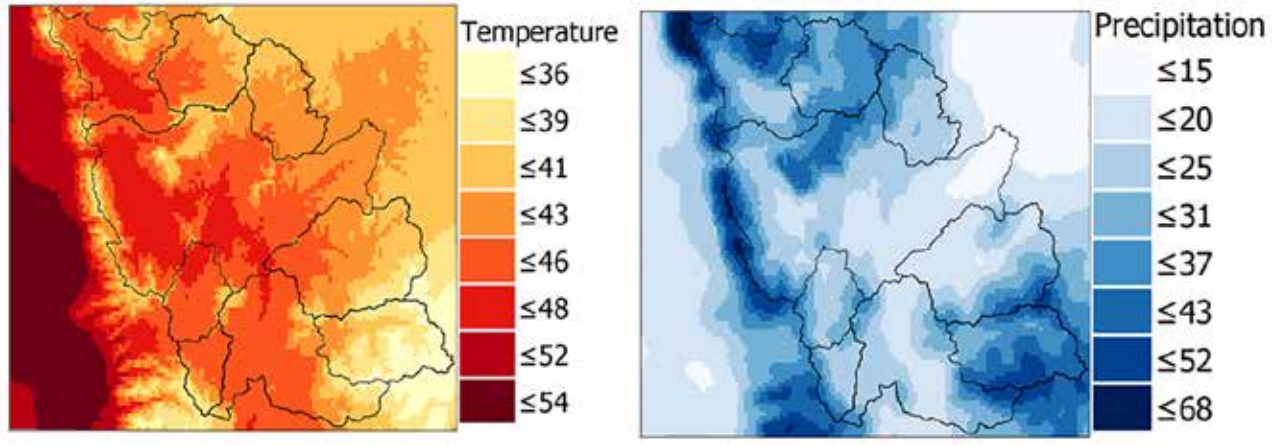

Figure 3. Mean annual temperature (degrees F) and precipitation (inches) for the study area derived from the 1981 – 2010 climate normal.

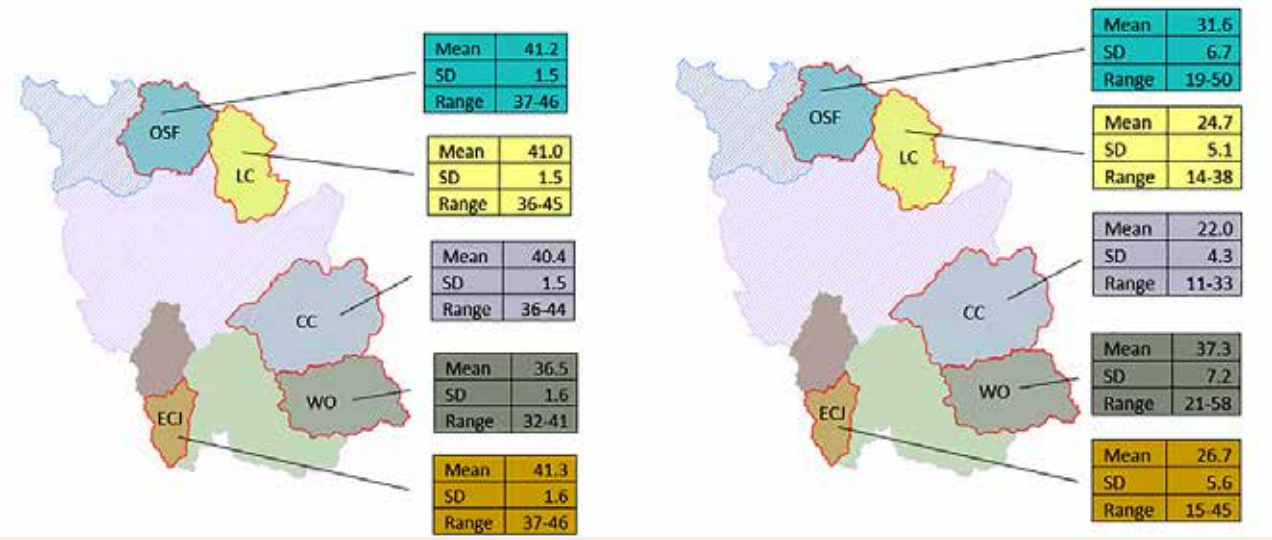

Figure 4. Mean annual temperature (left, degrees Fahrenheit) and precipitation (right, inches) for the five intensively studied headwater catchments: South Fork of the Ogden River (OSF), Lost Creek (LC), Chalk Creek (CC), Weber River above Oakley (WO) and East Canyon Creek above Jeremy Ranch (ECJ). The standard deviation (SD) and range are also reported.

Temperatures in all sub-basins have warmed by roughly 1.6°F in the past four decades, similar to a recent analysis for the watersheds east of Salt Lake City (Gelderloos 2018). In contrast to reports for other areas of the western United States, higher elevations of the Weber River basin do not appear to be warming more rapidly than lower elevations; in fact, higher elevation areas are warming more slowly than valley locations (Knowles et al. 2006). This result is somewhat surprising because most of Utah warmed by 2-3°F since 1900, which includes valley locations of the Weber River basin; in other parts of the western United States, high elevation location have warmed more than nearby low elevation locations. Interannual variability in temperature was similar in ECJ, CC, LC, and OSF catchments with coefficient of variation (CV) ranging from 0.17-0.18 (the CV measures dispersion in data and is the standard deviation divided by the mean). In contrast, temperature in the Weber River above Oakley, which is much colder that the other four subcatchments, was much more variable, with a CV of 0.35 (Figure 4).

In contrast to recent warming throughout the basin, long-term precipitation records (Figure 6) show no significant changes over time. Interannual variability in precipitation is higher than for temperature (Figure 5), and all catchments respond similarly to both relatively wet and relatively dry years. This pattern is similar to that observed by Gelderloos (2018) for the seven creeks east of Salt Lake City, but differs from a slow increase in precipitation observed at other locations in throughout the Western US (McCabe and Dettinger 1999; McCabe and Wolock 2002).

Similar to annual precipitation, April 1st snow water equivalent is highly variable with the greatest variability observed at the Ben Lomond Peak snotel site where April 1st SWE varies from 10 to 70 inches (Figure 7). The lower elevation Chalk Creek site and Ben Lomond Trail have several years in the historical record when the entire snowpack is melted by April 1st. The high interannual variability in April 1st SWE makes it difficult to detect statistically significant trends, but there does appear to be a slight, but non-significant downward trend in SWE. Data from the Ben Lomond Peak, Horse Ridge and both Chalk Creek sites is from 1979 – 2019, the Ben Lomond Trail site data is from 1981 – 2019 and the Thaynes Canyon site has data from 1989 – 2019 (NRCS National Water and Climate Center 2019b).

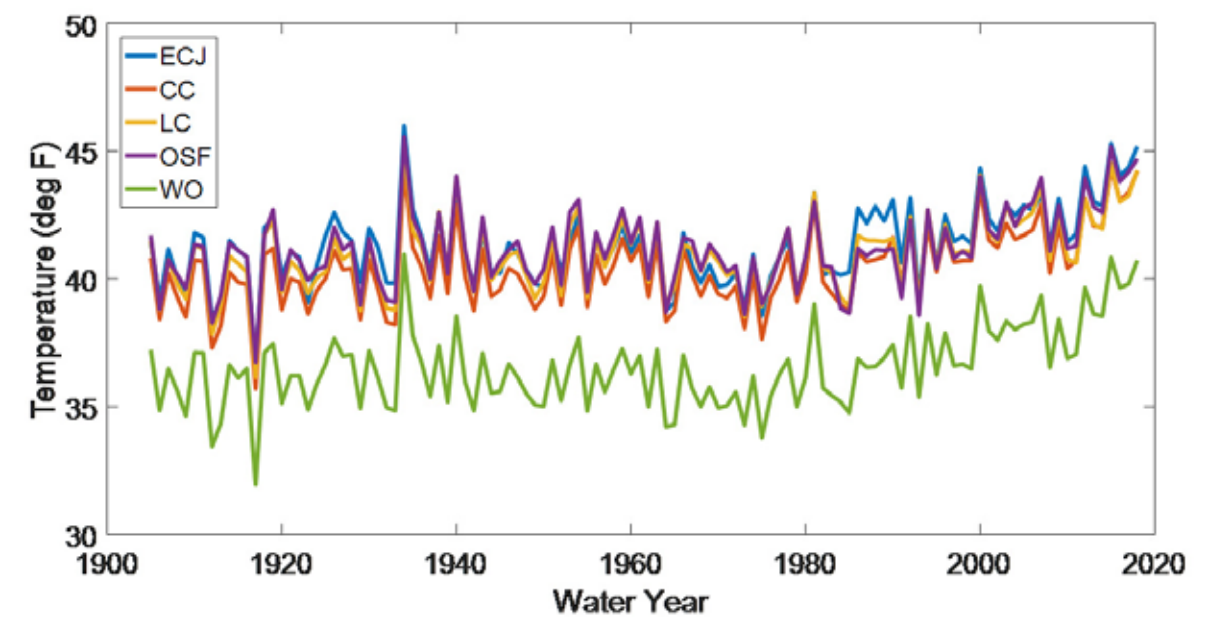

Figure 5. Annual temperature in East Canyon Creek above Jeremy Ranch (ECJ), Chalk Creek (CC), Lost Creek (LC), the South Fork of the Ogden River (OSF), and the Weber River above Oakley (WO). All five intensively studied headwater catchments show a marked rise in temperature beginning in the late 1970's.

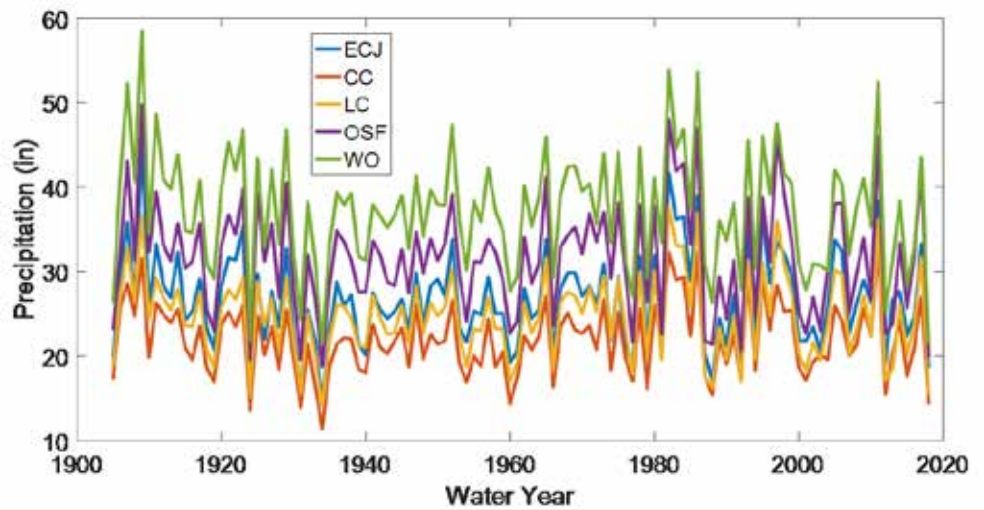

Figure 6. Annual precipitation in East Canyon Creek above Jeremy Ranch (ECJ), Chalk Creek (CC), Lost Creek (LC), the South Fork of the Ogden River (OSF), and the Weber River above Oakley (WO). The coefficient of variation (CV) values for individual sub-basins ranges from 0.19-0.21.

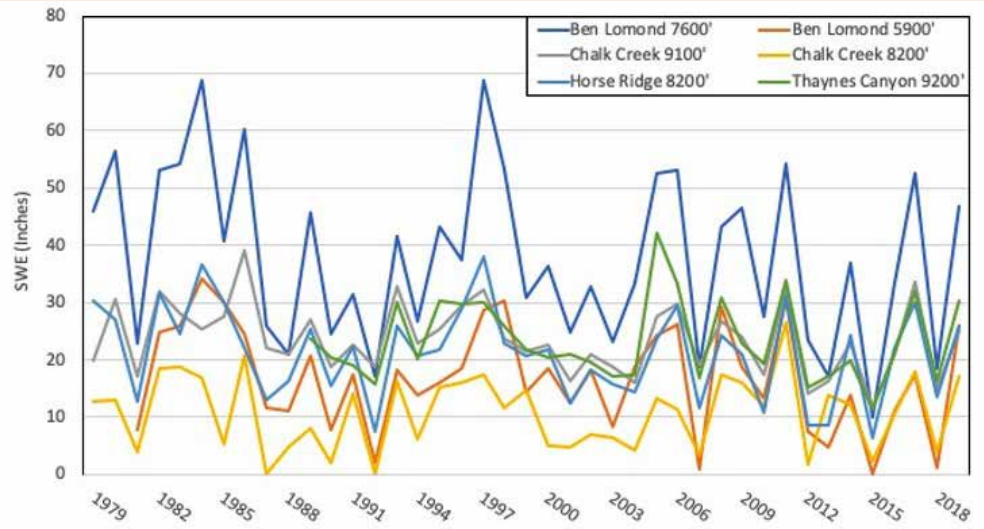

Figure 7. April 1st snow water equivalent (SWE) at six snotel sites in the Weber River basin.

D. VARIABILITY IN HISTORICAL STREAMFLOW RESPONSE TO CLIMATE

Key Points

- There was no significant change in streamflow in any sub-basin of the Weber River Basin from 1920-2018.
- Streamflow exhibits much greater variability than temperature or precipitation. *Very high confidence*.
- Similar to streamflow, water yield (runoff efficiency) varies across subcatchments ranging from 13% in Lost Creek to 48% in Weber River above Oakley. *Very high confidence*.
- Water yield is more variable than temperature or precipitation, but less variable than streamflow.

Daily streamflow values from each USGS stream gauge were aggregated to annual streamflow values. These values represent the total annual streamflow volume of each sub-basin. The Weber River above Oakley and the South Fork of the Ogden River are the most water-productive sub-basins, while Chalk Creek, Lost Creek, and East Canyon Creek generally have lower annual streamflow (Figure 8). Chalk Creek, Lost Creek, and East Canyon exhibit much greater interannual variability (coefficient of variation 0.51- 0.56) than Weber River above Oakley and South Fork of the Ogden River (Figure 9, coefficient of variation 0.31 and 0.41).

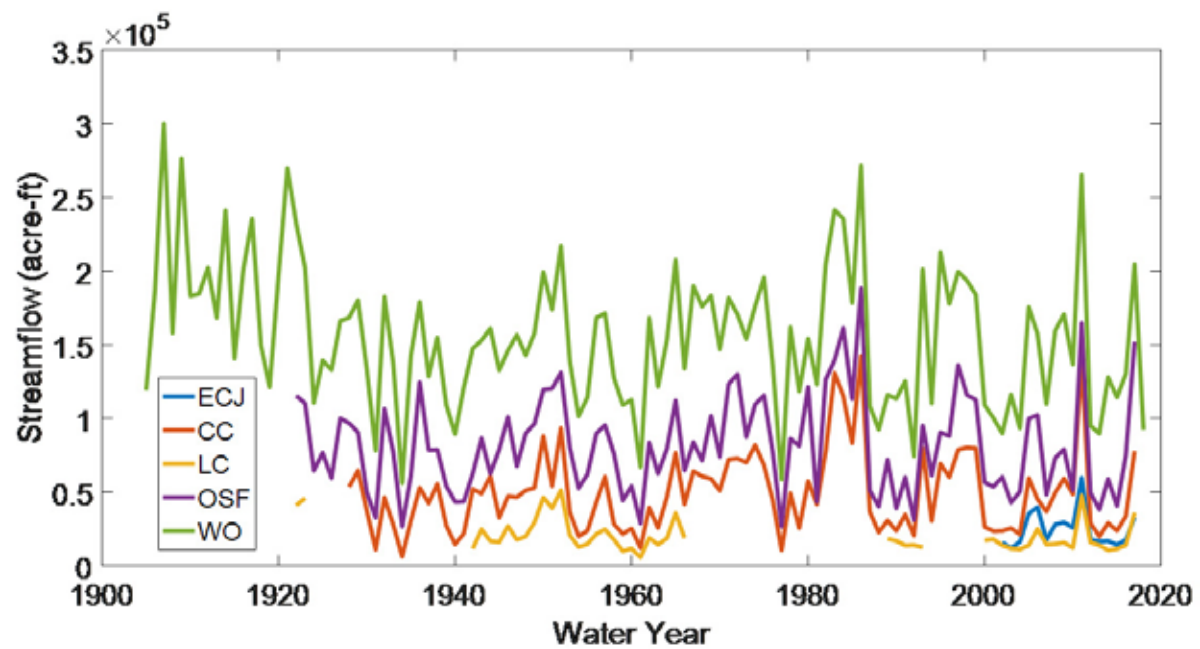

Figure 8. Annual streamflow in East Canyon Creek above Jeremy Ranch (ECJ), Chalk Creek (CC), Lost Creek (LC), the South Fork of the Ogden River (OSF), and the Weber River above Oakley (WO).

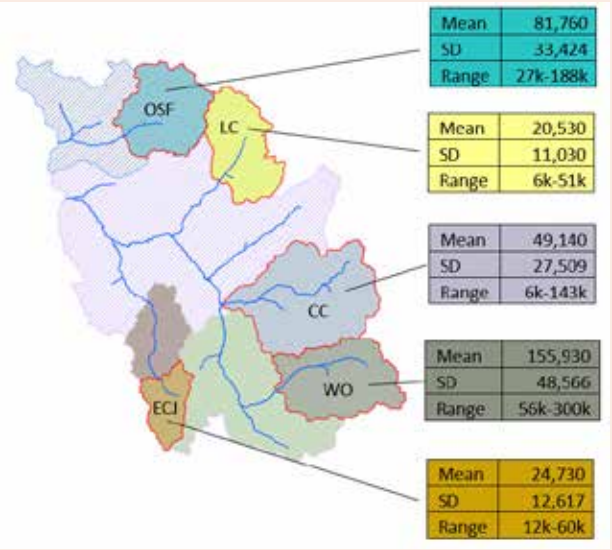

Figure 9. Mean, standard deviation (SD), and range of annual streamflow (acre-ft) in the South Fork of the Ogden River (OSF), Lost Creek (LC), Chalk Creek (CC), Weber River above Oakley (WO) and East Canyon Creek above Jeremy Ranch (ECJ).

Long-term streamflow records indicate that annual streamflow is much more variable than precipitation or temperature; coefficients of variation (CV) for streamflow ranged from 0.31-0.56 for individual sub-basins, while CV for precipitation ranged from 0.17-0.19. In general, variability is higher in drier and warmer catchments than in colder and wetter locations. However, streamflow response to climate exhibits both interannual and inter-sub-basin variability. In a given year, water yield or runoff efficiency (defined as the ratio of streamflow to precipitation) capture this variability by representing the fraction of incoming precipitation that is partitioned to streamflow.

Long-term annual water yield values range from 13% in Lost Creek to 48% in Weber River above Oakley (Figure 11). Variability ranges from CV of 0.18 in Weber River above Oakley to 0.45 in Lost Creek (Figure

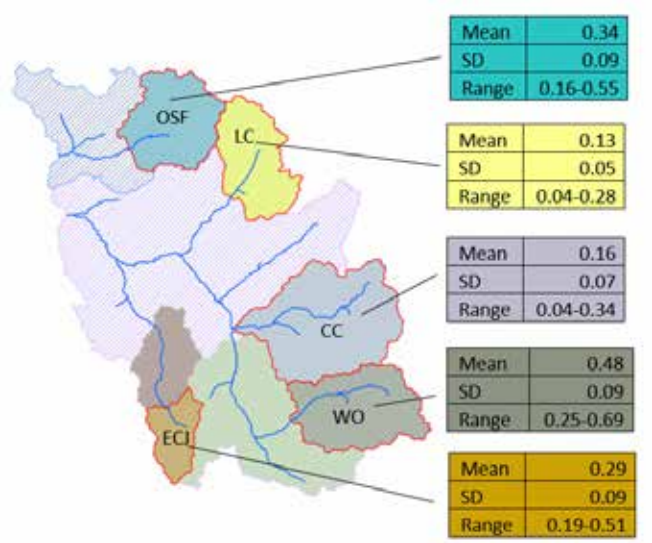

Figure 10. Mean, standard deviation (SD) and range of water yield (runoff efficiency) in the South Fork of the Ogden River (OSF), Lost Creek (LC), Chalk Creek (CC), Weber River above Oakley (WO) and East Canyon Creek above Jeremy Ranch (ECJ).

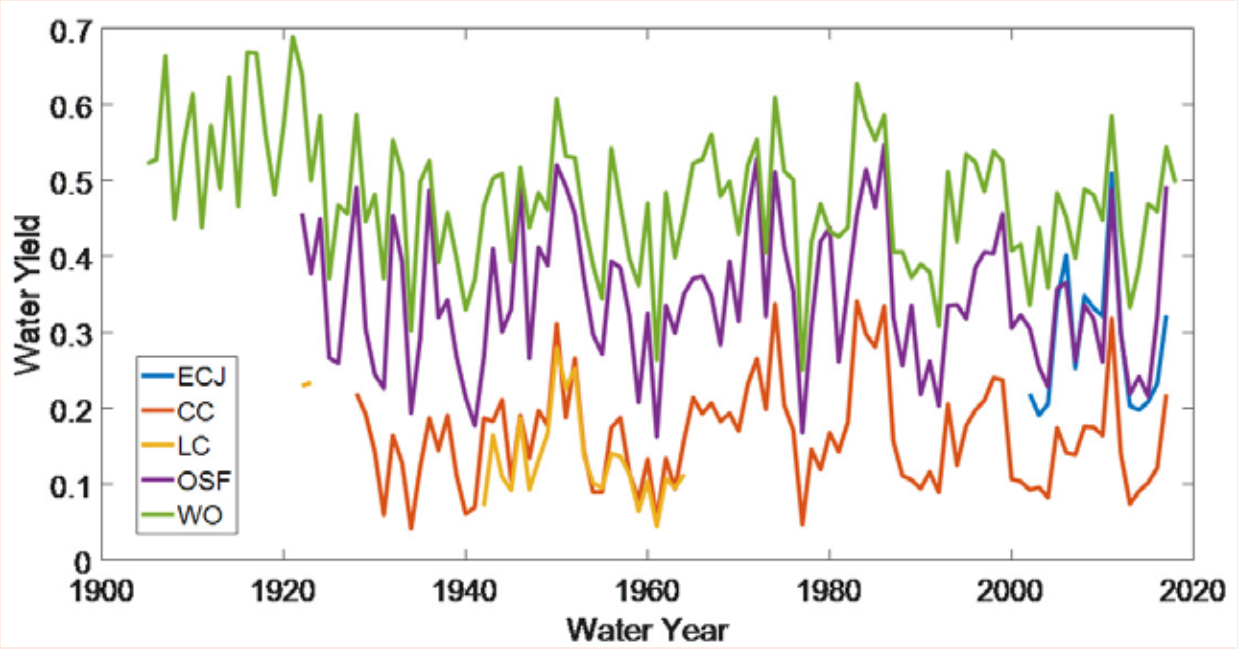

Figure 11. Water yield (runoff efficiency) in East Canyon Creek above Jeremy Ranch (ECJ), Chalk Creek (CC), Lost Creek (LC), the South Fork of the Ogden River (OSF), and the Weber River above Oakley (WO).

10). Water yield is less variable than streamflow in these five sub-basins and exhibits a similar pattern across sub-basins; water yield in Weber River above Oakley and South Fork of the Ogden River are less variable than water yield in Chalk Creek, Lost Creek, and East Canyon Creek. Similar to annual precipitation and streamflow, there is no significant trend in water yield in these five sub-basins during the period of record. Nearby watersheds show similar variations in water yield across both space and time as observed in the Weber River basin. Mean water yields in the seven creeks of Salt Lake Valley vary from 0.18 to 0.63, with CV ranging from 0.13 to 0.56 (Gelderloos 2018). These differences in water yield in space and time are due to unique landscape characteristics within the catchments and how these attribute interact with climate (Troch et al. 2009; P. Brooks et al. 2011; Voepel et al. 2011; Gelderloos 2018). In Section 4, we determine the primary factors controlling these differences in how precipitation is partitioned to streamflow.

3. PROJECTIONS OF FUTURE CLIMATE FOR THE WEBER BASIN

The following section provides an analysis of the future climate conditions of the Weber River basin. The analysis uses downscaled climate projections for the basin at locations relevant for management decisions at the mid- and end-of-century time periods. In addition to projections of temperature and precipitation, other factors such as snow characteristics, extreme precipitation, potential evapotranspiration and evaporation will be evaluated. The purpose of this portion of the report is to provide specific climate projections to aid WBWCD in its goal to develop new strategies to conserve and extend water supplies in light of the changing climate. We provide a brief introduction to the datasets used in this analysis, then communicate findings from the study with associated uncertainties, and lastly provide a summary of climate projections.

A. INTRODUCTION TO CLIMATE MODELING

Key Points

- A large set of global climate model (GCM) simulations are publicly available covering four greenhouse gas emission scenarios.
- The spatial resolution of these GCMs is too coarse for use in mountainous terrain, and so-called *downscaling* methods must be used to increase the resolution.
- Our downscaling based on statistical methods (*statistical downscaling*) enables rapid processing of all the available GCMs.
- Our more computationally intensive downscaling using high resolution modeling (*dynamical downscaling*) is limited to a single GCM simulation, but provides more physically based results.

A global climate model (GCM) is a computer program which simulates the state of the Earth's atmosphere, ocean, land surface, sea ice, and land ice. The program is built on the equations which represent the laws of physics. A GCM typically consists of tens of thousands of lines of computer code and is run on supercomputers with thousands of processor chips. Scientists change the concentration of greenhouse gases like carbon dioxide in these models, and study how aspects of climate like temperature and precipitation respond. Historical simulations are run to study and better understand past changes, and future simulations are run to study how the system will respond to various scenarios of fossil fuel combustion and greenhouse gas emissions. The various greenhouse gas emission scenarios are referred to as Representative Concentration Pathways (RCPs), and are used to specify how concentrations of fossil fuel combustion byproducts like carbon dioxide will change into the future.

In recent years, the international climate modeling community has developed publicly available, standardized, and coordinated sets of global climate model (GCM) simulations referred to as the Coupled Model Intercomparison Project Phase 5 (CMIP5; Taylor et al. 2012). The CMIP5 dataset includes more than 20 GCMs using four future greenhouse gas emission scenarios called Representative Concentration Pathways (van Vuuren et al. 2011). RCP 8.5 is a very high emission scenario where emissions continue to increase at the current annual rate through the end of the 21st century. RCP 6.0 and RCP 4.5 are intermediate scenarios with progressively lower emissions; for RCP4.5, greenhouse gas emissions reach a peak by mid-century and then decline. RCP4.5 is the scenario closest to the pledged goals in the Paris Accord (a 2016 international agreement where most countries in the world committed to

Photo: Hayden Peak over Mirror Lake, High Uinta Mountains, Utah. Credit: Ken Lund/Creative Commons.

reduce greenhouse gas emissions). RCP 2.6 is a low concentration scenario assuming highly-aggressive greenhouse gas emission reductions and carbon sequestration by the end of the current century (IPCC 2018).

Because of the global scale of the CMIP5 experiments and technological and economic limitations, they were run at coarse horizontal resolutions corresponding to approximately 75 mile x 75 mile grid spacing with simplified topographies and land-surface modelling. The large grid cell spacing limits the application of GCM datasets in complex terrain such as Northern Utah where climate parameters like precipitation vary dramatically over short horizontal distances. Because GCMs use large grid cells, local studies of climate change impacts often use a technique known as information downscaling in order to calculate modeling results at locally relevant scales. There are two main techniques to accomplish this: *statistical downscaling* and *dynamical downscaling* (Gutmann et al. 2012). We use datasets produced using both techniques in the analysis below.

In *statistical* downscaling of precipitation, for example, statistical relationships are found between fine-scale historical observations of precipitation and the GCM precipitation output during the historical period. These statistical relationships are then applied to the future GCM output in order to better approximate the local precipitation in the future. The advantage of statistical downscaling is its computational efficiency—computational techniques can rapidly process a large set of simulations corresponding to many GCMs over a broad range of emission scenarios. The main disadvantage of statistical downscaling is its assumption that the statistical relationships, derived from the climate of the past, are valid in the climate of the future.

The statistically downscaled dataset utilized in this report is the Localized Constructed Analogs (LOCA) dataset (Pierce et al. 2014). LOCA is a technique developed by the University of California-San Diego that uses the statistical power of so-called "analog days" to assign a high resolution pattern to future GCM precipitation. An analogue day is a day in the historical past which has a similar large-scale weather pattern to the day being downscaled in the simulated future. LOCA is more computationally expensive than other statistical downscaling methods, but it better represents extreme days and improves the spatial coherence of the downscaled precipitation. LOCA data is available for 32 global climate models under RCP 8.5 and RCP 4.5 (Pierce 2014).

Dynamical downscaling involves running a high-resolution regional climate model over a portion of the Earth, Utah in this case. Output from a coarse-resolution GCM provides input to the high-resolution climate model about the state of the atmosphere (e.g., temperature and humidity) at the edges of the model simulation. These atmospheric states on the edges of the model simulation are referred to as "boundary conditions," and we provide more detail on our specific boundary conditions below. The technique is highly computationally intensive, so it is not feasible to undertake for a broad range of climate models or carbon emission scenarios. The advantage is that it uses the fundamental laws of physics governing the atmosphere to model the future, but at a higher spatial resolution so that it adds locally-relevant information that was not available from the original GCM. This is very important in complex terrain. Many GCMs will only have two grid points each in the regions of the Wasatch and Uinta Mountains, meaning that GCM representation of terrain is unrealistically smooth. In contrast, a dynamically downscaled climate model can resolve individual canyons and mountain ridges. This is important because not only does the weather respond to the mountains here, it is driven by them.

The dynamically downscaled dataset used in this analysis was generated using the Weather Research and Forecasting (WRF) model (Skamarock et al. 2005) modified to include a customized model for the Great Salt Lake as described in (Scalzitti et al. 2016a; Scalzitti et al. 2016b and Strong et al. 2014). To specify the state of the atmosphere on the edges of our simulations (the "boundary conditions"), we began with the weather systems of the past and modified them with changes in temperature and moisture which are characteristic of global warming. This approach is known as pseudo global warming. In this case, the temperature and humidity changes were based on the Community Climate System Model (CCSM) from the National Center for Atmospheric Research in the RCP 6.0 scenario, and the historical weather period was 1995 to 2005, which included some of the best and worst water years on record. CCSM was chosen for its skill in capturing historical

climate in the Great Basin (Smith et al. 2015). Beginning with historical weather is a strength of pseudo global warming, because it circumvents model bias (e.g., the tendency for a GCM to be too cool), the frequency and structure of storms is realistic, and individual storms can be directly compared to their counterparts in the warmer and moister future simulation. The downside to pseudo global warming is that it may not entirely capture large-scale changes in the weather such as changes in the winter storm track.

The two techniques of downscaling each have their roles in this analysis. LOCA statistical downscaling is useful for its availability in many different global climate models and carbon emission scenarios. However, the lack of spatial resolution in the original GCMs is a serious hindrance to understanding variations in climate throughout the Weber River basin. Even with the higher resolution afforded by the downscaling, the input to the model is essentially the same at each LOCA point, so there is little spatial variation, even though we know that the Uinta and Wasatch Mountains will often have very different winters. The WRF dynamical downscaling becomes useful in analyzing the spatial differences in temperature, precipitation, and snowpack throughout the Weber River basin. The challenge in interpreting the WRF dataset is that it provides no information about uncertainty between carbon emission scenarios, and its relationship with the LOCA data is obscured since it uses the RCP6.0 emission scenario that is not available in the LOCA dataset. It overcomes some of the uncertainty by being based on historical weather patterns and therefore is not tied too closely to an individual GCM. In summary, the LOCA dataset is best used to illustrate magnitudes and uncertainties of the large-scale changes to the system, and the WRF dynamically downscaled dataset is best used to examine changes in physical processes and also spatial heterogeneity in the region.

B. TEMPERATURE PROJECTIONS

Key Points

- Moderate greenhouse gas emissions increase maximum temperatures by approximately 4°F by 2050 and 7°F by 2100. *High confidence*.
- High greenhouse gas emissions increase maximum temperatures by 6°F by 2050 and 12°F by 2100. *High confidence*.
- Year-to-year variability in warming is relatively small; there are many hot years in a row and fewer historically normal years. *High confidence*.
- The greatest warming will take place in the springtime as the snowpack melts sooner and bare ground is exposed which absorbs more solar radiation. *Very high confidence*.
- The strongest warming in the short-term will take place in valley locations such as Morgan and Ogden Valleys. *High confidence*.
- Snyderville Basin, Morgan and Ogden Valleys will eventually warm 50% more than Uinta Mountain areas. *Medium confidence*.

LOCA Statistical Downscaling

The largest uncertainty in future climate modeling is the impact of human activity on the climate system, not the uncertainty between different climate models. For example, the middle 25% to 75% of the LOCA-downscaled climate models results indicate an annual maximum temperature increase of approximately 3°F for both RCP4.5 and RCP8.5. However, the median model projection of annual maximum temperature for RCP8.5 in 2100 is 5°F greater than for RCP4.5. The relatively large impact of human behavior (i.e., level of emissions) on future uncertainty is an important context for the range of climate modeling results presented below.

Projections of future temperatures are relative to a base period of 1976 to 2006. This base period represents the last 30 years of what is referred to as the "historical" period in the CMIP5 studies. Results are presented

for an average of grid points located in the Uinta headwaters region of the Weber River. There is little difference in this dataset between the individual grid points, as discussed in Section 3a above.

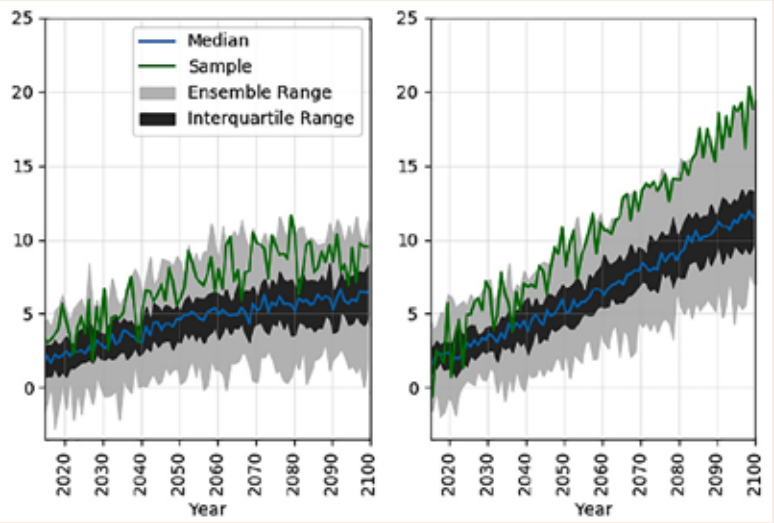

Figure 12. Change in annual average daily temperature (°F) relative to 1976-2006 mean for western Uinta Mountains above the Weber-Oakley stream gauge. RCP 4.5 is presented in the left panel and RCP8.5 is presented in the right panel, light gray shading indicates the total range of the 20 model simulations, dark gray shading indicates the middle 50% of the 20 model simulations, the blue curve indicates the median, and the green curve shows an individual model simulation to illustrate magnitude of interannual variability.

Under the RCP4.5 scenario, there will be a 3 to 5°F increase in annual maximum temperature by 2050 in this region (Figure 12). The range of 3 to 5°F represents the interquartile range, or 25% -75%, of the models in the analysis. After 2050, warming slows, and by the end of century RCP4.5 predicts a 5 to 8°F warming compared to the 1976-2006 average. In the RCP8.5 scenario (high emissions), there will be an exponential temperature increase with 4 to 6°F of warming by mid-century and 10 to 14°F of warming by 2100. A degree Fahrenheit of warming corresponds to approximately 300-foot higher snow levels, so these temperature changes indicate snow levels rising by 1200 to 1800 feet by mid-century and 3000 to 4200 feet by 2100.

Figure 12 shows a green line to represent how a single model in the sample evolves over time. This is to show how a specific model tends to have a certain departure from the mean in its temperature predictions, meaning that warmer models tend to run warm throughout the century. A corollary is that the interannual variability in warming is relatively small; there are many hot years in a row and fewer historically normal years no matter what the rate of warming turns out to be.

The higher resolution of dynamical downscaling, compared to statistical downscaling, enables a meaningful analysis of the spatial variability of climate parameters in the various sub-basins of the Weber River basin. To illustrate the spatial variability in future temperatures in the Weber River basin, temperature projections are superimposed on a map of the sub-basins (Figure 13). Warming is stronger at the end-of-century than for mid-century. The smallest increase in temperature occurs over the Great Salt Lake and other water bodies; because

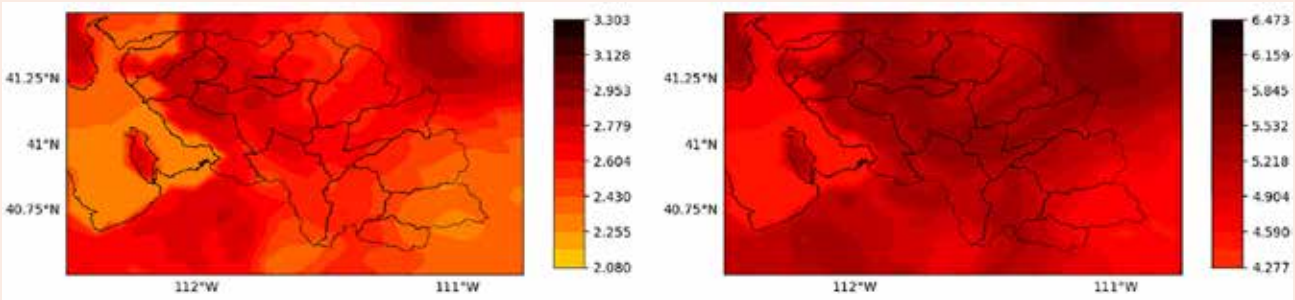

Figure 13. Based on dynamical downscaling, change in annual mean temperature (°F) for a mid-century decade (2035-2044; left panel) and end-of-century decade (2085-2094; right panel) relative to the historical period of 1985-2010. Note the color scales differ between the panels. The Great Salt Lake and the sub-basins of the Weber River are outlined in black.

water has a high heat capacity, areas over lakes warm more slowly than areas over and surfaces. However, there is still an increase to the water surface temperature of 2 to 2.5°F by mid-century and more than 4°F by the end-of-century, which may be significant enough to impact the ecology of these water bodies. The strongest warming in the short-term will take place in valley locations such as Mountain Green and Ogden Valley as well as the urban core of Ogden (2.5 to 3°F increase). In the longer-term, the strongest warming will take place all in the Wasatch Back valleys (5.5 to 6°F increase) with annual average temperatures increasing 50% more than the Uinta Mountains (4°F increase). Temperature change results for specific locations are tabulated in the Appendix 2.

To understand seasonal changes in the spatial pattern of warming, projections of future temperature change relative to the historical period are presented by month (Figures 14 and 15 as maps, Figures 16 and 17 at specific locations). The greatest warming will take place in the springtime as the snowpack melts sooner, which exposes bare ground and absorbs more solar radiation. Snowpack has a cooling effect by reflecting solar radiation; its early removal has a strong impact on local temperatures. This effect will be felt sooner at lower elevation locations as the ground becomes snow-free earlier in the season compared to higher elevation locations. During winter and summer, the greatest warming is observed in the low elevations of the Wasatch Front and Morgan Valleys, with the urban heat island effect most pronounced during summer. The autumn will see relatively little warming in the near future; warming in spring is three times greater than autumn warming. Smaller autumn temperature increases are likely due to weather patterns being less impacted by climate change in the near-term. Later in the century temperature increases in autumn are more similar to other seasons, indicating that the

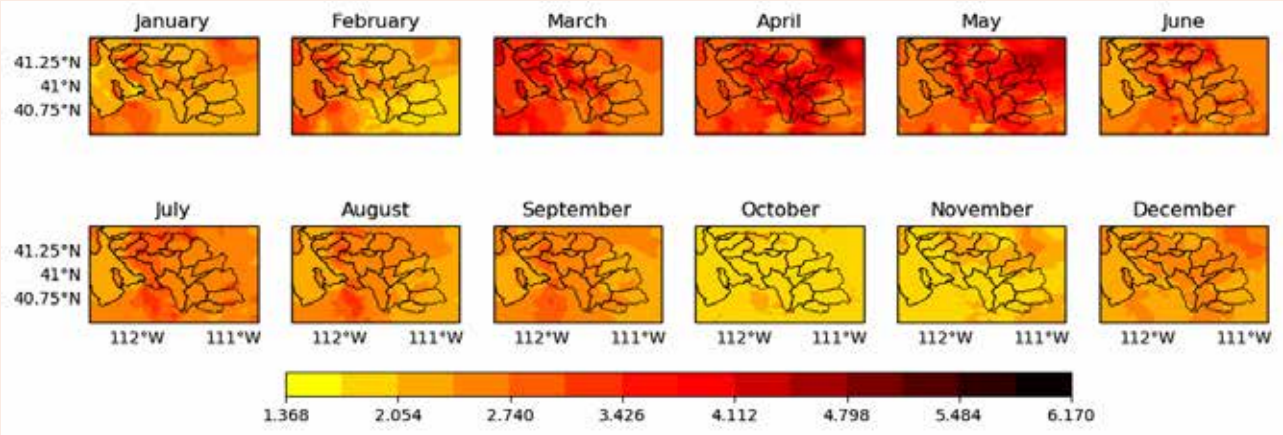

Figure 14. Based on dynamical downscaling, change in monthly mean temperature (°F) for a mid-century decade (2035-2044) relative to the historical period of 1985-2010. The Great Salt Lake and the sub-basins of the Weber River are outlined in black.

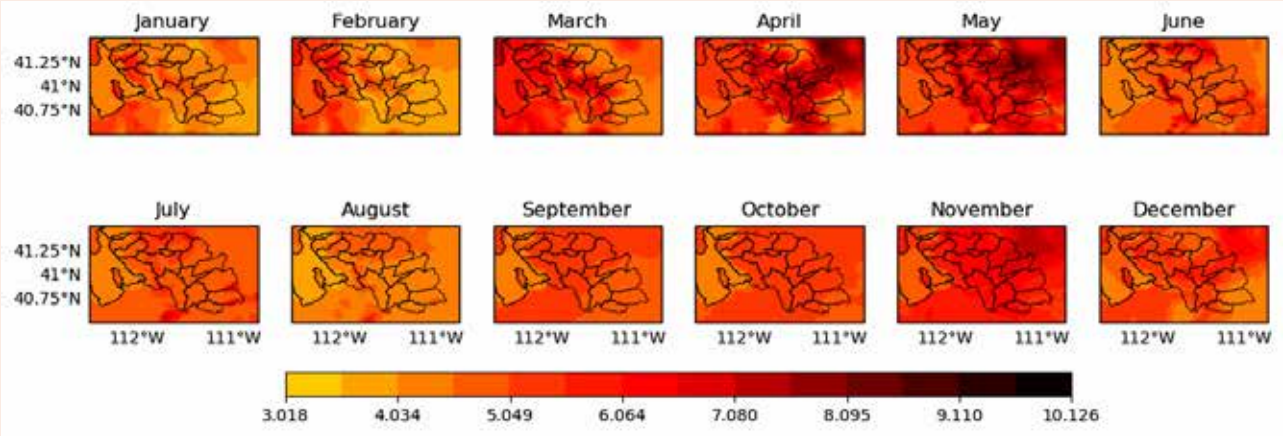

Figure 15. Same as Figure 13, but for an end-of-century decade (2085-2094).

process that was limiting local warming during autumn weakens under the heightened warming. There is very little spatial variability in warming during late summer through early winter for both mid- and end-of-century projections (Figure 16 and 17). There is greater spatial variability in warming during winter and spring. Winter and spring warming vary by up to 1.5°F between locations for mid-century projections. For end-of-century projections of temperature, spring and winter warming vary by p to 3.5°F between locations.

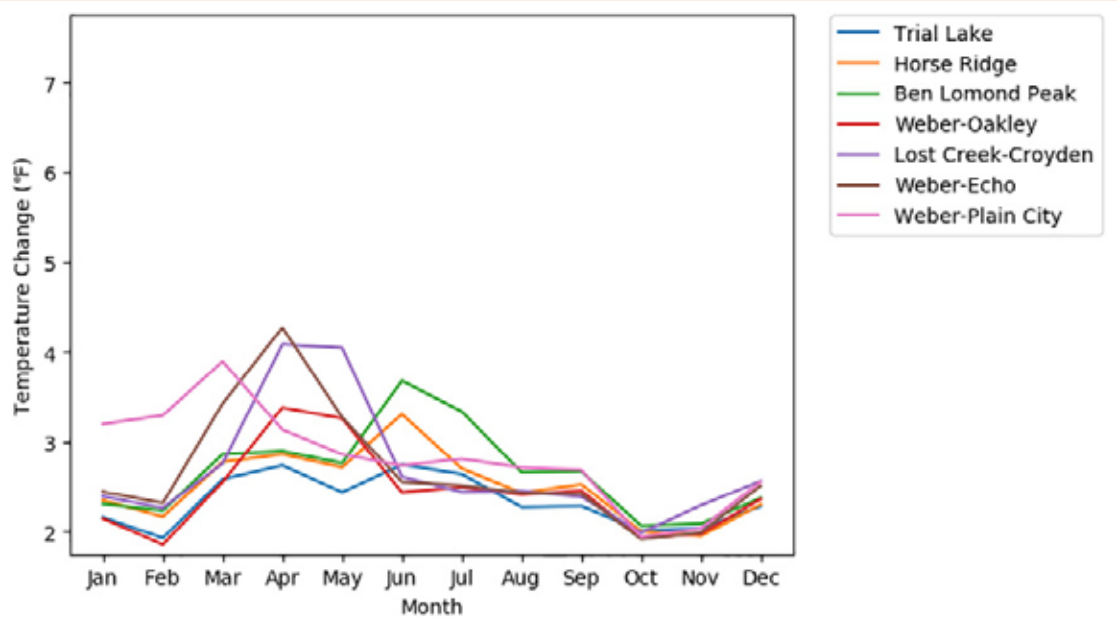

Figure 16. Based on dynamical downscaling, change in monthly mean temperature (°F) for a mid-century decade (2035-2044) relative to the historical period of 1985-2010 at key locations in Weber River watershed.

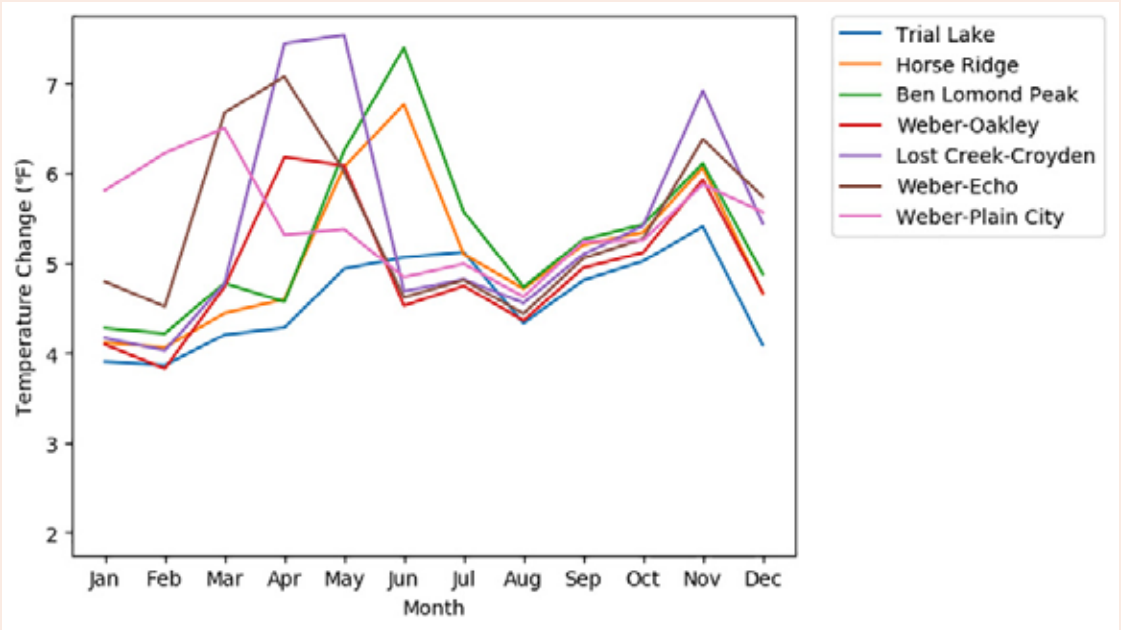

Figure 17. Based on dynamical downscaling, change in monthly mean temperature (°F) for an end-of-century decade (2085-2094) relative to the historical period of 1985-2010 at key locations in Weber River watershed.

C. PRECIPITATION PROJECTIONS

Key Points

- Northern Utah is near a transition zone in regards to precipitation projections with wetter future conditions expected to the north and drier future conditions expected to the south. *High confidence.*
- Most climate models project a slight increase in precipitation for the Weber River basin. *Medium confidence*.
- By mid-century, the greatest precipitation increases occur in January and February in the Wasatch and Uinta Mountains. *Medium confidence*.
- Precipitation is projected to decrease in May and June throughout the 21st century. *Medium confidence*.
- Mountain precipitation may increase in November and December throughout the century, but warming will increase the fraction of November and December precipitation that falls as rain. *High confidence*.
- A large increase in September precipitation is due to an interaction of monsoon moisture and fall Pacific storms. *Low confidence*.

Northern Utah is situated in a region where most climate models project a slight increase in precipitation. In the western United States, northern regions are predicted to see a large increase in precipitation while desert areas to the south may see reductions to precipitation (USGCRP 2017). Northern Utah is near the transition zone where more precipitation will fall to the north and less to the south in the western United States, but will likely see a slight increase in precipitation on average. In the LOCA dataset, this change is on the order of a 5% precipitation increase, but the middle 50% of results still includes instances of drought out to 2100 (Figure 18). The most significant difference between the two emission scenarios in the LOCA dataset is that there is greater uncertainty in RCP8.5; projections show greater interannual variability with more intense wet years and drought years. The green line on the figure represents a single model as a sample. In contrast to the temperature change, this sample includes many above-average and below-average years. That is to say, the interannual variability is larger than the variability between models, and that the region is likely to continue to see wet years and dry years at approximately the same frequency as in the historical record.

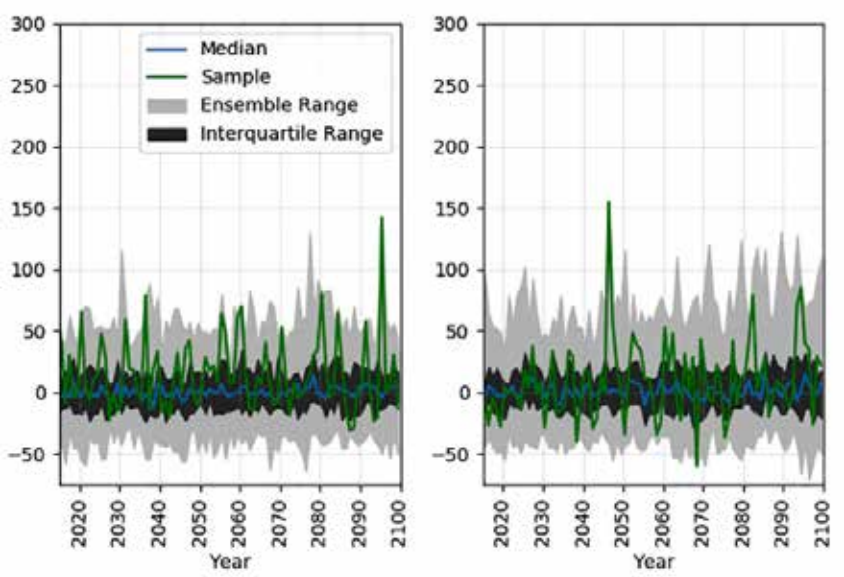

Figure 18. Change in annual mean precipitation (shown as a percent change from historical) relative to 1976-2006 mean for the western Uinta Mountains above the Weber-Oakley stream gage. RCP4.5 is presented in the left panel and RCP8.5 is presented in the right panel, light gray shading indicates the total range of the simulations, dark gray shading indicates the middle 50% of the simulations, the blue curve indicates the median, and the green curve shows a representative individual simulation.

The data from dynamical downscaling gives a different, and valuable, view of the future precipitation in the region. In contrast to LOCA, it shows a broad increase in precipitation across northern Utah, on the order of

5% by mid-century and 10% by the end-of-century (Figure 19). The differences may be ascribed to the large-scale precipitation outcome in the specific global climate model simulation chosen for dynamical downscaling, and also to differences in the two downscaling techniques. LOCA uses the relationships of the past, and may especially struggle in a future where the mountains have subtly different impacts on storms due to the different temperature profiles and moisture content of the atmosphere. Another way to state this concept is that future weather patterns may be different than past weather patterns; LOCA downscaling assumes that future weather patterns will be similar to past weather patterns. In the WRF model used in dynamical downscaling, the spatial distribution of the increase in precipitation is broadly the same in both the mid-century and end-of-century periods. The highest relative increase takes place in the Wasatch Back valleys near Echo Reservoir, Morgan,

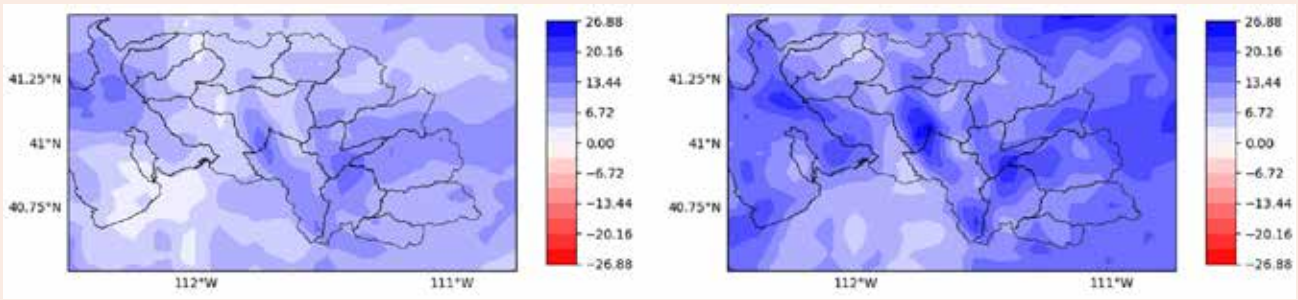

Figure 19. Based on dynamical downscaling, change in annual mean precipitation (percent difference) for a mid-century decade (2035-2044; left panel) and end-of-century decade (2085-2094; right panel) relative to the historical period of 1985-2010 for RCP6.0. The Great Salt Lake and sub-basins of the Weber River are outlined in black.

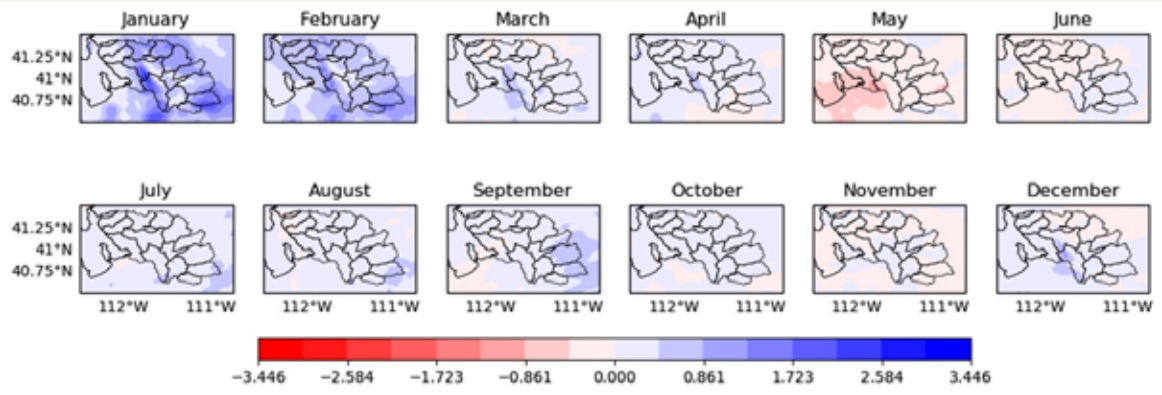

Figure 20. Based on dynamical downscaling, change in monthly mean precipitation (inches) for a mid-century decade (2035-2044) relative to the historical period, 1985-2010. The Great Salt Lake and sub-basins of the Weber River are outlined in black.

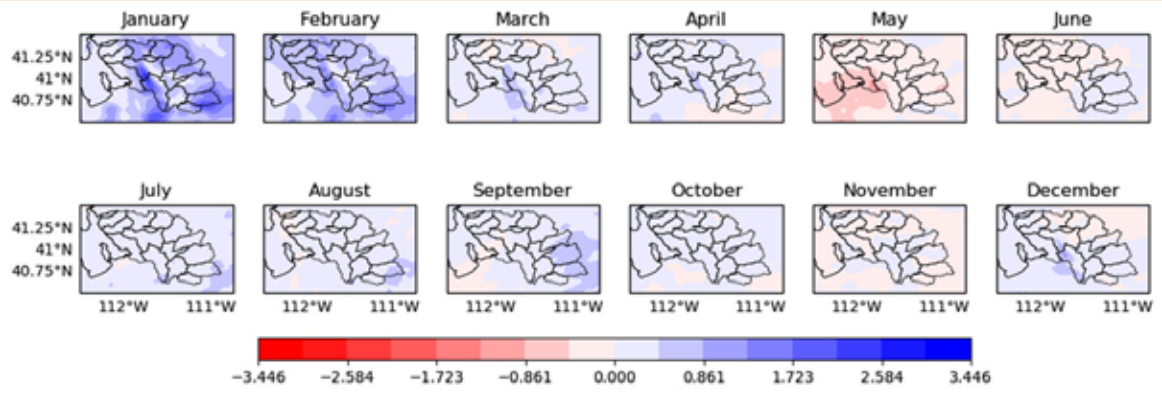

Figure 21. Same as Figure 18, but for an end-of-century decade (2085-2094).

and Snyderville. The smallest relative increase takes place in the Ben Lomond area, but that is because that mountain already receives so much moisture. Changes in precipitation for specific locations are tabulated in the Appendix 2.

By mid-century, the greatest precipitation increases take place during January and February in the Wasatch and Uinta Mountains with three inches of additional water received in some places (Figure 20). Summertime also sees a large increase in precipitation due to a more active monsoon, but because so little rain falls in summer, it is a small contributor relative to the winter. A decrease in precipitation during the late spring months of May and June is observed throughout the century. This is especially relevant since it may impact amount of moisture available in spring and potentially the starting date of the irrigation season. By the end of the century, reductions in March – June precipitation may cause drought conditions to emerge in valley locations. In contrast, November and December see a large increase in mountain precipitation (Figure 21). Unfortunately, dynamical downscaling for this scenario indicates it will be too warm by then for most of that to fall as snow. The month of September also stands out for its large increase in precipitation due to the interaction of the monsoon moisture and fall storms. Figures 22 and 23 show projected changes in monthly precipitation at ten locations for mid-century and end-of-century.

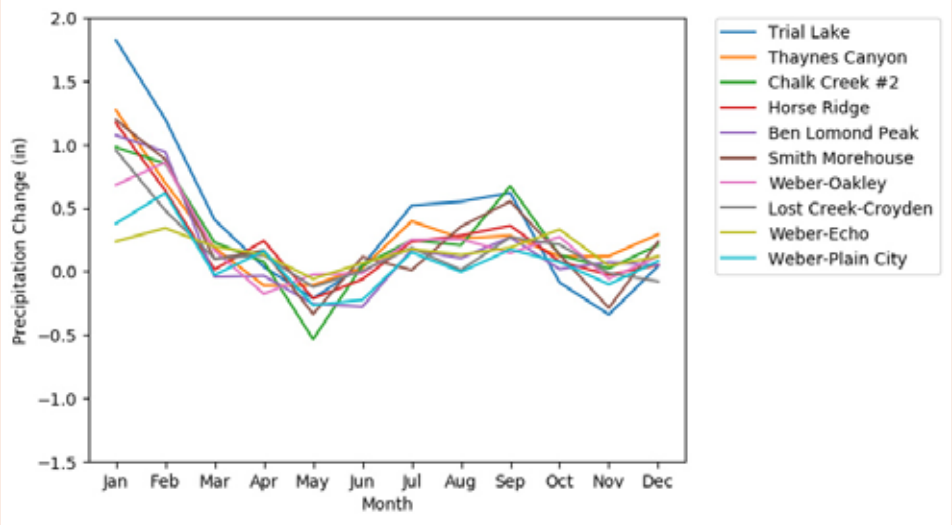

Figure 22. Based on dynamical downscaling, change in monthly mean precipitation (inches) for a mid-century decade (2035-2044) relative to the historical period, 1985-2010 at key points in Weber River watershed.

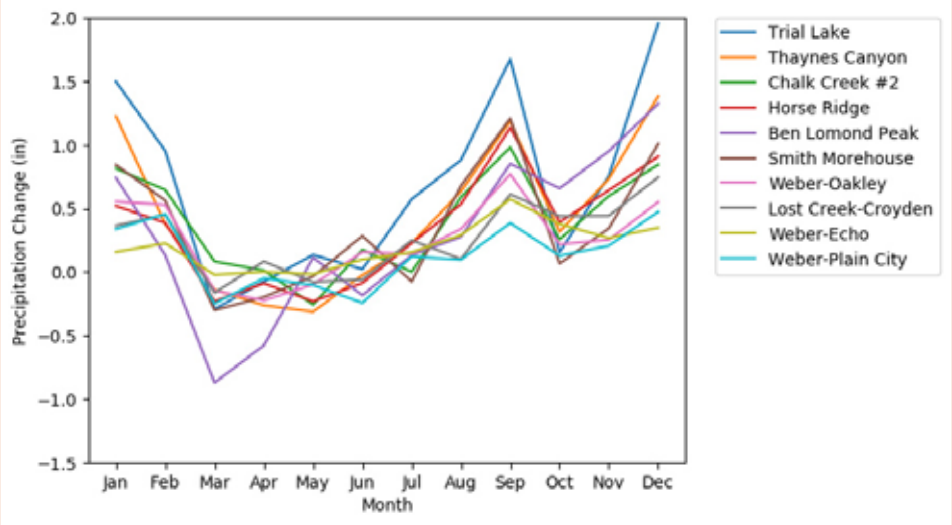

Figure 23. Same as Figure 22, but for an end-of-century decade (2085-2094).

4. PROJECTIONS OF FUTURE WEBER RIVER STREAMFLOW

Any approach at modeling streamflow under future climate will have uncertainties associated with data used to drive the model, the structure of the model itself, and evaluation procedures used during model validation. To address these interacting sources of uncertainty, we employ three widely-used modeling approaches to provide projections of future Weber River streamflow. Convergence among model predictions increases confidence, while the suite of streamflow predictions allow for direct comparison with related work from other regions that is likely to use only one modeling approach, Specifically, we provide:

- Predictive streamflow models of sub-basins of the Weber River basin were developed using historical data that includes streamflow and other hydrological parameters.
- Streamflow is projected for 2055 and 2085 using a Variable Infiltration Capacity (VIC) model.
- Streamflow is projected for mid-century by performing a temperature and precipitation sensitivity analysis of a streamflow model used by forecasters at the Colorado Basin River Forecast Center.

A. STATISTICAL STREAMFLOW MODELS OF SUB-BASINS

i. Development of statistical models with historical climate

Key Findings

- Statistical models of streamflow are developed using historical data presented in Section 2. These models capture 92%-98% of the historical variability in streamflow in the Weber River basin.
- Across all sub-basins, the three strongest predictors of annual streamflow are precipitation, antecedent groundwater storage (groundwater levels before melt begins), and snowmelt dynamics.
- These modeling results quantify how climate influences streamflow at three distinct temporal scales:
  - On an annual time scale, the amount of precipitation is a critical driver of streamflow.
  - On a multi-year time scale, the climatic influences on groundwater recharge are an important driver of streamflow.
  - On a seasonal time scale, the controls on snowmelt dynamics are the key driver of streamflow.
- Snowmelt rate is decreasing in the headwaters of the Weber River above Oakley. Slower snowmelt generally occurs when melt begins early because solar angles are still relatively low (lower input of solar radiation). Early, slow melt generally causes lower streamflow than a later, faster melt.
- A slower melt rate of the Weber River above Oakley snowpack could reduce water yield in future years.

To develop statistical models of both annual and daily streamflow specific to WBWCD, we compiled climate and streamflow data described in Section 2 with sub-basin characteristics (elevation, aspect, vegetation cover, etc.) in a series of linear and stepwise multiple-linear (MLR) regressions to identify factors statistically related to streamflow. Following these initial analyses, predictive factors were screened for co-linearity and the weaker

Photo: Rockport Reservoir, Utah. Credit: John/Adobe Stock.

statistical predictor was discarded. For example, winter and annual precipitation are strongly related to each other and to streamflow. Because annual precipitation is a stronger predictor of annual streamflow than winter precipitation, only annual precipitation was retained in subsequent analyses. The resulting factors were retained for MLR modeling. With the final model structure including all factors that were both statistically significant and added more than 3% improvement in model prediction.

Modeling annual streamflow volumes

Not surprisingly, annual precipitation was the strongest factor controlling variability in streamflow (Hornberger et al. 2014) in all sub-basins. In general, the higher the mean annual precipitation for a sub-basin, the greater the predictive ability annual precipitation added to the statistical model (higher r^2 value in Figure 24). Surprisingly, and in contrast to assumptions encoded in other models, neither annual nor seasonal temperatures added predictability (explained remaining variance) in our model. It is important to note that this does not mean that a potential increase in ET driven by rising temperatures is unlikely to occur. Rather, it suggests that the influence of temperature on streamflow occurs primarily at longer or shorter time steps than annual. The next strongest predictor of annual streamflow in all sub-basins was antecedent groundwater storage inferred from January baseflow measurements.

Although initially surprising, these findings are consistent with extensive recent literature on streamflow routing and longer residence time water (Brooks et al. 2015; Huntington and Niswonger 2012; Godsey et al. 2009) on streamflow generation. The results indicate that as the amount of water stored in groundwater increases, a larger fraction of new precipitation entering is partitioned to streamflow. This mechanism explains how an average precipitation year following several years of drought (during which groundwater storage was slowly depleted) may result in lower water yield or runoff efficiency than average for a basin. Our approach to quantify antecedent groundwater storage is analogous to recession analyses for dynamic storage and flood forecasting (Stoelzle et al. 2013; Birkel et al. 2011; Ajami et al. 2011; Wittenberg and Sivapalan 1999), but has only recently been applied to snowmelt-derived water resources (Gelderloos 2018). Briefly, our approach involves confirming that January streamflow is not influenced by contemporaneous or recent climate, is not undergoing directional changes, and exhibits only small, random temporal variability. These requirements were

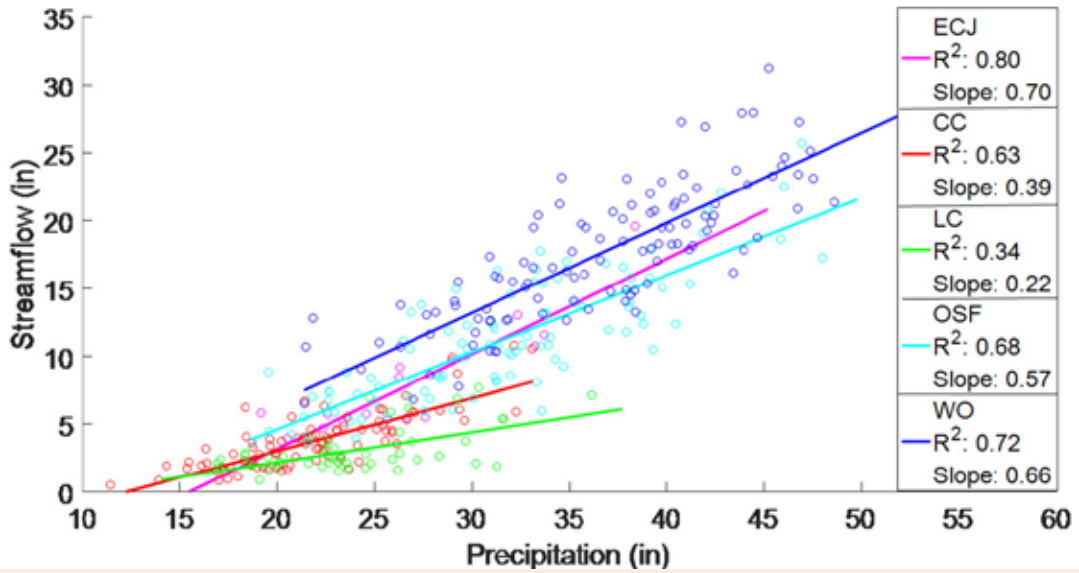

Figure 24. Statistical relationships between precipitation and streamflow in the five headwater catchments. All relationships are significant; the equations and statistics are presented in Table 12 of Appendix 1.

met for all sub-basins in all but a few years (which were excluded from analyses) and we infer that January streamflow is indicative of antecedent subsurface storage.

Following annual precipitation and antecedent groundwater storage, the third most important factor in predicting streamflow across all sub-basins was snowmelt. This is not surprising since the majority of precipitation in the Weber River basin falls as snow in winter and both isotopic and physical models of streamflow in the western United States highlight the importance of snowmelt processes (Clow 2010; Bales et al. 2006). In general, when snow melts faster, a larger fraction of the total snow storage becomes streamflow (streamflow generation is more efficient). In contrast, when snow melts more slowly, streamflow generation is less efficient (Barnhart et al. 2016). Observations show that melt is beginning earlier and proceeding more slowly in the Weber River basin, a trend that is expected to continue as climate warms. Importantly for future water supply, these patterns are expected to reduce water yield, or runoff efficiency in the future.

In the final statistical model (Figure 25), annual precipitation, antecedent groundwater storage and snowmelt dynamics account for 92% to 98% of interannual streamflow variability. No other climate or landscape factors added predictability to the statistical streamflow model.

Modeling daily streamflow values and hydrograph construction

Translation of annual water yield or streamflow predictions into an annual hydrograph requires quantifying how the timing of streamflow responds to climate. Historical streamflow data is used to develop statistical representations of streamflow on every day of the year. These statistical representations, referred to as cumulative discharge functions (CDFs), were developed under different precipitation and temperature scenarios. Years with average temperatures warmer than 85% of the historic record were classified as hot years. Those hot years were classified as dry (precipitation < 40% of historic record), average (precipitation > 20% but < 80% of historic record) or wet (precipitation > 60% of historic record). CDFs from each of those categories were then averaged to yield a typical CDF under hot-dry, hot-average, and hot-wet conditions. The overlap between scenarios yields a smoother CDF curve that is less prone to influence by a single, abnormal year. This process was repeated for average and lower temperature scenarios as well, with specific values shown in Table 14 of Appendix 1. CDFs

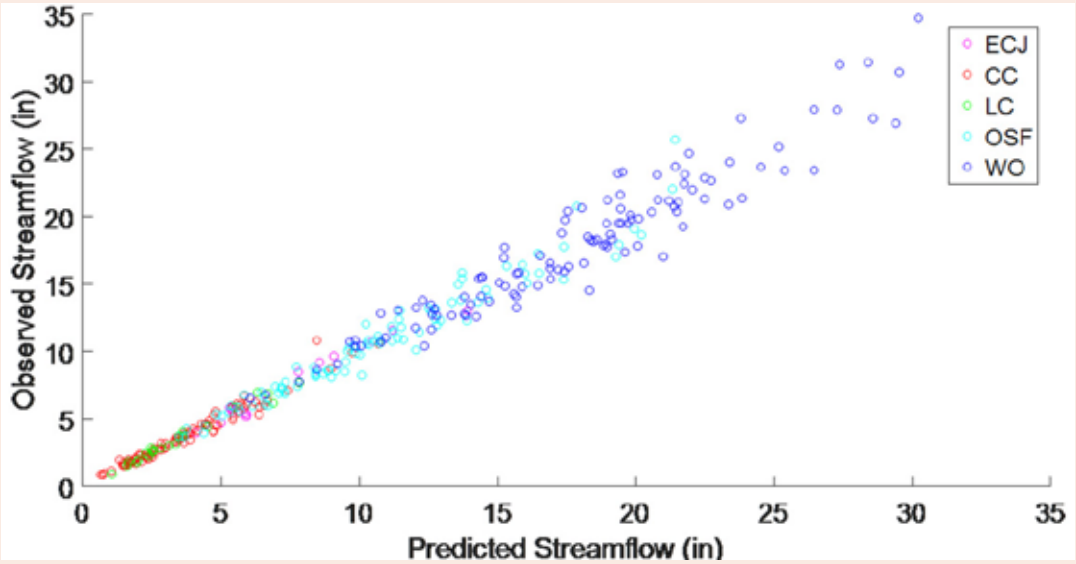

Figure 25. Multiple Linear Regression (MLR) models of streamflow for the five headwater catchments describe 92% to 97% of interannual variability in streamflow. MLR models include precipitation, antecedent January baseflow, and snowmelt dynamics. Equations and statistics for each catchment can be found in Table 13 of Appendix 1.

from a selection of these scenarios can be seen in Figure 26. Only CDFs with temperatures that fall within the hot scenario are used to project Weber River streamflow. We use CDFs, in combination with estimated annual streamflow from our statistical streamflow models, to develop hydrographs for four future climate scenarios.

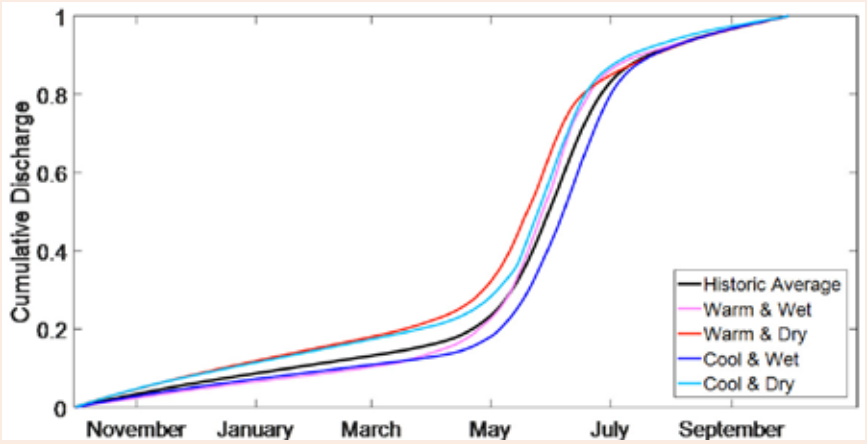

Figure 26. Cumulative discharge functions for the Weber River above Oakley under different climate scenarios.

ii. Streamflow response to future climate

Key Findings

- Streamflow projections for the headwaters of the Weber River above Oakley were developed for three precipitation scenarios (low, moderate and high) under a moderate (RCP4.5) and high (RCP8.5) emissions scenario for mid-century.
- Under the moderate emission scenario with medium precipitation, streamflow volume is 5% higher than the historical average (*Medium confidence*). Peak streamflow is 20% higher (*Medium confidence*), occurs 10 days earlier and base flow conditions return sooner (*High confidence*).
- Under moderate emissions with high precipitation, total annual streamflow is 5% higher than the historic maximum. Under moderate emissions with low precipitation, total annual streamflow is roughly equal to the historic minimum.
- Under the high emission scenario with medium precipitation, streamflow volume is 16% lower than the historical average (*Medium confidence*), peak streamflow is reduced by 32% (*Medium precipitation*) and snowmelt begins 2-3 weeks earlier (*High confidence*).
- The high emission, high precipitation scenario highlights the possibility of severe early-season flooding, with continuous melt-induced flow starting as early as February. *Low confidence*.
- The high emission, low precipitation scenario suggests the possibility of severe drought, with total streamflow 30% lower than the lowest year on record. *Medium confidence*.
- Snowmelt rate is decreasing in the headwaters of the Weber River above Oakley. Slower snowmelt generally occurs when melt begins early because solar angles are still relatively low (lower input of solar radiation). Early, slow melt generally causes lower streamflow than a later, faster melt. *High confidence*.
- A slower melt rate of the Weber River above Oakley snowpack could reduce water yield in future years.

To develop flow predictions under future climate conditions for the Weber River above Oakley, we use the LOCA downscaled climate projections from section 3b-c. Future climate scenarios were developed to simulate three different precipitation scenarios, each under two different emission/temperature scenarios for a mid-century time period (2050s). Mean annual precipitation for the Weber River above Oakley is 37.4 inches. Annual

precipitation 19.9 inches for the low precipitation scenario, 38.5 inches for the medium precipitation scenario, and 65.2 inches for the high precipitation. The medium precipitation scenario represents the mean of projected precipitation values. The low and high precipitation scenarios represent the 20th and 80th percentile of the minimum and maximum precipitation ensemble projections. The medium scenario is the most plausible, while the low and high scenarios represent more extreme scenarios that are less likely, but possible. The moderate emission scenario (RCP4.5) assumes a mean annual temperature of 38.9°F, a 2°F increase over historical means, and the high emission scenario (RCP8.5) assumes a mean annual temperature of 41.3°F, a 4.4°F temperature increase over historical means. As with all modeling approaches presented in this report, confidence is higher when temperature and precipitation of future climate scenarios fall within the historical range of climate. The low and medium precipitation scenarios are within the historical range of precipitation, but the high precipitation scenario is slightly outside the historical range. Temperature in the moderate emission scenario is within the historical range of temperature, but temperature in the high emission scenario is outside of the historic range.

Statistical models from Section 4a.i are used to estimate streamflow amount (using the MLR model) and streamflow timing (using the CDF model) under each climate scenario. Estimates of streamflow amount are shown in Table 1.

Table 1. Annual streamflow estimates (acre-feet) for the Weber River above Oakley under three precipitation projections in moderate emission (mid-century RCP4.5) and high emission (mid-century RCP8.5) scenarios. For reference, historical mean annual streamflow is 156,000 acre-feet.

	LOW PRECIPITATION	MEDIUM PRECIPITATION	HIGH PRECIPITATION
Moderate Emissions	56,057	162,930	316,080
High Emissions	39,300	130,900	262,280

It is important to note that these scenarios assume that antecedent groundwater storage is at the historical average for each sub-basin. Quantifying the multi-year climate impacts on groundwater storage is a priority for future research.

Peak streamflow is 20% higher, occurs 10 days earlier and returns to base flow conditions sooner than the historical average for the medium precipitation scenario under moderate (RCP4.5) emissions (Figure 27). Projected total annual streamflow is 162,930 acre-ft, 5% higher than the historical mean. Under the high precipitation scenario and moderate emissions, snowmelt induced flow begins 20 days earlier and total annual streamflow is 316,080 acre-ft, 5% higher than the historic maximum. Under low precipitation, total annual flow is roughly equal to the historic minimum (56,057 acre-ft).

In the high emission scenario, the validity of our model is more uncertain because projected temperatures are outside the range of historical observations. For these scenarios, a space-for-time substitution is used which assumes that the Weber River above Oakley partitions precipitation similar to the warmer South Fork of Ogden River, where projected temperatures are within the historical range. We use the statistical streamflow model and CDFs from the South fork of the Ogden River to estimate the amount and timing of streamflow for the Weber River above Oakley. This substitution captures the future likelihood of higher evaporative losses and earlier timing of melt.

Snowmelt-induced streamflow, peak flow and a return to baseflow occurs 2 to 3-weeks earlier for the medium precipitation scenario under high emissions compared to historical means (Figure 28). Peak flow decreases by 32% in this scenario and total annual streamflow is 130,900 acre-ft, 16% lower than the historical mean. The

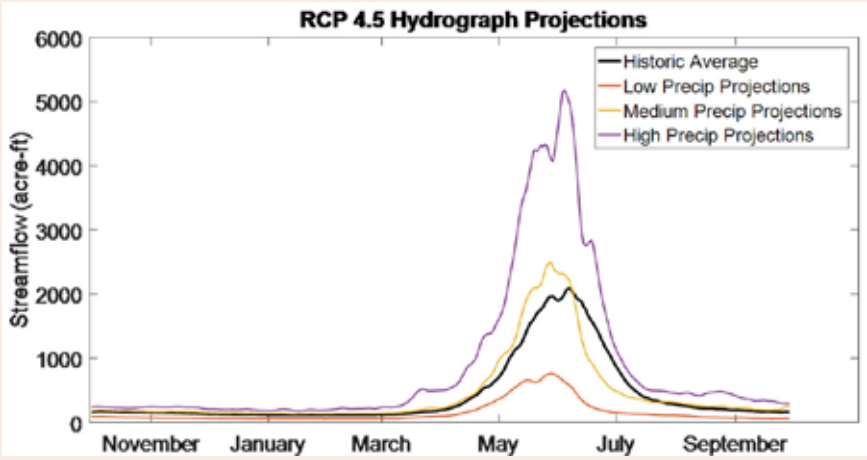

Figure 27. Monthly hydrographs for low, medium, and high precipitation scenarios under moderate emissions for a mid-century (2050s) time period for the Weber River at Oakley. Total annual streamflow is calculated using the MLR model for streamflow while the shape of the hydrograph is determined using the typical Cumulative Discharge Function for each scenario.

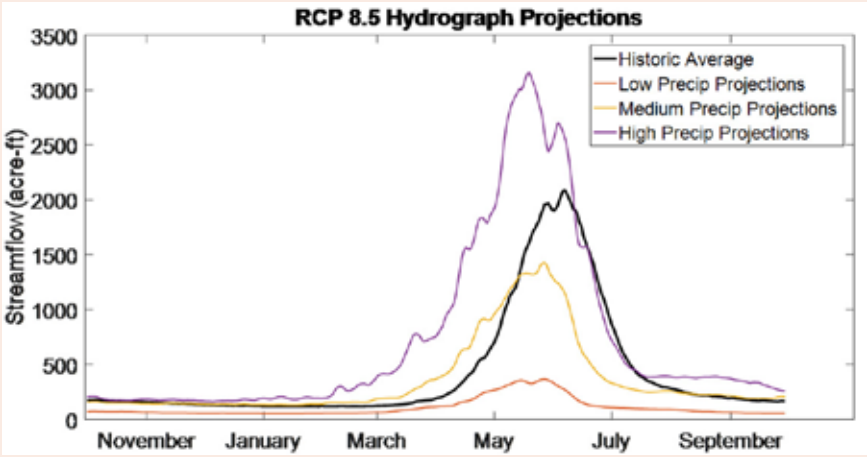

Figure 28. Monthly hydrographs for low, medium, and high precipitation scenarios under high emissions for a mid-century (2050s) time period for the Weber River at Oakley. Total annual streamflow is calculated using a space for time substitution using the MLR models from South Fork of the Ogden River where historical temperatures are similar to the 4.4°F temperature increase used in the high emissions (RCP8.5) scenario.

high precipitation scenario (under high emissions) highlights the possibility of severe early-season flooding, with continuous snowmelt-induced flow starting as early as February. In the low precipitation scenario there is severe drought, with total streamflow 30% lower than the lowest year on record. Total flow in the low precipitation high emission scenario would be just 39,300 acre-feet, compared to the historical mean of 156,000 acre-feet.

iii. Potential future work

Knowledge gaps and sources of uncertainty:

- Because antecedent groundwater storage is the strongest predictor for the fraction of annual precipitation that becomes streamflow there is a critical need to determine the factors controlling recharge.
- Preliminary analyses from regional catchments suggest that variability in groundwater storage represents a multi-year climate signal that may attenuate or exacerbate the effects of an individual dry year.
- Because melt rate is an important factor controlling the fraction of the snowpack partitioned to groundwater and streamflow, there is a need to determine how winter and spring climate will interact to control melt rate.

Because antecedent baseflow is the strongest predictor for the fraction of annual precipitation that becomes streamflow there is a critical need to determine the factors controlling subsurface storage. Preliminary analyses from regional catchments, including Weber River Basin, suggest that baseflow/ storage exhibits a regular periodicity over roughly five-year cycle, but the underlying causes of periodicity, and how it may change in the future, are unknown. Hydrochemistry and tracers also suggest that a large fraction of streamflow is surprisingly old water, and that even during or after precipitation events, stored water is “flushed” out of the subsurface (Kirchner 2003; Godsey et al. 2009; Brooks et al. 2015). The contribution of multiple year-old water

to streamflow is in direct contrast with most hydrologic models that assume water balance closure each water year. Potential evapotranspiration (PET) is projected to increase in the Weber basin (section 5), and PET limits the amount of precipitation that is available for streamflow and baseflow (Gnann et al. 2019). The importance of baseflow in explaining streamflow variability, as well as the potential for changes to baseflow under future climate highlight the need for further research into what factors control baseflow in the Weber River basin.

The importance of snowmelt timing and rate on modeling streamflow suggest an overarching importance of spring climate on hydrologic response. Temperature is just one of several factors important to melting a snowpack, and it has a relatively small energy contribution compared to solar radiation (DeWalle and Rango 2008). Warm temperatures in early spring may be enough to initiate earlier melt (Clow 2010), but due to the relatively low solar angles, melt occurs more slowly than it would later in the spring (Trujillo and Molotch 2014). Earlier, slower melt may result in higher evapotranspiration and lower water yield (Barnhart et al. 2016). During a cool or wet spring, melt occurs later but at a faster rate due to the higher solar angle and greater radiant energy input. In most locations this results in a larger fraction of the water in snowpack is partitioned to streamflow and groundwater. Future research should examine what climatic conditions in spring and winter control melt dynamics in the Weber River basin, and to what extent these conditions will be altered by climate change.

B. Variable Infiltration Capacity (VIC) model projections

Key Findings

- A VIC hydrologic model calibrated for the Weber River at Oakley was used with downscaled climate projections to predict future streamflow for 2055 and 2085.
- Four climate scenarios were selected based on a climate model's temperature or precipitation projection relative to the mean of all climate models: warm/dry, hot/dry, warm/wet and hot/wet.
- In the moderate emissions scenario (RCP4.5), annual Weber River streamflow decreased by 7% in 2055 for a hot/dry scenario. Weber River streamflow increased by 2055 for the other scenarios with the greatest increase observed for a warm/wet scenario (11.2%). *Low confidence*.
- In the high emissions scenario (RCP8.5), annual Weber River streamflow is projected to increase for all scenarios by 2055 with an increase of nearly 13% for a warm/wet scenario. *Low confidence*.
- Monthly projections of Weber River streamflow show that streamflow in winter and early spring increase while late summer and fall streamflow (baseflow) decrease. In one scenario, peak streamflow occurred nearly two months earlier and the peak's magnitude was greatly reduced. *High confidence*.

The second technique used to project future Weber River streamflow is based on a calibrated Variable Infiltration Capacity (VIC) model coupled with downscaled projections of climate developed using the Bias Correction Spatial Disaggregation (BCSD) method (BOR 2013). A VIC model is a hydrological model that uses climate parameters such as temperature, precipitation, soil moisture, relative humidity, etc., as the physical basis for modeling streamflow. Once a VIC model is calibrated to the historical climate and streamflow for a river basin, it can be used as a tool to project future streamflow. For this analysis, projections of temperature and precipitation from the BCSD downscaled climate dataset were used as inputs in the VIC model calibrated for the Weber River at Oakley. The VIC model projections of Weber River streamflow were part of a report developed for the Utah Division of Water Resources (UDWRe) that provided VIC model projections of streamflow for eight river basins in Utah (Wood and Bardsley 2015).

The UDWRe report uses data from 24 downscaled global climate models (GCMs) to project future Weber River streamflow. For this analysis four future scenarios were chosen to represent four plausible future climate states. Prior to selecting downscaled GCMs for each future climate scenario, the eight GCMs (of the 24) that most accurately recreated historical climate in the Pacific Northwest and Intermountain West regions were selected

(Rupp et al. 2013). Of the eight models selected for projecting future Weber River streamflow, one model was selected for each climate scenario. The four climate scenarios selected represent plausible future climates that are described by their relative changes in temperature and precipitation. The four climate scenarios are: warm/dry, hot/dry, warm/wet and hot/wet. A fifth climate scenario is the mean projected streamflow of the eight GCMS selected for use in this analysis. In the description of each climate scenario, "w›arm" means a temperature increase lower than the mean projection, "hot" means a temperature increase higher than the projected mean, "dry" means a precipitation outcome lower than the projected mean and "wet" means a precipitation outcome higher than the projected mean. Table 2 lists the eight climate models selected and the model used for each scenario.

Table 2. List of the GCMs selected to project Weber River streamflow and the model used for each climate scenario.

SELECTED MODELS	CLIMATE SCENARIOS	MODEL
Bcc-csm1-1-m	Warm/dry	Had-GEM-ES-365
CCSM4	Hot/dry	CCSM4
CNMR-CM5	Warm/wet	Had-GEM-CC-365
Had-GEM-CC-365	Hot/wet	IPSL-CM5A-MR
Had-GEM-ES-365		
IPSL-CM5A-MR		
MIROC5		
NorESM1		

Using the mean or median result from a group of climate models, along with a measure of the variability around the mean median, provides a single projection that incorporates information from a large group of models and typically adds robustness to a projection of climate. The use of individual models to project climate variables can be a useful technique if there is evidence to suggest a particular model simulates regional climate better than others or if a specific climate model represents a particular climate scenario of interest (i.e., hot and dry).

VIC model projections of future Weber River streamflow are presented in two forms. One, annual streamflow as a percentage change relative to the historical modeled streamflow (1981 – 2010) for 2055 and 2085 under a moderate and high emissions scenario. Two, monthly streamflow projections for 2055 under a moderate and high emissions scenario. For a moderate emission scenario, Weber River annual streamflow is projected to increase in 2055 and 2085 for all scenarios except the hot/dry scenario where projected streamflow decreases by 4 – 8% (Table 3). In 2055, the greatest projected increase in streamflow occurred for the warm/wet scenario and in 2085, the greatest increase in annual streamflow occurred for the hot/wet scenario. For RCP8.5, Weber River annual streamflow increased in all scenarios (Table 4). Projected annual streamflow increased over 10% by 2055 for the warm/wet and hot/wet scenarios. In 2085, annual Weber streamflow is projected to increase by 13% for the hot/wet scenario and 26% for the warm/wet scenario.

Table 3. Percentage change in annual Weber River streamflow at Oakley compared to historical modeled streamflow for a moderate emission scenario (RCP4.5). A calibrated VIC model was used for water volume projections.

	MEAN	WARM/DRY	HOT/DRY	WARM/WET	HOT/WET
2055	5.9%	2.1%	-7.1%	11.2%	8.0%
2085	8.1%	6.4%	-4.4%	15.1%	18.0%

Table 4. Percentage change in annual Weber River streamflow at Oakley compared to historical modeled streamflow for a high emissions scenario (RCP8.5). A calibrated VIC model was used for water volume projections.

	MEAN	WARM/DRY	HOT/DRY	WARM/WET	HOT/WET
2055	7.7%	1.4%	0.1%	12.8%	10.9%
2085	13.5%	1.6%	8.2%	26.2%	13.6%

The timing of peak Weber River streamflow is projected change in the future. Historically, streamflow peaks in June and May streamflow is similar in magnitude; streamflow is relatively low in winter, spring, and fall. Figure 29 shows projections of monthly streamflow and historical streamflow for RCP8.5 in 2055. Projected monthly streamflow for mean, warm/dry, warm/wet and warm/dry scenarios peaks in May. The annual pattern of streamflow in these scenarios is similar to historical modeled streamflow, but the hydrograph is shifted one month earlier so that projected streamflow is relatively higher in winter and spring and lower in late summer and fall (i.e. lower baseflows). The hydrograph for the hot/wet scenario is very different than the historical hydrograph; streamflow is more evenly distributed throughout the year, and the peak is much lower and shifted one month earlier. Late fall and winter streamflow is significantly higher than the historical streamflow while late summer and fall streamflow is lower. The projected changes in the hydrograph for the hot/wet scenario likely reflect a shift in winter precipitation from snow to rain; snow is likely still falling at high elevations in the headwaters of the Weber River, with more rain will fall at mid-elevations.

By the end of the century, the hydrographs for all future scenarios are projected to shift so that peak monthly streamflow occurs one month earlier than historical streamflow. Projected peak monthly streamflow occurs in May for all scenarios (Figure 30). Unlike projections for 2055, in 2085, the seasonal pattern of streamflow is very similar for all scenarios. In the historical record, there is a prolonged, two-month peak in streamflow. Peak monthly streamflow projections for all scenarios is higher than historical streamflow, but that peak occurs more rapidly (i.e. faster snowmelt). Also like projections for 2055, projections of streamflow for all scenarios

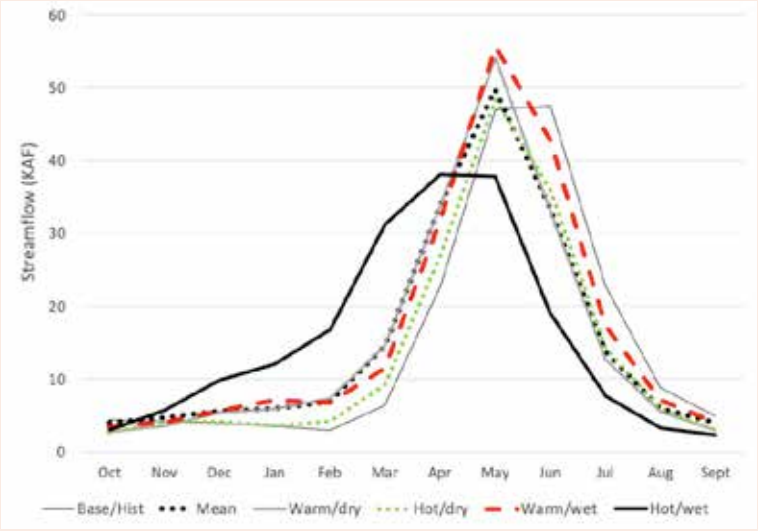

Figure 29. Projected changes in monthly streamflow (in thousands of acre-feet) for 2055 under a high emissions scenario (RCP8.5) using a calibrated VIC model. The *Mean* scenario is the mean of four models used in the other scenarios. The *Base/Hist* scenario is the historical (1980-2010) average water volume from the calibrated VIC model.

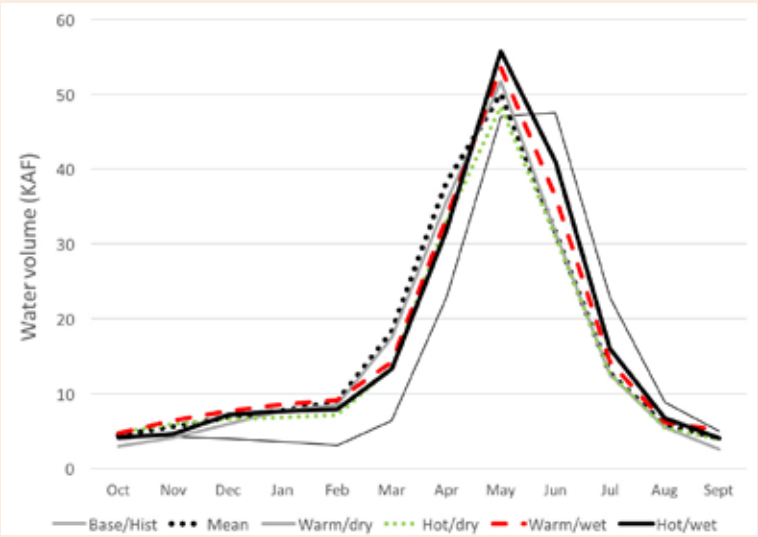

Figure 30. Projected changes in monthly streamflow (in thousands of acre-feet) for 2085 under a high emissions scenario (RCP8.5) using a calibrated VIC model. The *Mean* scenario is the mean of four models used in the other scenarios. The *Base/Hist* scenario is the historical (1980-2010) average water volume from the calibrated VIC model.

in 2085 have higher streamflow in winter and spring with lower relative streamflow in late summer and fall (i.e. lower baseflow). Projected increases in winter streamflow likely reflect an increase proportion of winter precipitation that is falling as rain. High peak monthly streamflow in May suggests that a significant snowpack still forms in the headwaters of the Weber River basin. Earlier projected peak monthly streamflow likely reflects an increase in spring temperatures which, in part, drives earlier snowmelt. All the changes in the hydrograph described here are consistent with downscaled climate projections presented in Section 3B-C.

C. Temperature and precipitation sensitivity analysis

Key Findings

- An operational streamflow model used by the Colorado Basin River Forecast Center was used as a tool to project Weber River streamflow.
- Projections of streamflow using this technique were much lower than projections from the VIC model. Most scenarios project a decrease in future Weber River streamflow and variability between climate scenarios was greater.
- Projections for 2055 show the greatest decrease in streamflow for the hot/dry scenario (-20.2%) and the greatest increase in streamflow for the hot/wet scenario (+29%). *Low confidence*.
- In 2055, peak monthly streamflow is projected to occur one month earlier for all climate scenarios compared to the historical streamflow record. *High confidence*.

A temperature and precipitation sensitivity analysis was used to develop projections of Weber River streamflow. The analysis has two components. One, downscaled climate projections of temperature and precipitation. Two, a streamflow model used by the NOAA Colorado Basin River Forecast Center (CBRFC) to forecast Weber River streamflow one day to three months into the future. To use the CBRFC model to project streamflow, historical temperature and precipitation data (1980 – 2010) was altered to simulate five future climate scenarios and used as an input to the CBRFC model. The output from the streamflow model was projections of future Weber River streamflow for 2055 and 2085. By altering the historical climate data, we are testing how sensitive streamflow is to changes in temperature and precipitation. For example, how would streamflow respond if temperature is 4°F warmer, or precipitation increases by 10% compared to historical climate. The following analysis was also included in the Weber Basin Drought Contingency Plan and a more detailed explanation of the method is available Appendix 3-C of the Plan (WBWCD 2018b).

As with streamflow projections obtained through the VIC model in Section 4b, downscaled projections of climate were developed using the Bias Correction Spatial Disaggregation (BCSD) method (BOR 2013). The five climate scenarios were chosen from 234 monthly runs of different global climate models under different emission scenarios to represent distinct future climates. The five scenarios were warm/wet, warm/dry, hot/wet, hot/dry and median of all model results. These climate scenarios are defined in section 4b. Table 5 shows the change in temperature and precipitation used for each scenario. The CBRFC streamflow model for the Weber River basin is comprised of the Sacramento Soil Moisture Accounting Model coupled with the Snow-17 temperature index snow model and is driven by the most recent 30-year historical period of climate, 1980 – 2010 in this case (Bardsley et al. 2013). The historical streamflow record for the Weber River comes from a headwater stream gauge in Oakley, UT. This method was also used to project streamflow for the seven creeks east of Salt Lake City managed by Salt Lake Department of Public Utilities (Bardsley et al. 2013).

Table 5. Five scenarios of temperature and precipitation change for 2050 compared to 1981-2010. Temperature is in Fahrenheit, precipitation is in percentage change.

SCENARIO	TEMPERATURE	PRECIPITATION
Central tendency	4.1°	+4%
Warm/wet	2.3°	+12.7%
Warm/dry	2.2°	-5.9%
Hot/wet	5.6°	+10.%
Hot/dry	5.8°	-6.2%

Results from the temperature and precipitation sensitivity analysis of Weber River streamflow were much more variable than projections of streamflow from the VIC model (Section 4b). Annual streamflow projections for 2055 were greater than historical streamflow for the hot/wet (+12%) and warm/wet (+29%) scenarios. Streamflow projections for the central tendency, warm/dry and hot/dry scenarios were all less than historical streamflow. Table 6 shows 2050 and 2085 projections of annual Weber River water volume at Oakley for all five climate scenarios. While projections for 2085 streamflow may not be relevant for WBWCD planning, we provide these data for a comparison with 2055 projections. The historical annual streamflow for the Weber River at Oakley is 153,000 acre-feet. Amongst all projections, annual streamflow varied from 96,000 acre-feet to 197,000 acre-feet. The warm/wet scenario produced 25-30% increases in total water volume, while the hot/dry scenario produced 20-35% reductions to total water volume. Projections for annual water volume in 2085 were overall drier compared to 2050 projections and the central tendency of all 2085 model results predicts a 9% decline in water volume.

Table 6. Percentage change in annual Weber River water volume at Oakley relative to the historical average under five climate scenarios.

	CENTRAL TENDENCY	WARM/DRY	HOT/DRY	WARM/WET	HOT/WET
2055	-3.7%	-16.7%	-20.2%	29.2%	12.4%
2085	-9.0%	-11.9%	-36.9%	24.5%	-1.0%

Historically, annual Weber River streamflow peaked in June with slightly lower streamflow in May. Monthly peak streamflow in all future scenarios occurred in May. Monthly peak streamflow in the warm/wet scenario and the hot/wet scenario were greater than historical streamflow (Figure 31). The mean (central tendency) streamflow scenario had a similar peak to the historical peak, but occurred one month earlier. The warm/wet scenario is striking because streamflow is greater than the historical record in all months March – August. In the warm/wet scenario, May and June flows are 10,000 to 20,000 acre-feet higher than historical flows. The hot/dry scenario is striking for the opposite reason; projections of March – August flow are always lower than historical flows. Streamflow in all scenarios except the warm dry scenario is higher in late winter and spring compared to historical streamflow, likely reflecting warmer late winter/early spring temperatures and an earlier onset of snowmelt. Late summer/early fall streamflow is lower than historical streamflow for all scenarios except the warm/wet scenario, reflecting decreased baseflows under future climate.

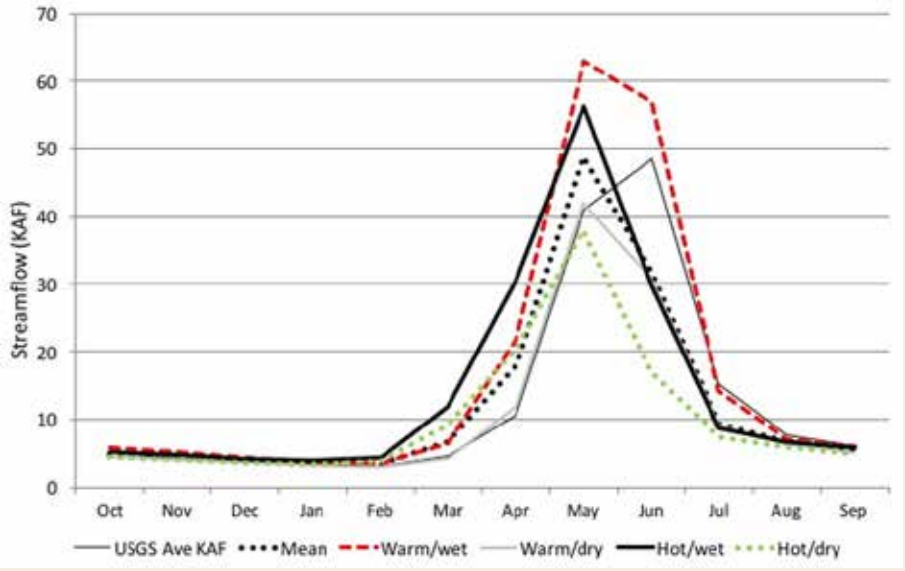

Figure 31. Average observed monthly streamflow from 1980 – 2010 (USGS KAF Ave) and projections of 2050 Weber River monthly streamflow for four climate scenarios. Streamflow observations and projections were from a headwater gage on the Weber River in Oakley, UT.

5. SPECIFIC IMPACTS OF CLIMATE CHANGE

A. CHANGES IN POTENTIAL EVAPOTRANSPIRATION AND WATER USE

i. Introduction

Future changes in climate are expected to have two primary impacts on water supply. One, changes in temperature, precipitation and precipitation type will impact the amount and timing of WBWCD's annual water supply. Two, warming temperatures are associated with an increase in outdoor water demand. Changes in climate variables, such as temperature, humidity, wind speed and solar radiation may increase potential evapotranspiration (PET), or the atmosphere's "thirst" for water. Higher PET will increase the amount of water required to maintain current outdoor landscapes and higher PET is typically associated with higher outdoor water demand.

Potential evapotranspiration (PET) is defined as the amount of water lost to the atmosphere from an environment through evaporation and plant transpiration given an unlimited supply of water. Temperature is perhaps the most important climate parameter influencing PET, but relative humidity, wind speed and solar radiation are also factored into the calculation. All four variables, not just temperature, play important roles in determining the magnitude of PET.

Global climate models agree that temperatures will increase steadily in northern Utah throughout the 21st century (USGCRP 2017), but there is less certainty in changes to wind speed, solar radiation and relative humidity. In general, wind speeds in the western United States are expected to slow by 2100, which would tend to decrease PET (Kulkarni and Huang 2014). Solar radiation is most affected by the amount of cloudiness. Globally, higher temperatures are associated with increased evaporation from oceans and increased cloudiness, but cloudiness in Utah is determined by regional climate factors. For example, one important factor in determining cloudiness during Utah's summer is the North American monsoon. The Weber River basin is typically on the northwestern edge of the North American monsoon. While precipitation from the monsoon does not always reach the area, increased cloud cover from monsoonal weather patterns can increase relative humidity and decrease solar radiation, which lowers PET.

The following section presents results of an analysis of the impact of future changes in climate on potential evapotranspiration and outdoor water use. The primary goal of this analysis is to develop a linear regression model using observations of PET and outdoor water use. The PET/water use model will be used to create projections of outdoor water use for two neighborhoods in the Ogden area of Weber Basin's service area.

ii. Potential Evapotranspiration

Key Findings

- Potential evapotranspiration (PET) is a measure of the atmosphere's "thirst" from water through evaporation of water from soils and transpiration of water from plants.
- Projections of future PET were developed using a downscaled climate dataset.
- In 2050, PET is projected to increase by 5% given a moderate emissions scenario (RCP4.5) and by 8% under a high emissions scenario. *Medium to high confidence*.

Photo: Northern Wasatch Front, east of Ogden, Utah. Credit: im me/Creative Commons.

Long-term historical records of PET do not exist because few meteorological stations in Utah measure all the necessary climate variables to calculate PET. The record of PET in northern Utah extends back to 2001 at one site at the University of Utah. In the Ogden area, there is a weather station near Riverdale Road (41.175°N, 112.009°W) that measures all climate variables necessary to calculate PET since 2013. Since 2013, growing season PET (April – October) has varied from 31 to 36 inches. Since there is a relatively strong warming trend in northern Utah over the last 20-30 years, it is possible that PET has increased, however, there is no long-term climate record to assess historical trends in PET.

Despite a lack of long-term observations of PET, global climate models provide models of historical climate (1950-2005) and models of projected climate (2006-2099). As discussed in previous sections, global climate models are not the appropriate tool for projecting climate in locations such as Utah where complex mountainous terrain strongly influence climate. Instead, downscaled data from global climate models are used here. To project changes in PET, the MACA (Multivariate Adaptive Constructed Analogs) downscaled global climate model data set, which is based on a subset of 17 global climate models from the CMIP5 archive, is used (Abatzoglou and Brown 2012). MACA is a statistically downscaled climate dataset which has a spatial resolution of 1/24th of a degree or 2.5 miles. All future projections of PET are for a 2.5 mile x 2.5 mile grid cell in Ogden, UT (center point of grid cell is at 41.1878°N, 112.0224°W). Three separate datasets from the MACA downscaled climate datasets are used: historical, RCP4.5 (moderate emissions) and RCP8.5 (high emissions). The historical dataset is *modeled* historical climate data from 1950-2005. Historical *modeled* data may differ slightly from *observed* historical climate data. The modeled historical data is used as a comparison to future projections of climate.

Two different approaches are used for presenting projections of future PET. One, the median result of PET from ten downscaled global climate models is presented in Figure 32. Two, specific downscaled global climate models are used to illustrate specific future climate scenarios. Two future PET scenarios were chosen to represent a warm/wet climate future with modest increases in PET and a hot/dry climate future with large increases in PET. The warm/wet scenario uses data from the CNMR-CM5 model and the hot/dry scenario uses data from the IPSL-CM5A-MR model. Models selected in this analysis performed well in reproducing regional climate in the Pacific Northwest and the northwestern Great Basin and they represent very different but plausible future climate scenarios (Rupp et al. 2013).

Historical and projected PET in Ogden, UT under moderate (RCP4.5) and high emissions (RCP8.5) scenarios is presented in Figure 32. Each point in the figure is the median annual PET from ten climate models and averaged over 30 years. For both moderate and high emissions scenarios, annual PET is projected to increase throughout the 21st century. Projected increases in annual PET by 2035 are similar for the two emissions scenarios. By

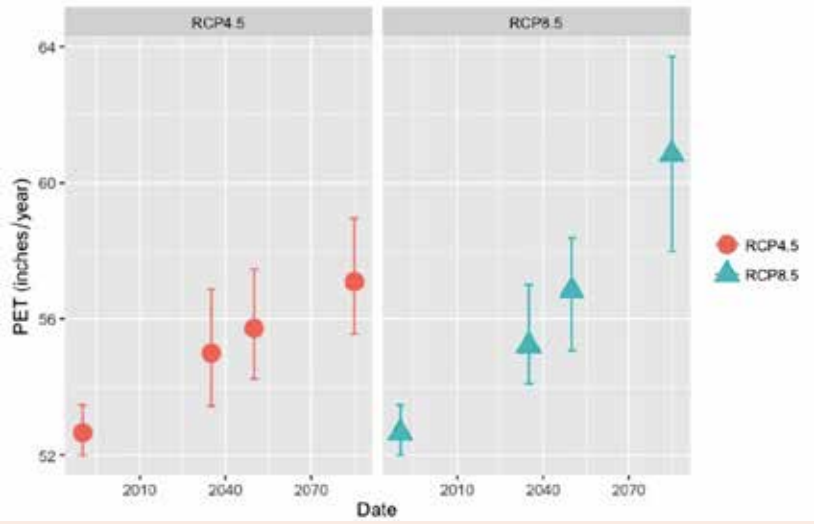

Figure 32. Modeled historical (1990) and projected annual potential evapotranspiration (PET) for Ogden, UT for RCP 4.5 (moderate emissions) and RCP8.5 (high emissions) scenarios. Data obtained from ten downscaled global climate models. The filled symbols represent the median result of 30-year means of daily PET centered around 1990, 2035, 2060 and 2085. Error bars represent the 10th and 90th percentile of model results.

2050 and 2085, annual PET increases significantly more in the high emissions scenario compared to the moderate emissions scenario. Table 7 shows percentage increase in annual PET in 2035, 2050 and 2085 compared to the modeled historic period. By 2050, the median model projections of annual PET indicate an increase of 5% to 8%. By 2085, RCP4.5 projections of PET begin to level off, while RCP8.5 projections of PET continue to increase, with a median projected 16% increase by 2085.

Table 7. Percentage increase in annual PET for moderate (RCP4.5) and high (RCP8.5) emission scenarios. Represents median of ten models.

YEAR	RCP4.5	RCP8.5
2035	+4.8%	+5.3%
2050	+5.3%	+8.3%
2085	+8.5%	+16.0%

iii. Water use projections

Key Findings

- Using water use data from the Ogden area and observations of PET, a model was created to relate PET to water use. PET explained 60% of the variability in water use.
- The PET/water use model was used as a tool to project future water use for four neighborhoods in the Ogden area.
- A low and high PET scenario was used to project water use. The CNMR model was used for a low PET scenario and the IPSL model was used for a high PET scenario.
- By 2050, water use in four Ogden-area neighborhoods is projected to increase by 6% for a low PET scenario and by 10% for a high PET scenario. *Medium confidence*.
- Increases in outdoor water use due to climate change should be considered in long-term water planning.

Intuitively, projections of higher temperatures and higher PET suggest that outdoor water use will also increase in the coming decades. If PET is higher, more water will be needed to maintain current outdoor landscapes in the Weber River basin. It is useful to know that PET is projected to increase by 5 - 8% by 2050, but that information alone will not help plan for how much more water will be needed to maintain current landscapes. To begin to answer the question of how much *more* water will be needed with increased PET, a linear regression model relating weekly PET to weekly water use was developed.

Several assumptions were required to develop a PET/water use model and to use it as a tool to project future water use. There are also limitations to the analysis due to its simplicity and availability of data. First, projections of future water use are based on a limited number of individual water users (208) and projections are not scaled up to basin-wide water use. Future projections of water use assume that landscapes and patterns of water use will remain constant in the future. Landscapes and patterns of water use will likely change in the future. A major limitation of the PET/water use model is that there is a limited amount of PET and water use data available (7 years). Seasonal (April - September) PET and water use data was available only from 2013-2018; a longer record would likely produce a more robust relationship between PET and water use. Because of the seasonal nature of both PET and water use there are statistical problems with autocorrelation between the two variables that cast some doubt on the validity of the model. Despite the assumptions and limitations of this approach, projections of future water use with a simple PET/water use model provide an estimate of outdoor water use as climate changes.

The PET/water use model was constructed using linear regression to relate weekly cumulative PET to weekly cumulative outdoor water use from 2013 - 2018. The robustness of the PET/water use model is limited by the relatively short records of daily water use and observed PET. Daily water use data was obtained from 208 metered water users in the Ogden, South Ogden, South Weber, and Washington Terrace neighborhoods provided by WBWCD. Water use data was available from mid-April through October. Observations of PET were obtained from a site maintained by Utah DOT on Riverdale Road in Ogden. The linear regression model was constructed using April-September PET because PET affects only outdoor water use; it was assumed that outdoor water use was limited or did not occur during October-March.

Two individual models representing two different future climate scenarios were chosen to project water use. The CNMR-CM5 and IPSL-CM5A-MR models were chosen because these two models performed well compared to other models at recreating historical climate in the Pacific Northwest and Great Basin (Rupp et al. 2013). These two models also represent very different, but plausible, representations of future climate and PET in northern Utah. CNMR-CM5 projects moderate increases in temperatures and increased precipitation, a "warm/wet" scenario. IPSL-CM5A-MR projects larger increases to temperature and little or no increase in precipitation, a "hot/dry" scenario. The two models, as expected, project different levels of PET by 2050. The median RCP8.5 projection of seasonal PET for 2050 using the CNMR model is 35 inches/year, compared to 36.5 inches/year for the IPSL model. The two models provide a plausible high and low projection of PET for Ogden, and will serve as the high and low estimates of water use.

Modeled historical PET in all global climate models systematically overestimated observed PET. Figure 33 shows modeled historical and observed seasonal (April – September) PET. Historical PET is the median of ten models. Because the PET/water use model was constructed using observed PET, but water use projections used future *modeled* PET, modeled PET data must be adjusted or scaled in order to be used as an input in the PET/water use model. To account for the overestimation of observed PET by climate models, projections of PET were scaled to observed PET by comparing mean weekly *modeled* PET from 2013-2018 (RCP4.5) to mean weekly observed PET from 2013-2018. A scaling factor of 0.8500 was used for CNMR-CM5 PET projections and a scaling factor of 0.8779 was used for IPSL-CM5A-MR PET projections. If a scaling factor were not used, estimates of 2050 water use would be unrealistically high.

Figure 34 presents the results from a linear regression model using April-September PET as the independent variable and April-September water use as the dependent variable ($r^2 = 0.6044$, p-value < 0.001, degrees of freedom = 129, $y = 5.4403x - 2.0943$). Each data point in the graph represents PET and water use for a given week. Data in the linear regression are from April 25 – October 2 during 2013 – 2018; data from 2014 are only available from June 14 – October 1. Several statistical issues exist with the model. Both variables, PET and water use, are autocorrelated;

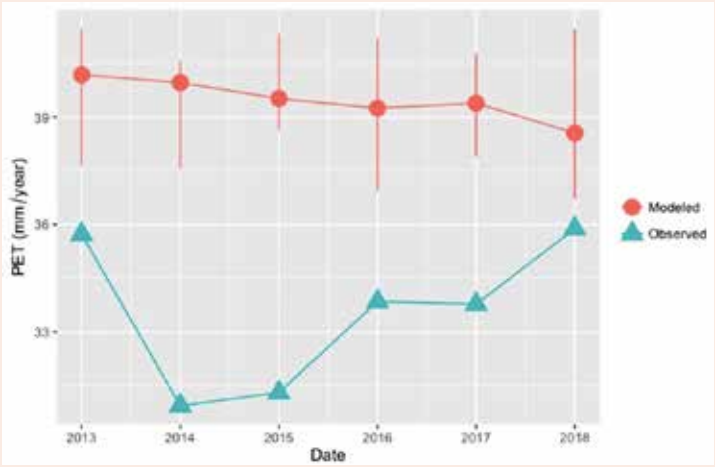

Figure 33. Modeled and observed potential evapotranspiration (PET) from the Riverdale Road in Ogden from 2013 - 2018. Modeled PET is from the MACA downscaled global climate model dataset. Error bars for modeled PET represent the 10th and 90th percentile of ten models.

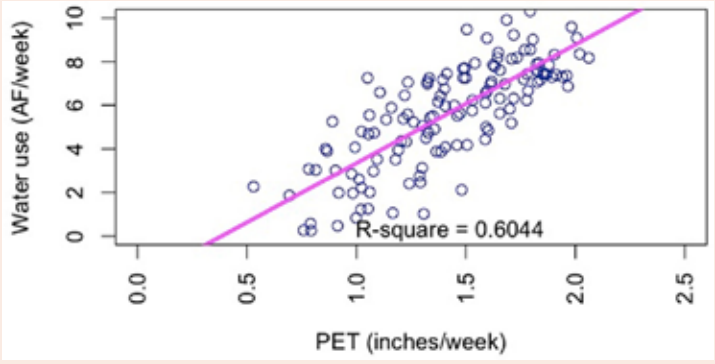

Figure 34. Linear regression model between observed weekly potential evapotranspiration (PET) and observed weekly water use (in acre-feet). PET data was from Riverdale Road in Ogden and daily water use data was from four neighborhoods in Ogden during April to September 2013-2018.

Table 8. Middle- and end-of century projected changes in water use for four neighborhoods in Ogden. Observed water use was the average of April 18 – October 2 water use in 2013 and 2015-2018. Two climate models were used to project future potential evapotranspiration (PET): CNMR-CM5 (CNMR) and IPSL-CM5A-MR (IPSL) for moderate emissions scenario (RCP4.5) and a high emissions scenario (RCP8.5).

MODEL	2050 WATER USE (ACRE-FEET)	% CHANGE	2085 WATER USE (ACRE-FEET)	% CHANGE
Observed Mean	129.7	---	129.7	---
CNMR (RCP4.5)	132.0	+1.8%	135.5	+4.5%
CNMR (RCP8.5)	137.9	+6.3%	143.4	+10.6%
IPSL (RCP4.5)	139.8	+7.8%	141.7	+9.2%
IPSL (RCP8.5)	142.9	+10.1%	156.5	+20.7%

autocorrelation means that the variable is correlated to itself at different time lags. PET and outdoor water use are autocorrelated because both variables generally increase in value to a peak during summer and decrease into fall. Autocorrelation does not necessarily invalidate a linear model, but it means the correlation between water use and PET is confounded by correlations of the variable with itself. The residuals of the linear regression model are not normally distributed, failing the Shapiro-Wilk normality test (W=0.99356 p-value = 0.818). Mathematical transformations of the PET and water use data did not significantly improve the distribution of data or variable autocorrelation. Despite the statistical shortcomings of the PET/water use model, it provides the best available projection of future water use for the Weber River basin based on the availability of data.

Projections of future outdoor water use are calculated by inputting projections of mean weekly PET from the warm/wet scenario (CNMR) or hot/dry scenario (IPSL) into the PET/water use linear regression model. Mean weekly PET for 2050 was calculated by averaging weekly PET from April 25 – October 2 from 2035 – 2064. Mean weekly PET for 2085 used data from 2070 – 2099. Thirty-year averages of weekly PET projections were used to ensure that changes in climate, not annual weather, were considered in PET projections. Table 8 presents water use projections for 2050 and 2085 using the two climate models and two emissions scenarios. The warm/wet climate scenario (CNMR) results in slight to moderate increases in projected water use (+2 to 6%) by 2050. However, the hot/dry scenario (IPSL) results in projected water use increases of 8 to 10% by 2050. Increases in water use are calculated by comparing water use projections in 2050 or 2085 to mean observed water use from 2013 – 2018. As expected, projections of water use in 2085 are significantly higher than projections for 2050. Water use increased by 4 to 10% by 2085 under a warm/wet climate scenario (CNMR), while the hot/dry scenario (IPSL) projected a 9 to 20% increase in end-of-century water use. Different climate models provide realistic predictions of future climate, but it is uncertain which climate model is most likely to accurately project future conditions. If a warm/wet climate scenario (CNMR) proves true and global emissions are significantly reduced in the next 10-15 years, then changes in PET will increase water use only slightly by 2050. If a hot/dry climate scenario proves correct, then moderate to significant increases in water use may occur in the 21st century. While there is no certainty in the level of future emissions, current national and international policies and trends in emissions suggest that the high emission scenario (RCP8.5) is a more likely future outcome than the moderate emission scenario (RCP4.5).

Figure 35 shows the seasonal pattern of observed outdoor water use and projected outdoor water use. Observed weekly outdoor water use is the mean of weekly water use from 2013 – 2018. The most interesting observation from a more detailed look a water use projections is that 2050 water use is much higher in the first half of the outdoor watering season. Projected water use in late April and May is approximately double compared to 2013-2018 water use. June 2050 water use is also projected to be higher than observed water use. Somewhat surprisingly, 2050 projections of July – September water use are very similar to observed water use. The pattern of high projections of water use in spring and early summer and relatively lower water use in late

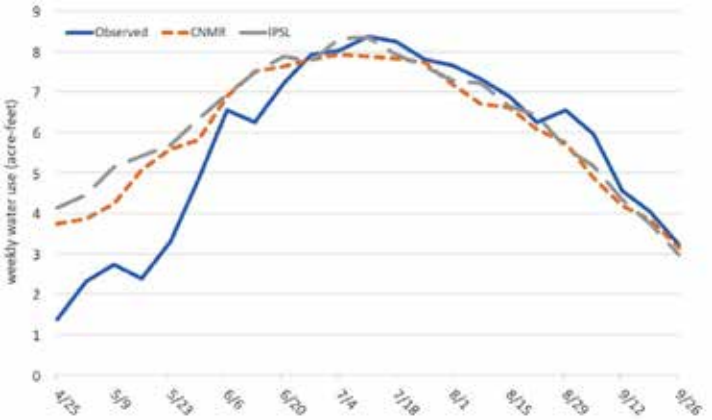

Figure 35. Observed and projected mean weekly water use for metered users from four neighborhoods (Ogden, South Ogden, South Weber and Washington Terrace). Observed weekly water use is from 2013 – 2018. Projections of weekly water use are for 2050 using a high emission scenario (RCP8.5).

summer in early fall is partly explained by downscaled projections of temperature and precipitation presented earlier in the report. The greatest projected monthly temperature increases for 2050 (2.5 - 4°F) occur in March – May (Figure 15) and coincide with decreased precipitation in March – June (Figure 19). Projected water use in August and September is slightly lower than observed water use. This result is also supported by climate projections. August and September 2050 temperature increases are slightly lower (~2°F, Figure 15) and September monthly precipitation is projected to increase by about 0.5 inches (Figure 21).

Further research and more data are needed to improve the PET/water use model in order to more accurately project future water use. The greatest limitations to this approach are the limited availability of both PET and water use data. The strength of correlation in between PET and water use in the model would likely improve if there were more years of data and if water use data for the entire month of April and March existed. Ideally, projections of water use could be used to estimate water demand for the entire Weber Basin service area in 2050. However, daily water use data, with a record of at least five years, is available from only a small number of customers. WBWCD is currently installing water meters throughout its service area; several years from now, there may be enough years of water use data in other locations to develop water use projections that cover a larger geographic area. A final data limitation if the lack of PET data; few sites measure all the variables necessary to calculate PET.

B. CHANGES IN SNOWPACK

Key Findings

- By mid-century, annual snowfall is projected to decrease by a third along the Wasatch Front and 10-15% in the lower areas of the Wasatch Back. *Medium confidence*.
- Elevations above 7500 feet in the Wasatch and Uinta Mountains are projected to see a 10% increase in snowfall by the end of the century. *Medium confidence*.
- Future winters may resemble 2016-2017, when warm storms brought a deep snowpack to the high mountains, but the lower elevations were bare for much of the winter due to warmer temperatures and low elevation rain.
- Locations at higher elevations that see the most snow will have the most dramatic shift toward an earlier timing in peak snowpack, while mid-elevation locations will see smaller changes. *High confidence*.

Projections of precipitation using LOCA statistically downscaled and WRF dynamically downscaled show modest increases annually with the greatest increases occurring in early winter and summer. Increases in temperature and changes to precipitation will affect the timing and magnitude of snow accumulation in the Wasatch and Uinta Mountains. By mid-century, annual snow water equivalent, which is the depth that snow would have if melted to liquid water, will decrease by a third along the Wasatch Front and 10-15% below 7,500 feet the Wasatch Back. In contrast to lower elevations, high elevations of the Wasatch and Uinta Mountains are projected to see a 10% increase in snow water equivalent (Figure 36). The switch from a reduction in snowfall at low elevation to an

increase in snowfall at high elevation occurs at around 7500 feet in the Wasatch Back. By the end of the century, snowfall along the Wasatch Front and Morgan Valley will be less than half of modern levels, and the only area with an increased snow water equivalent will be the Uinta Mountains. Separating it out by month, the largest increases in the near term will be in January and February along all of the higher terrain (Figure 37). However, this is balanced in the Ogden River basin by losses of up to an inch of snow water equivalent falling in November, December, and March. By the end of the century, December is expected to see more snowfall in the higher elevations with up to a 1.8-inch increase in the western Uinta Mountains (Figure 38). The Wasatch Mountains north of Grandview Peak will see decreases in snow water equivalent in every month (except December at Ben Lomond). Changes in monthly mean snow water equivalent at specific sites are presented for a mid-century (Figure 39) and end-of-century decade (Figure 40). Values for specific locations are tabulated in Appendix 2.

Two processes affect the spatial pattern of snowfall in a warming world. One, warmer air carries more water vapor before condensing into clouds and precipitation. Therefore, in a warmer climate, there is more moisture in the atmosphere on average to condense into precipitation. Two, a warmer world means higher snow levels. The increase in precipitable water is felt at the low levels as heavy winter rainstorms. Together, we can expect a future winter to be more like the winter of 2016-2017, where warm storms brought a deep snowpack to the high mountains, but the lower elevations were bare for much of the winter.

Another aspect of the snow storage that will change with warming is when the snowpack begins to decline. We calculated when the snowpack reaches its peak at several locations in the Weber River watershed (Figure 41).

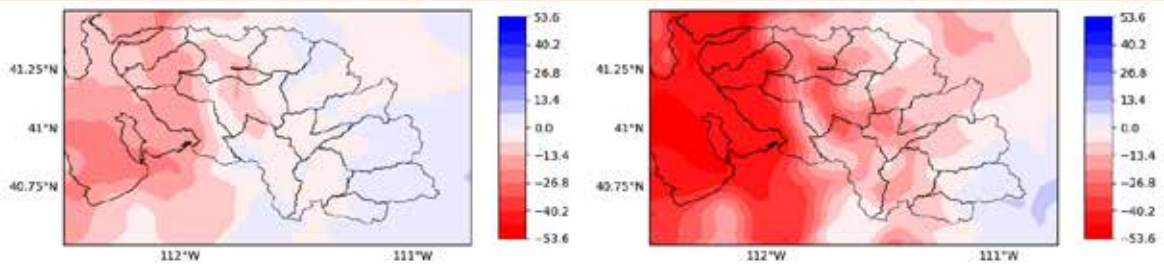

Figure 36. Based on dynamical downscaling, change in annual mean snow water equivalent (percent change) for a mid-century decade (2035-2044; left panel) and end-of-century decade (2085-2094; right panel) relative to the historical period, 1985-2010. The Great Salt Lake and sub-basins of the Weber River are outlined in black.

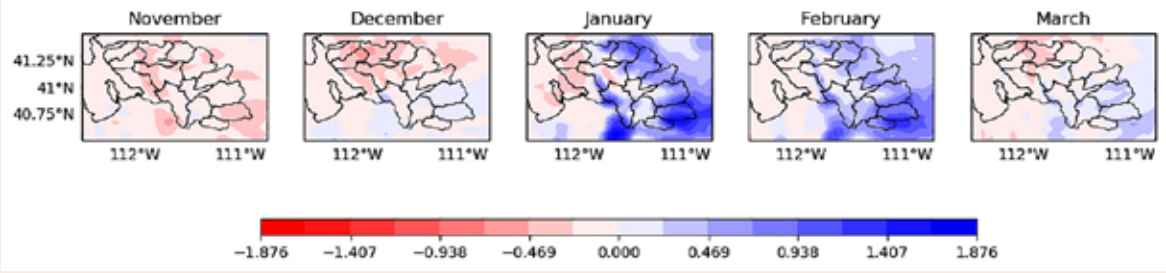

Figure 37. Based on dynamical downscaling, change in monthly mean snow water equivalent (inches) for a mid-century decade (2035-2044) relative to the historical period 1985-2010. The Great Salt Lake and sub-basins of the Weber River are outlined in black.

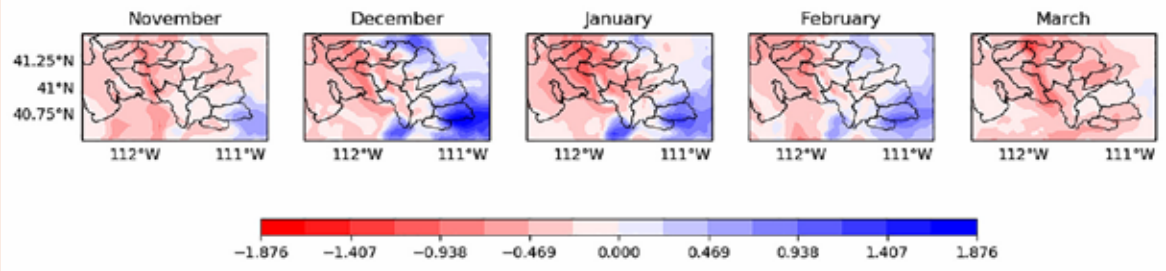

Figure 38. Same as Figure 37, but for an end-of-century decade (2085-2094).

Locations at higher elevations that see the most snow will have the most dramatic change in when melt begins. Places above Park City and in the Uinta Mountains may see runoff begin three weeks earlier in the springtime, while mid-elevation locations will see little change. Importantly, these results indicate that the timing of peak snow depth will become more vertically stacked, that is higher elevation locations will start to melt out at the same time as the mid-elevations. During the historical period, mid elevations typically began melt several weeks to a month earlier than high elevations.

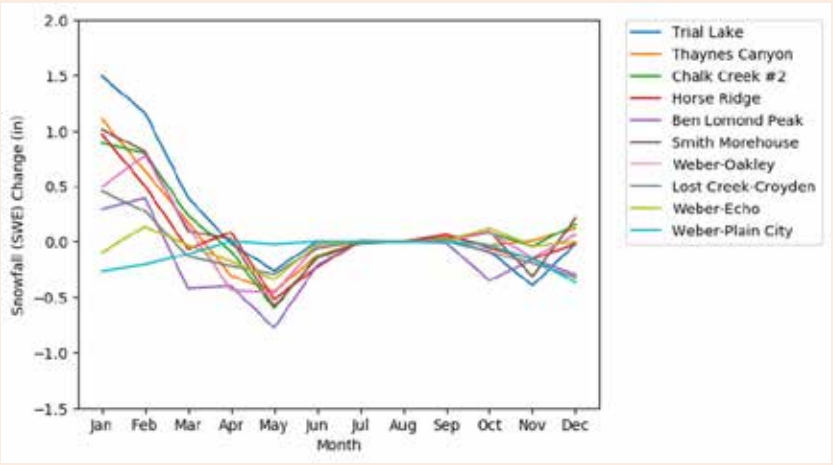

Figure 39. Based on dynamical downscaling, change in monthly mean snow water equivalent (inches) for a mid-century decade (2035-2044) relative to the historical period 1985-2010 at key locations in Weber River watershed.

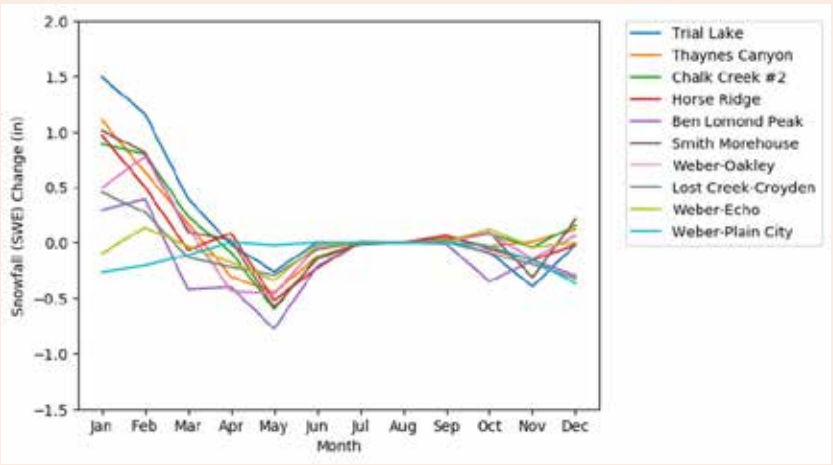

Figure 40. Same as Figure 3, but for an end-of-century decade (2085-2094).

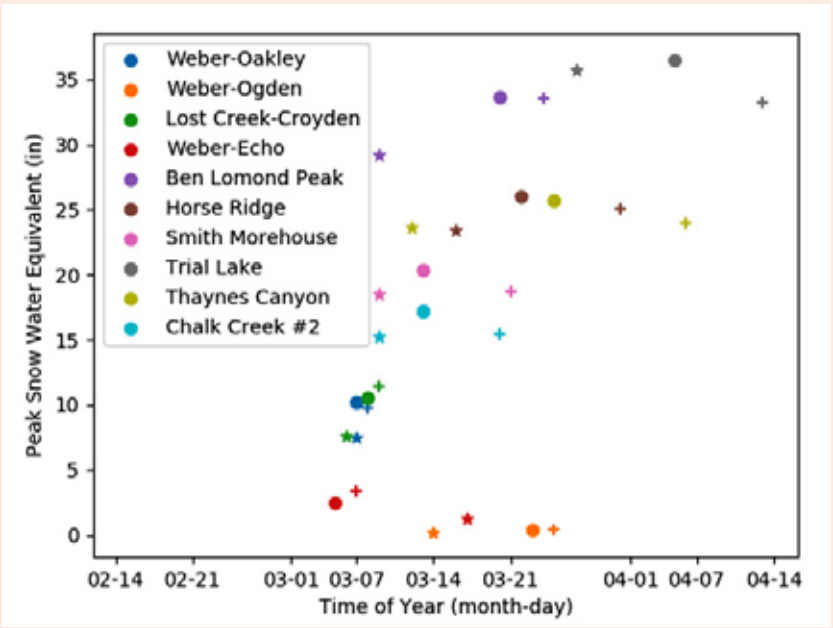

Figure 41. Time of year and value of maximum snow water equivalent (SWE) averaged over 10-year periods (1995-2005 for historical, 2035-2045 for mid-century, 2085-2095 for end-of-century) based on dynamical downscaling with the WRF model. Colors indicate individual locations specified in legend. Shape of marker indicates which time period is represented.

C. CHANGES IN EXTREME PRECIPITATION

Key Findings

- Extreme precipitation, by definition, occurs rarely but can have dramatic impacts.
- On the Wasatch Front, little change in extreme precipitation is projected for the next several decades. *Medium confidence*.
- By the end of the century, extreme once-per-decade storms will be 10% stronger than in the historical period. *Medium confidence*.

Extreme precipitation refers to very large values which occur rarely, but can have dramatic impacts. Extreme precipitation events can, for example, lead to mudslides or overwhelm systems built to capture storm water. We investigated changes in extreme precipitation in the dynamical downscaled WRF data using a technique called generalized extreme value (GEV) analysis. GEV analysis is a statistical framework for calculating how likely extreme events are, and the largest event we might expect to see in a given period of time. We calculated return intervals for 24-hour precipitation totals in various regions of the Weber River watershed. Table 9 shows how the intensity of a 10-year storm (a storm which has a 10% chance of occurring in a given year) changes with warming. Another way to think of a 10-year storm is we would wait 10 years on average to see a storm that large. Values are in inches. On the Wasatch Front, there is little change in the next several decades, but by the end of the century a 10-year storm will be 10% stronger than in the historical period.

Table 9. Historical and projected precipitation amounts over 24 hours for a 10-year rainfall event.

	WASATCH FRONT	WASATCH BACK	UINTAS
Historical	2.24	2.7	2.11
Mid-Century	2.24	2.98	2.28
End-of-Century	2.53	3.16	2.43

Table 10. Monthly projections of the change in evaporation from Willard Bay under the RCP6.0 scenario for mid- and end-of-century. Negative values represent a decrease in projected evaporation. Values are the change in acre-feet per month for each month of the year, and then acre-feet per year for the Total row.

MONTH	MID-CENTURY	END-OF-CENTURY
January	28	60
February	51	166
March	96	495
April	160	649
May	255	820
June	248	759
July	139	621
August	178	161
September	198	-112
October	118	-190
November	86	-92
December	8	23
Total	**1565**	**3368**

D. CHANGES IN EVAPORATION OF WILLARD BAY

Key Findings

- Evaporation increases in all months for mid-century and all months except September through November in the late century projections. *High confidence*.
- The strongest increases in evaporation occur during the warm months. *High confidence*.
- The mid-century increase in evaporation amounts to a loss of 1565 acre feet per year, and the late-century increase amounts to a loss of 3368 acre feet per year. *Medium confidence*.

A matter of concern for WBWCD is the change in evaporation rates off of Willard Bay. We use data from the WRF simulations (RCP 6.0) to get an estimate of how reservoir evaporation will change in the future. We note that WRF treats Willard Bay as a part of the Great Salt Lake, meaning it is hypersaline and therefore has reduced evaporation relative to fresh water. The calculations presented here increase WRF's evaporation by a correction factor of 1.3 to account for this. These results (Table 10) are thus highly preliminary and additional modeling with appropriate evaporation parameters and historical validation data is needed.

6. BOTTOM-UP SYSTEM VULNERABILITY ANALYSIS

A. INTRODUCTION

Future climate conditions are uncertain and may be described as point estimates with narrow ranges, as probabilities, or as a few scenarios of possibilities (Wang et al., 2020) . This vulnerability assessment looks at how uncertain future climate and additional factors – streamflow, demands, reservoir sedimentation, and reservoir evaporation – affect water availability, reservoir storage, and shortages to users in the Weber Basin of northern Utah. We use a bottom-up, multi-dimensional sensitivity approach (Brown et al., 2012; Brown et al., 2019) to identify the conditions and combinations of conditions where the Weber River Basin water system succeeds and fails.

It is increasingly difficult to model and plan for a large number of uncertain future conditions, such as the many possibilities for future stream flows, demands, reservoir sedimentation, and reservoir evaporation. Conventional top-down approaches define and propagate a few representative concentration pathways of future global carbon emissions through global circulation models. These models generate future temperature and precipitation outputs over the coming decades at coarse spatial scale. Top-down approaches then downscale the temperature and precipitation outputs to the scale of watersheds and stream gages. Next, top-down approaches use the downscaled future stream flows to run a water system model to identify the effects of future carbon emissions on system users. This cascade of modeling effort is computationally intensive and only allows examination of a limited number of emissions or climate scenarios.

In contrast, a bottom-up approach looks at the key factors that might affect the water system's future performance. In the Weber River Basin, these factors include future stream flow, demands, reservoir sedimentation, and reservoir evaporation rates. The bottom-up approach develops scenarios of possible future conditions for each factor. The bottom-up approach then tests how the water system will perform under individual and combinations of scenarios. In general, a bottom-up approach looks at a wider set of climate and additional factors. The bottom-up approach can be more flexible in developing the inputs that define a scenario of a possible future condition. A scenario can draw data from prior climate or demand studies. Where studies or models do not exist, a scenario can alternatively draw on a storyline managers or experts would like to explore.

The bottom-up approach, like many other scenario-based methods, focuses on simulating plans across many plausible states of the world rather than assigning likelihoods to future conditions (Alexander, 2018). A bottom-up approach also looks beyond best- or worst-case scenarios (Ben-Haim, 2019). The bottom-up approach looks at a wider picture of possible future conditions and helps managers better understand what conditions cause the water system to succeed and to fail. This knowledge can provide insight to the future conditions managers should pay attention to. And this knowledge can help managers adapt water system policies over time as they learn more about future climate and other conditions (Haasnoot et al., 2019).

The WBWCD is particularly interested in a bottom-up vulnerability study because WBWCD is vulnerable to reduced reservoir storage and shortages to users, in part because they are the junior water rights holder in the basin. The bottom-up approach works in the following steps:

Photo: Willard Bay, Utah. Credit: Jami/Adobe Stock.

1. Identify the inflow, demand, reservoir sedimentation, and reservoir evaporation factors that may impact system vulnerability.
2. Develop scenarios of potential future conditions for each factor.
3. Run a RiverWare model for the Weber River Basin for each scenario and scenario combinations.
4. Identify criteria that describe satisfactory system performance within the RiverWare results.
5. Determine which scenarios perform satisfactorily and unsatisfactorily. Visualize vulnerabilities.
6. Discuss results with managers and solicit feedback.

In this study, four uncertain climate and additional factors that can only be described with scenarios were considered based on available data. These factors were thought to affect district storage and shortages, and interests of the WBWCD:

1. Changes to future inflow. Inflows included past flows observed in the paleo record going back to 1400 AD, the instrumented record, and flows modeled in response to future temperature and precipitation changes,
2. Changes to future water demand due to uncertainties in increasing population, per-capita demand shifts, increased net landscape evapotranspiration, and shifting agriculture to urban land use,
3. Reduced reservoir storage due to sedimentation, and
4. Increased evaporation from Willard Bay Reservoir, the largest reservoir in the Weber Basin Water Conservancy District, due to increasing temperature and other climate factors.

The remaining sections describe the Weber River Basin study area, bottom-up vulnerability method applied to the Weber Basin water system, results, and conditions where the Weber Basin water system succeeds and fails.

B. WEBER BASIN STUDY AREA

The Weber River Basin, located in northern Utah, comprised of eight sub-basins, contains parts of both the Wasatch Mountains and the Uinta Mountains, and supplies water to the Great Salt Lake Valley, Ogden Valley, Morgan Valley and the Snyderville Basin. The Weber Basin water system includes 8 reservoirs, 4 water treatment plants, and several pipelines (WBWCD, 2020). The WBWCD was established in 1950 and provides agricultural and urban water for over 620,000 people in 5 counties. (WBWCD, 2013; WBWCD, 2020) . Most urban users live along the Wasatch Front between North Salt Lake and North Ogden.

C. METHODOLOGY

Key Findings

- Four factors are considered -- future uncertain streamflow, demand, reservoir sedimentation, and reservoir evaporation conditions -- that may affect future Weber River Basin system performance.
- Six scenarios of future streamflow—each 30-years in length at a monthly timestep—were drawn from three periods in the paleo record, two periods in the most recent century of gaged records, and a scenario for 2030 to 2060 streamflow under hot and dry climate (Section 4c). Total basin annual flows for these scenarios varied from approximately 800,000 to 975,000 acre-feet per year.
- Six scenarios of future annual demands ranged from 362,000 to 846,000 acre-feet per year. These scenarios represent select combinations of a larger set of 63 demand scenarios drawn from uncertain future population growth, total per capita water use, agricultural to urban water transfers, and increased landscape evapotranspiration.

- Three scenarios of future reservoir sedimentation -- 0%, 10%, and 30% filling of total storage – were developed from scarce data. These scenarios represent no buildup, gradual filling over time, and more severe filling.
- Three scenarios of future evaporation from Willard Bay reservoir were used: 3.2, 3.7, and 4.0 feet per year. These rates represent the current value used by the Utah Division of Water Resources (UDWRe), historical modeled value and a late 21st century values estimated in section 5d.
- The RiverSmart plug-in and a prior-existing Utah Division of Water Resources RiverWare model for the Weber River Basin was used to simulate 324 combinations of the inflow, demand, reservoir sedimentation, and reservoir evaporation scenarios.

The analysis used six scenarios of future Weber River streamflow at Oakley (the most upstream gage in the basin), six scenarios of future demands, three scenarios of sediment buildup in reservoirs, and three scenarios of evaporation rates for Willard Bay Reservoir. Each scenario represents a possible future condition (Figure 42). Scenarios of future inflow, demand, reservoir sedimentation, and reservoir evaporation were combined into 324 modeling runs. Each run was simulated for 30 years at a monthly timestep in the RiverWare modeling platform. Three reservoir storage and a water shortage criterion were developed to define when the system performed satisfactorily and when the system was vulnerable. Contour and time series plots were used to show the combinations of future inflow, demand, reservoir sedimentation and reservoir evaporation that led to satisfactory and unsatisfactory conditions.

Previous studies have been done to determine Weber River stream flow, dating back to 1408 AD and looking ahead to 2060 (JUB Engineers, 2018; Stagge et al., 2018). This climate vulnerability study uses data from the UDWRe Weber River Basin study, the WBWCD Drought Contingency Plan, the Paleoflow.org database, and earlier streamflow estimates (Section 4). The UDWRe study considered historical flows based on the Weber River at Oakley gage. The Drought Contingency Plan expanded on the UDWRe study and used the historical inflows, paleohydrology and climate forecasts. This study develops inflow scenarios from each of the previous studies and provides a wider view of the effect of hydrology in combination with demands, reservoir sedimentation, and reservoir evaporation on Weber Basin water availability.

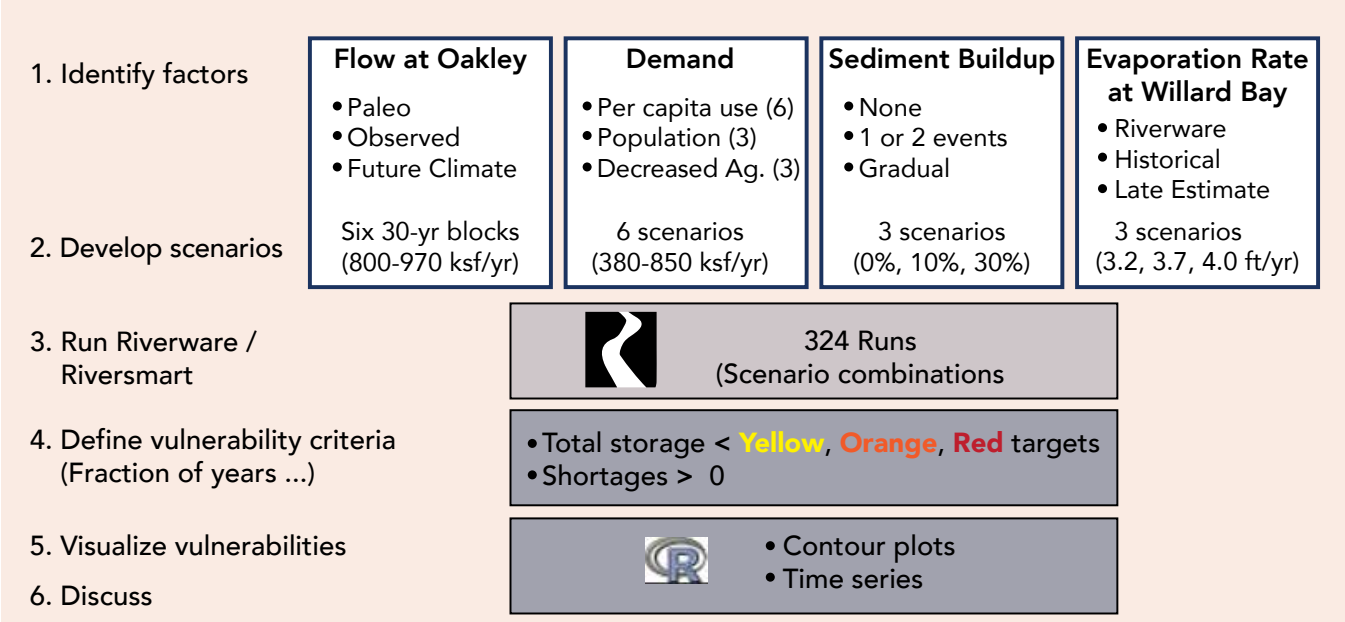

Figure 42. Methodology – Six key steps for vulnerability assessment.

i. Weber River flow at Oakley, Utah

Key Findings

- Six scenarios of future streamflow—each 30-years in length at a monthly timestep—were drawn from three periods in the paleo record, two periods in the most recent century of gaged records, and a scenario for 2030 to 2060 streamflow under hot and dry climate.
- Total basin annual flow for these scenarios varied from approximately 800,000 to 975,000 acre-feet per year.

To select future model inflow scenarios for the Weber River basin, we use three different datasets of streamflow. The three selected datasets are monthly Paleo-flows for the Weber River Basin reconstructed from tree-rings that date back to 1428 (Stagge et al., 2018) (Figure 43), the Western Water Assessment (WWA) climate scenarios for 2030 to 2060 (JUB Engineers, 2018)(Figure 44), historical gage inflow data from 1905 to 2019 (JUB Engineers, 2018), and streamflow projections from this report (Section 4).

The paleoflows on the Weber River at Oakley date back to 1409 AD and were reconstructed at a monthly timestep by using Weber basin (Bekker et al., 2014) and regional tree ring chronologies for multiple tree species and a reconstruction of the El Nino Southern Oscillation (ENSO) climate index (Stagge et al., 2018). A tree ring chronology is a dendroclimatology term that refers to a time-series of spacings between annual tree rings from one or more trees at a site that are de-trended and adjusted for tree age at the time the ring was formed. A statistical relationship is made between the adjusted tree ring width and streamflow. Typically, the regression is made on annual stream flow but Stagge et al. (2018) exploited regional tree chronologies for different species whose growth occurs in different months of the year and the ENSO index to reconstruct at the monthly time step. The R-squared value for the calculated Weber River monthly stream flow is 0.87. This value expresses the fraction of variance in observed reconstructed flows explained by the variance tree-ring widths (Stagge et al., 2018). The paleo-flow timeseries used in this study (Figure 43) can be found at paleoflow.org by setting the **Time Resolution** to *Monthly*, **Flow Gauge** to *Weber River at Oakley*, and selecting the desired **Flow Units**.

The historical gage data for the Weber River at Oakley is from 1905 to 2018 (USGS gage 10128500). Historical data time periods are selected based on their drought data.

Lastly, we used climate change scenarios developed by the WWA for the WBWCD Drought Contingency Plan (JUB Engineers, 2018). WWA developed the scenarios from many different global climate model runs for three emission scenarios. Five climate scenarios were used: Hot-Dry, Warm-Dry, Hot-Wet, Warm-Wet, and Central Tendency (JUB Engineers, 2018) (Figure 44). Each scenario was a 30 year average from 2030 to 2060.

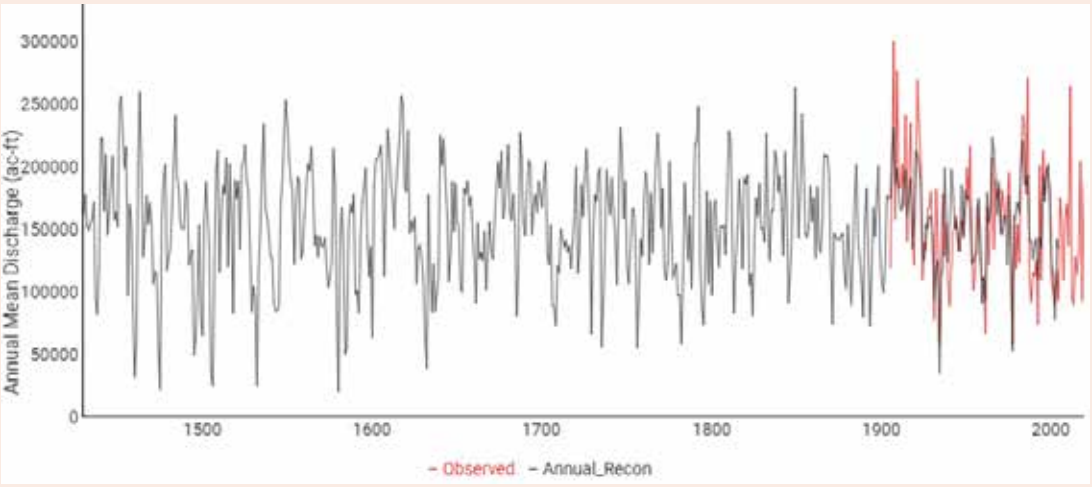

Figure 43. Weber River at Oakley stream flows. Black lines are annual flows reconstructed from tree-rings, and red lines show observed annual flows (Stagge et al., 2018).

For this study we used a forward looking linear average annual flow for 1 to 60 years to help inform the choice of a 30-year scenario length (Figure 45). The forward looking linear average annual flow was calculated by finding the average streamflow for the specified number of years and shifting the averaging period one year forward starting in 1408 AD in the paleo record and finishing in the historal record. The resulting range of period average values is shown by the box plots in Figure 45. Each box and whiskers considers approximately 600 averages.

By looking at the linear average annual results shown in Figure 46, we found that a 30-year averaging window had similar 25%, median, and 75% annual average values as longer averaging periods. At the same time, outlier 30-year periods have larger deviations in average annual flows and suggest more possible streamflow scenarios. The choice of a 30-year scenario length balances computational burden, variability in flow scenarios, and the stream flow data available in the WWA future climate scenarios.

From the paleo flow, historical, and future climate stream flows available, we selected six 30-year periods to represent a range of possible low future streamflow scenarios for the Weber Basin (Figure 46). The scenarios could include long drought duration and/or high drought intensity. Three scenarios come from the paleo record. Two scenarios for 1930 to 1960 and 1940 to 1970 emphasize low flow periods in the historical record. To help

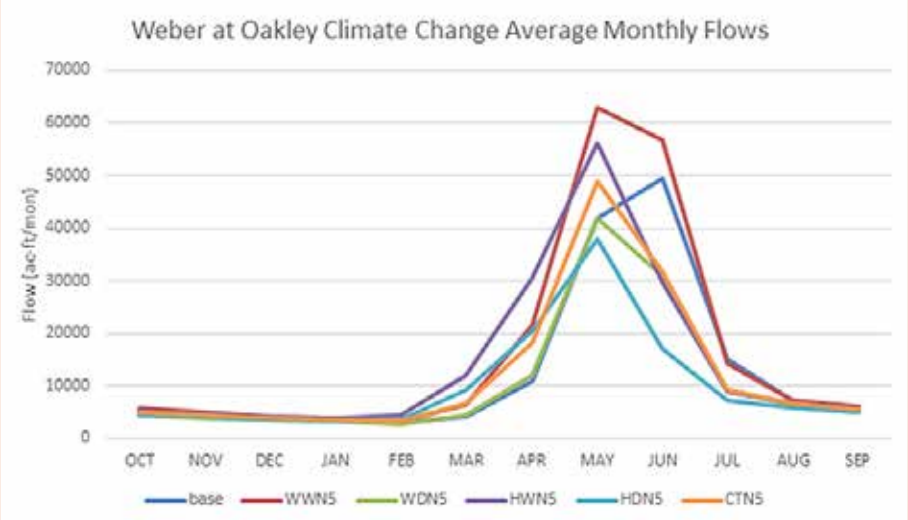

Figure 44. Averaged monthly stream flows for the Weber River at Oakley for a base case and five scenarios of changing temperature and precipitation (JUB Engineers, 2018).

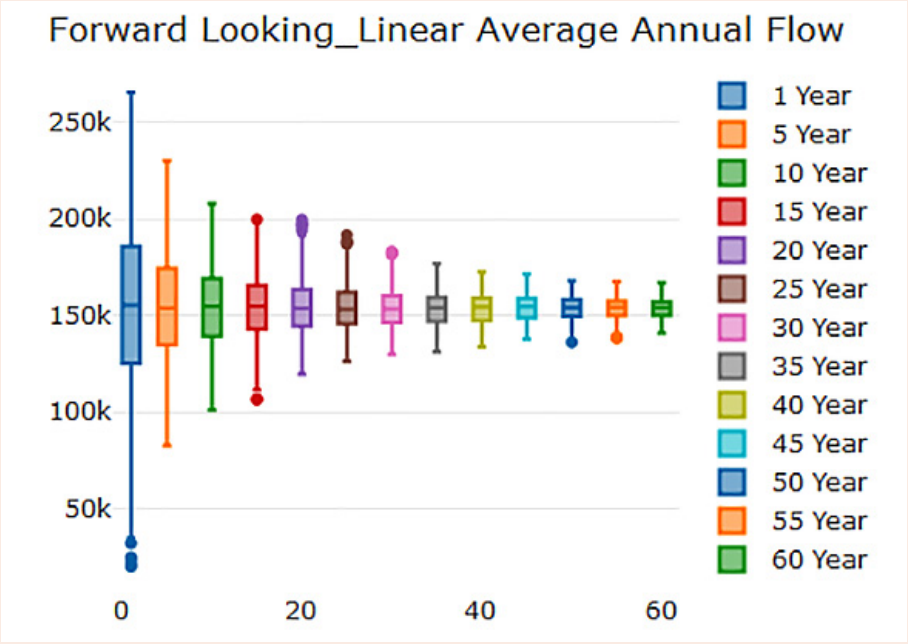

Figure 45. Boxplots of forward looking linear average annual flow across different averaging windows.

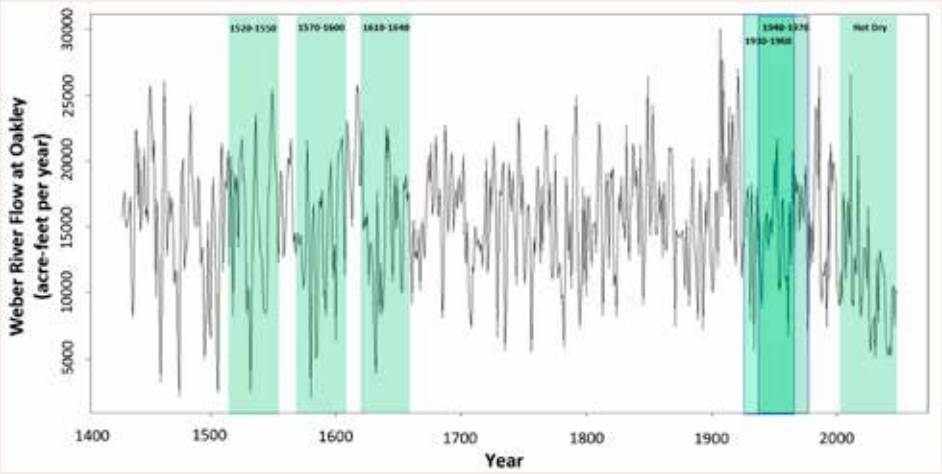

Figure 46. Weber at Oakley streamflow scenarios (green shading) over historical and reconstructed streamflow record.

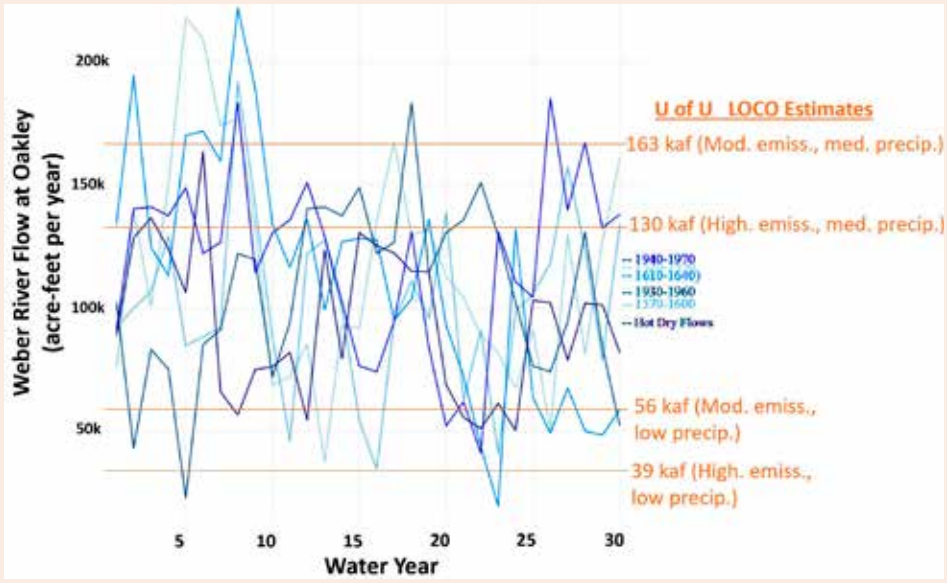

Figure 47. Comparison of the six selected scenarios of Weber River flow at Oakley by water year, and the University of Utah stream flow projections. Mean inflow is shown on the right.

later in comparing the flow scenarios, we refer to the 1940 to 1970 scenario as a base since this scenario also represents the most recent period. We include the Hot-Dry future climate scenario because it is the most severe of the five climate inflow scenarios WWA developed (JUB Engineers, 2018).

Figure 47 shows streamflow for the five scenarios by water year with the 30-year average flow shown on the right y axis. Annual stream flows can vary by factors of 2 above the means or drop to 25% of the mean. The streamflow projections in section 4a fall above and below the means of the selected scenarios and suggest that low precipitation, moderate or high emissions conditions will give stream flows even lower than the low scenarios considered here.

The relations between streamflow at Oakley and every other gage in the Weber River Basin were previously calculated by regressing historical flow at other gages to flow at the Weber River at Oakley gage (JUB Engineers, 2018).

ii. Basin water demand

Key Findings

- Six scenarios of future annual demands ranged from 362,000 to 846,000 acre-feet per year.
- These scenarios represented select combinations of a larger set of 63 demand scenarios drawn from combinations of uncertain future population growth, total per capita water use, agricultural to urban water transfers, and increased landscape evapotranspiration.

Water demand scenarios for this study were calculated by considering four subfactors. The first subfactor is change in population for the years 2015, 2070, and 2150. The second subfactor is the change in per-capita potable and secondary water use for each service area. Secondary water is a Utah-specific term for secondary distribution systems that provide untreated water for outdoor irrigation. The third subfactor is the transfer of agricultural irrigation water to municipal use. And the final subfactor is climate change's effect on landscape evaporation and its effect on secondary water usage. We considered several levels (values) for each demand subfactor which we explain further below.

Population Growth

The University of Utah projections for the state of Utah show that the population will continue to grow at a high rate through 2150 (University of Utah, 2019). Throughout the Weber River basin, population is forecast to increase in all counties. There are particularly large population changes in Morgan and Summit Counties (University of Utah, 2019; WBWCD, 2013) which we use for this study. We use three scenarios corresponding to population projections for 2015, 2070 and 2150 (Table 11).

Table 11. The total population for Weber Basin for the selected population scenario years.

YEAR	POPULATION (PERSONS)
2015	623,960
2070	978,500
2150	1,263,000

Per-Capita Water Use

Per-capita water usage is the amount of water that one person in a household uses for an average day. There are two types of per-capita water use: secondary water use (outdoor use), and potable use (indoor use). The 2015 values for both secondary and potable per-capita water use were taken from the 2015 *Municipal and Industrial Water Use report* by the Utah Division of Water Resources (Table 12) (UDWR, 2018).

Table 12. The 2015 Weber Basin community system water data by county and water use type (Base Case), (UDWR, 2018).

COUNTY	BOX ELDER		DAVIS		MORGAN		SUMMIT		WEBER		BASIN TOTAL	
Population	3,340		336,100		8,500		34,930		241,090		623,960	
Portable Water Use	ac-ft/year	GPCD	ac-ft/year	GPCD	ac-ft/year	GPCD	ac-ft/year	GPCD	ac-ft/year	GPCD	ac-ft/year	GPCD
Residential	527.3	141	28,539.33	76	893.3	94	5,895.7	151	18,642.6	69	54,498.2	78
Commercial	50.2	13	7,232.8	19	73.0	8	3,692.7	94	6,209.7	23	17,258.3	25
Institutional	21.1	6	3,232.5	9	40.5	4	401.4	10	1,976.3	7	5,671.8	8
Industrial	0.0	0	1,111.1	3	50.4	5	8.8	0	3,369.9	12	4,540.2	6
Total Potable++	**598.5**	**160**	**40,115.6**	**107**	**1,057.2**	**111**	**9,998.7**	**256**	**30,198.5**	**112**	**81,968.5**	**117**
Secondary Water Use	ac-ft/year	GPCD	ac-ft/year	GPCD	ac-ft/year	GPCD	ac-ft/year	GPCD	ac-ft/year	GPCD	ac-ft/year	GPCD
Residential	2819	75	40,450.2	107	1,023.6	108	1,277.6	33	34,147.0	126	77,180.2	110
Commercial	0.0	0	242.8	1	7.3	1	0.0	0	1,046.7	4	1,296.9	2
Institutional	45	1	7,777.0	21	211.4	22	2,233.8	57	3,841.4	14	14,068.1	20
Industrial	0.0	0	0.0	0	0.0	0	0.0	0	0.0	0	0.0	0
Total Secondary++	**286.4**	**77**	**48,470.0**	**129**	**1,242.3**	**130**	**3,511.4**	**93**	**39,035.1**	**145**	**92,545.2**	**132**
Potable Reliable Supply	ac-ft/year		ac-ft/year		ac-ft/year		ac-ft/year		ac-ft/year		ac-ft/year	
Springs	309.2		200.4		772.5		3,630.7		4,260.1		9,172.8	
Wells	2,163.0		27,763.9		1,771.0		18,691.9		48,674.2		99,064.1	
Surface	0.0		29,520.8		3,000.0		14,893.9		40,094.2		87,508.9	
Total Reliable	**2,472.2**		**57,485.1**		**5,543.5**		**37,216.5**		**93,028.4**		**195,745.8**	

++ **Total GPCDs are county weighted**

The total potable and total secondary gallon per-capita per day (GPCD) values are used to calculate the base demand using the year 2015 population data for each county (Table 13). We assumed Utah County demand would stay constant at 35 KAF/year because the supplied water to Utah County is a contract amount and because Utah County is not within the Weber Basin.

The Weber River Basin is divided into 20 service areas in the UDWRe RiverWare model (Table 14). Using the GPCD data and population projections for each county within a service area, the average annual demand value was calculated. Table 14 shows the calculated municipal demand for each service area in the Weber Basin.

Table 13. Potable and secondary water use by county with the calculated average annual demand (Base values for 2015 population).

COUNTIES	POPULATION	POTABLE USE (GPCD)	SECONDARY USE (GPCD)	DEMAND (AF/YEAR)
Utah	NA	NA	NA	35,500
Box Elder	3,340	160	77	887
Davis	336,100	107	129	88,849
Morgan	8,500	111	130	2,295
Summit	34,930	256	90	13,538
Weber	241,090	112	145	69,404
2015 Total	**623,960**			**210,473**

Table 14. The calculated annual municipal demand by service area, and county.

WEBER BASIN SERVICE AREAS	SERVICE AREAS BY COUNTY	DEMAND (AF/YEAR)
SA1 Weber Provo Diversion Canal	Utah	35,500
SA2 Oakley to Wanship	Summit	8,701
SA3 Wanship to Echo	Summit	3,002
SA4 Echo to Devils Slide	Morgan	419
SA5 Lost Creek	Morgan	293
SA6 Devils Slide to Stoddard	Morgan	1,010
SA7 Park City	Summit	1,835
SA8 East Canyon	Morgan	503
SA9 Stoddard To Gateway	Morgan	70
SA10 Gateway Canal	Davis	52,306
SA11 Davis Weber Canal	Davis	36,543
SA12 Weber Basin Project Ogden Valley	Weber	7,027
SA13 Ogden Brigham and S Ogden Highline Canals	Weber	8,050
SA14 Ogden River Below Pineview	Weber	6,109
SA15 Slaterville	Weber	19,245
SA16 Warren Canal	Weber	4,982
SA17 Ogden Bay Bird Refuge	Weber	15,863
SA18 GSL Minerals	Weber	3,356
SA19 Gateway to Slaterville	Weber	4,772
SA20 Additional WB Demand	Future	Future

To simulate the change in per-capita water usage, we use a percentage reduction to the per-capita water usage. The first percentage reduction is based on the 2025 water usage goals created for the state of Utah of a 25% reduction from 2015 values (Hansen Allen & Luce and Bowen Collins & Associates, 2019) . To reach the 25% reduction of per-capita water usage, a 10% reduction is implemented to potable water use and a 34% reduction is implemented to secondary water use. In addition to reach the 25% reduction, a 35% reduction of per-capita usage is also considered in this study. This 35% reduction is implemented with a 20% reduction to potable use and a 44% reduction to secondary use. This demand reduction only considers the demand from municipal water not water used for agriculture.

Evapotranspiration Impacts on Secondary Water Use

Projections of potential evapotranspiration (PET) throughout the WBWCD vary from 5-9% under moderate emissions and to 8-16% under high emissions (Section 5a). This study considers evapotranspiration by accounting for it in future municipal and industrial outdoor water use. To model the effect of evapotranspiration, we use the values for projected change in secondary water usage calculated for four Ogden area neighborhoods using a linear regression model (Section 5a). These values are a 6% increase in secondary water usage from a low PET scenario and a 10% increase from a high PET scenario. These values of a 6% and a 10% increase in secondary water use are the values used for the PET scenarios in this study.

Agricultural-to-Urban Water Transfers

Total water usage is made up of two parts in the Weber Basin, municipal (urban usage), and agricultural usage (field irrigation or animal water). Agricultural lands in Utah today are being urbanized and the amount of irrigated agricultural land is decreasing (Li et al., 2019) . The conversion of agricultural land to urban uses is implemented in this study by looking at the Utah Division of Water Rights Conversion Report from October 2018 (Greer, personal communication, 2019). This report provides the conversion of water rights from one type of use to another. Using Equation 1, we calculate a unitless Water Conversion Factor from the volume of Agricultural Irrigation Water (acre-feet) converted to Municipal Water (acre-feet).

$$Water\ Conversion\ Factor = \frac{Municipal\ Water}{Agricultural\ Irrigation\ Water} \quad \textbf{(Equation 1)}$$

Considering the 721 change applications for the Weber Basin, water conversion factors vary from 12.8% to 100% with bottom quartile and mean values of 63% and 71%. A conversion factor of 63% means 1 acre-foot of agricultural water usage translates into 0.63 acre-feet of municipal water usage. These values only consider the conversion of agricultural irrigation water to municipal use and do not account for the many other types of water usage such as industrial or agricultural stock water. Therefore, this data may not fully reflect agriculture to urban transfers occurring in the Weber basin; but are the best available data to represent agricultural conversions.

We use scenarios of 0% (base case), 63%, and 71% conversions. The analysis method used assumes that all increased municipal water use comes from retired agricultural land. First, we calculated the change in municipal water use from 2015 to 2070 and 2150. Second, we calculated the change to agricultural irrigation water (from 2015 to 2070 and from 2015 to 2150) by dividing the change in municipal water by the agricultural conversion factor (0%, 63%, and 71%). Third, we calculate the 2070 and 2150 amount of agricultural usage by subtracting the 2015 agricultural usage by the 2070 and 2150 change in agricultural usage. Lastly, we add the future agricultural usage for 2070 and 2150 to the municipal usage. The agriculture to municipal water usage was done on a service area basis. The change from agriculture water usage to municipal water usage is a rough estimate and does not consider more detailed processes of land use change or growth.

Selecting Demand Scenarios

We combined the three population growth scenarios, six per capita use values, three scenarios of potential evapotranspiration, and three scenarios of agricultural to urban conversions into 63 demand scenarios. These

combinations of demand subfactors suggest a range of future annual basin-wide demands from 360 KAF to 850 KAF per year (Figure 48, each connected set of blue line segments represents an annual demand scenario; the line segments cross the grey vertical axes at the value for the demand factor; light to dark blue lines indicate increasing total annual demand and are also indicated on the right-most vertical annual demand axis). This range contrasts with the current demand of 550 KAF per year (Figure 7, red line).

Out of the 63 different demand combinations, we selected 6 demand scenarios as the lower and upper bounds for each population projection year (Figure 48, large, red circles). These selected demands also span the range of all demand combinations (Figure 49, small, light blue circles).

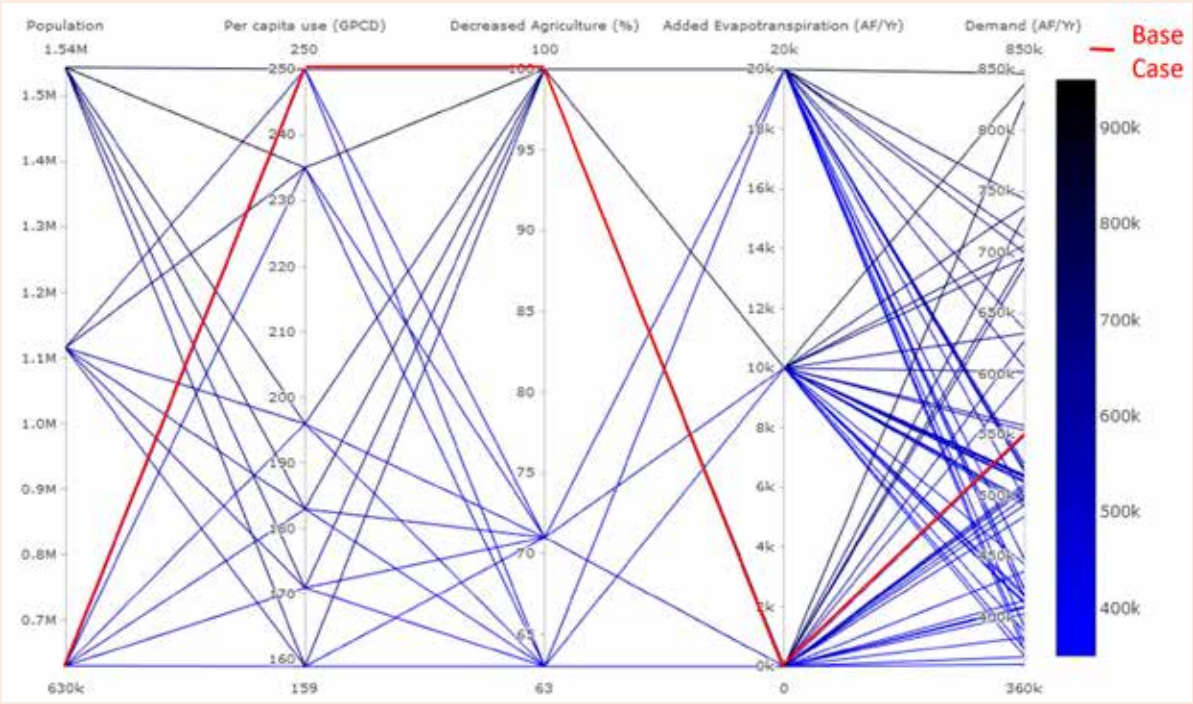

Figure 48. Parallel plot of demand subfactors shows the effects each subfactor has on the overall demand. Total annual demand scenarios are shown on the right axis. Light blue to dark blue line color also shows the increase in total demand (color bar legend). The 2015 base case for demand is shown as a red line.

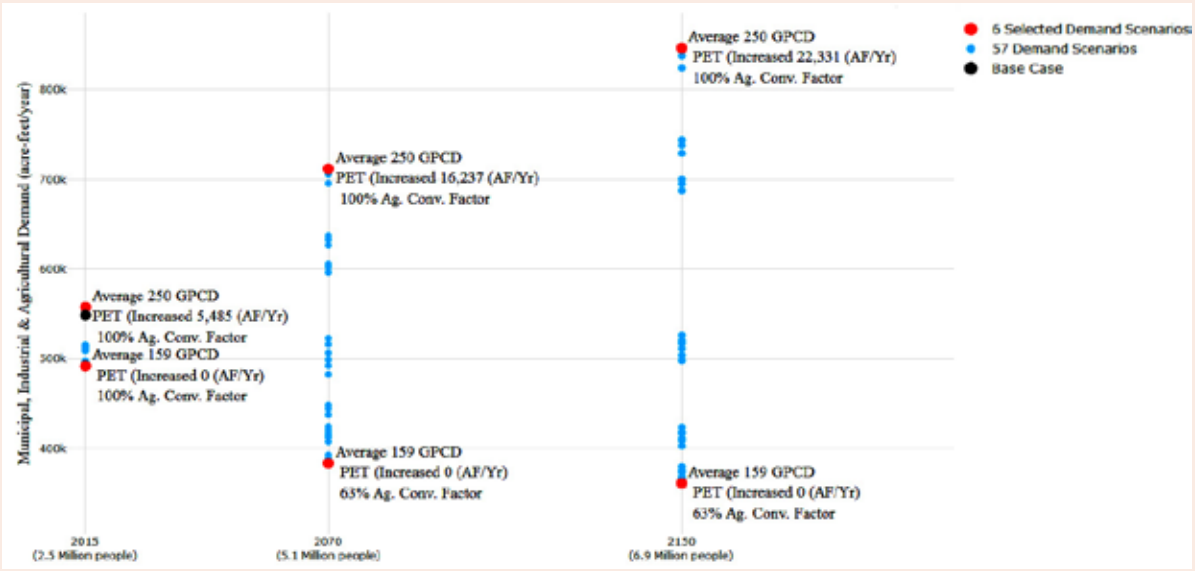

Figure 49. Total annual averaged demands by forecast year show all 63 demand scenarios (small light blue circles), 6 selected demand scenarios (larger red circles), and base case annual demand (black circle).

iii. Reservoir sediment buildup

Key Findings

- Data for future reservoir sedimentation was scarce.
- We constructed three scenarios of 0%, 10%, and 30% filling of total storage that represent the current assumption of no buildup, gradual filling over time, and more severe filling.

There are two types of reservoir sedimentation, long-term and short-term. Long-term sedimentation is the accumulation of sediment through gradual erosion and other processes over long periods of time. The calculated average for Utah's reservoirs is considered to be 0.2% of total capacity lost per year. Values of 0.1%, 0.2%, and 0.1% are reported for Echo, Wanship, and East Canyon Reservoirs respectively in the Weber River Basin (Stonely et al., 2010) . Short-term sedimentation is the quick accumulation of sediment from a flashflood, floods after wildfires, or a rockslide during one or two events (Belmont and Murphy, 2019). Short-term events can mobilize 5,000 to 10,000 acre-feet of material in a single event and completely fill in a small reservoir such as Smith and Morehouse or Causey (Belmont and Murphy, 2019). Belmont and Murphy (2019) suggest that for larger reservoirs in the region, it was plausible that up to 10% of the reservoir storage could be lost due to either long-term or short-term sedimentation (Belmont and Murphy, personal communication, 2019). To find a range of changes to total reservoir storage in the Weber Basin due to sedimentation, Weber Basin reservoirs were separated into three reservoir sizes (Table 15). The time to fill 50% of active reservoir volume with sedimentation rates of 0.1% to 0.2% is 500 years and 250 years respectively (Stonely et al., 2010). Because the variability of sedimentation yields into reservoirs is extremely large, true sedimentation is based on the individual characteristics of each watershed and reservoir. Absent of an individual sediment flow study for each watershed, no precise values for the effect on the WBWCD's system can be estimated. Thus, we choose reservoir sedimentation rates of 0%, 10%, and 30% to approximate no, gradual, and more severe buildup over time. In RiverWare modeling of each sedimentation scenario, all reservoirs are assumed to begin the thirty-year simulation period with the specified percentage of storage filled. Sedimentation is implemented at the beginning of the model runs not throughout time.

Table 15. Weber Basin reservoir storage capacity and storage lost due to two sedimentation scenarios (acre-feet).

Weber Basin Reservoir Storages				
NO.	NAME	MAX STORAGE	RESERVOIR STORAGE LOST TO SEDIMENTATION	
			10%	30%
Res 1	Smith and Morehouse	8,350	835	2,505
Res 2	Rockport	61,260	6,126	18,378
Res 3	Echo	73,940	7,394	22,182
Res 4	Lost Creek	22,510	22,510	6,753
Res 5	East Canyon	51,200	5,120	15,360
Res 6	Causey	7,870	787	2,361
Res 7	Pineview	110,150	11,015	33,045
Res 8	Willard Bay	247,302	24,730	74,191

iv. Evaporation rate at Willard Bay

Key Findings

- Three scenarios of future evaporation from Willard Bay reservoir had rates of 3.2, 3.7, and 4.0 feet per year.
- These rates represented the current value used by the Utah Division of Water Resources (UDWRe) and historical and late 21st century values estimated in section 5d this report.

Three different reservoir evaporation rates for Willard Bay Reservoir draw on climate estimates made in Section 5d (Table 16). Willard Bay was used because Willard Bay is the biggest reservoir with the biggest surface area in the Weber Basin.

Table 16. Evaporation rate scenarios for Willard Bay shown as a feet per year value.

SCENARIO	DATA SOURCE	EVAPORATION RATE (FT/YEAR)
Base	UDWRe RiverWare Model	3.2
Historical	University of Utah Study (1995 to 2005)	3.7
Late 21st Century	University of Utah Study (2085 to 2095)	4.0

The base rate of 3.2 feet per year was used in the UDWRe RiverWare model for the Weber River Basin and derived from an earlier UDWRe Fortran version of the model (JUB Engineers, 2018). Considering the Willard Bay at full capacity, the UDWRe historical evaporation rate of 3.2 feet per year translates to approximately 31,000 acre-feet per year of evaporated volume. In contrast, the U of U used the Weather Research and Forecasting (WRF) model for the years 1995 to 2005 to estimate a historical evaporation rate of 3.7 feet per year which translates to 37,000 acre-feet per year of evaporation with Willard Bay at full capacity (Section 5d). The WRF model with Representative Concentration Pathway (RCP) 6.0 was used to estimate a late 21st century (2085 to 2095) reservoir evaporation rate of 4.0 feet per year or 39,000 acre-feet per year, which represents the high estimate of evaporation projections for this study.

We apply the three Willard Bay evaporation scenarios to the other reservoirs in the basin by scaling up the base case monthly evaporation rate for each other reservoir by the same percentage increase. Reservoir evaporation for all reservoirs is zero during winter months (November to February) to represent ice on the reservoirs. The layer of ice on top of the reservoirs creates a barrier, which during winter months prevents evaporation from the reservoir surface and also prevents precipitation (snow or rain) from reaching the reservoir water body.

v. RiverWare modeling

Key Findings

- The existing UDWRe RiverWare model for the Weber River Basin was used.
- The RiverSmart plugin was configured to automate the 324 model runs.

RiverWare is a water system modeling program created by the Center for Advanced Decision Support for Water and Environmental Systems (CADSWES) at the University of Colorado, Boulder (Zagona et al., 2001). The UDWRe created a RiverWare model for the Weber River Basin from a prior custom-coded Fortran model. The model has nine reservoir objects, 19 inflow objects, 20 demand/service areas, and 43 rules that are organized into seven groups and a set of finalization rules (JUB Engineers, 2018). The rule groups specify the order water (i) is drawn from reservoirs and delivered to service areas, and (ii) stored in protected reservoir pools. Simplified, the model balances inflows, demands, and reservoir storage on a monthly basis. Water starts at inflow objects and moves through the water system based on the demand and storage rules set up by the UDWRe.

The model is used to analyze the impact of inputs such as inflows, demands, reservoir capacity, and reservoir evaporation over a 30-year, monthly simulation period. The model outputs reservoir storage for each reservoir, water deliveries to each service area, and shortages (the difference between a service area's delivery request and actual delivery).

We used the CADSWES RiverSmart plugin tool to automatically set up and run a large number of model runs comprised of various combinations of inflow, demand, reservoir evaporation, and reservoir sedimentation scenarios. We set up the RiverWare model and RiverSmart plugin tool as follows.

RiverWare Setup Steps:

1. Setup the Data Management Interface (DMI) configuration to define inputs for stream flow, demands, reservoir sedimentation, and reservoir evaporation (see DMI setup section)
2. Setup the Multiple Run Module (MRM) to define different scenarios for stream flow, demands, and reservoir inputs (See MRM setup section)
3. Create a total storage slot in the Other Data, data object. This slot sums storage for each reservoir object

DMI Setup Steps:

1. Create a new Excel DMI for the hydrology, demand, sedimentation, and reservoir evaporation scenarios (see CADSWES, 2020) . This DMI points to the Excel files that have the data values for each scenario.
2. Open the DMI configuration check and confirm warnings
3. To run the RiverSmart plugin, the DMI configuration must be formatted exactly as shown in Figure 50.

The inflow data is set up for each of the 19 inflow gage objects in an Excel file and read into RiverWare using the RiverWare DMI tool. The DMI tool reads in the Excel file and saves the data in RiverWare slots. There are six Excel sheets read in, one for each of the selected factor scenarios. These selected data sheets are called traces in RiverWare (Table 17).

The DMI tool reads six Excel data sheets of the annual demand values (See Table 18). Each Excel sheet has the annual demands for 20 service areas in the Weber Basin.

The annual demand values are assumed to remain the same for the full 30-year RiverWare simulation time. There is no methodology in the RiverWare model to implement varied annual reservoir sedimentation. Thus, RiverWare reads in an Excel file that designates Trace 1 runs as the 0% change, Trace 2 runs as 10% change, and Trace 3 runs as 30% change to maximum reservoir storages. Lastly, evaporation for this study is considered by changing the evaporation rate for each of the reservoir objects in RiverWare. Each reservoir object receives values interpolated outside of RiverWare and input into the model using the evaporation DMI. The three evaporation scenarios are implemented as three separate RiverWare models.

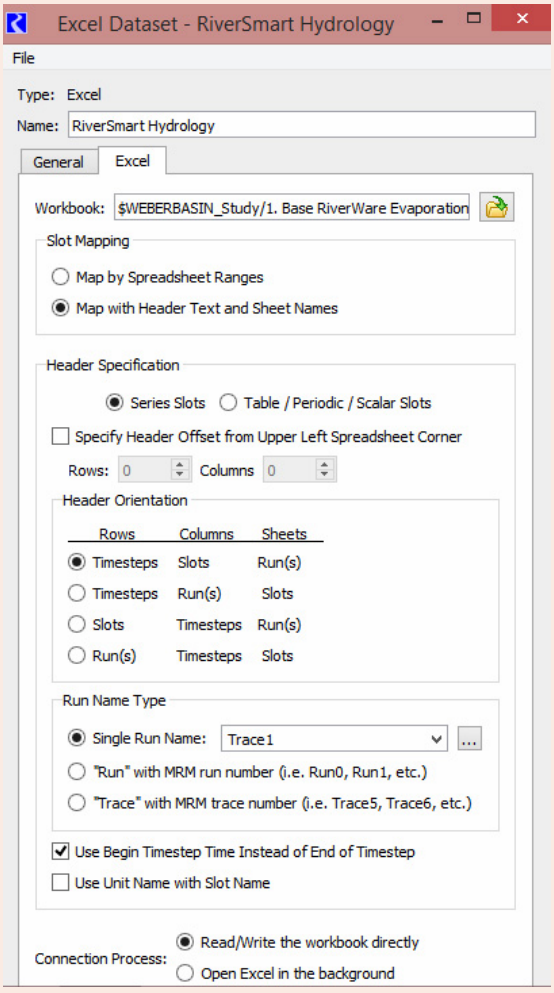

Figure 50. Screenshot of the Data Management Interface (DMI) configuration that shows the required settings to run RiverWare and RiverSmart model runs.

Table 17. RiverWare inflow traces and their correcting inflow scenario with average June 1st values.

RIVERWARE TRACE NOTATION	INFLOW SCENARIOS RUN NAME	AVERAGE JUNE 1ST INFLOWS (AF/YR)	WHY SELECTED
Trace 1	Western Water Assessment (Hot Dry Climate Scenario)	796,000	Worst case scenario – Intensity drought
Trace 2	1940 to 1970 (Historical Inflows)	954,700	Historical inflows – Base case
Trace 3	1930 to 1960 (Historical Inflows)	880,200	Historically known droughts
Trace 4	1610 to 1640 (Paleo-Flows)	925,000	Intensity droughts
Trace 5	1520 to 1550 (Paleo-Flows)	971,500	Duration droughts
Trace 6	1570 to 1600 (Paleo-Flows)	852,000	Duration and intensity droughts

Table 18. Selected average annual demand input run scenarios (traces).

RIVERWARE TRACE NOTATION	POPULATION SIMULATION YEARS	AVERAGE ANNUAL DEMAND SCENARIOS VALUES (AF/YR)	WHY SELECTED
Trace 1	2015	492,000	Lower bound of 2015 scenarios
Trace 2	2015	557,800	Upper bound of 2015 scenarios
Trace 3	2070	384,000	Lower bound of 2070 scenarios
Trace 4	2070	711,800	Upper bound of 2070 scenarios
Trace 5	2150	361,000	Lower bound of 2150 scenarios
Trace 6	2150	846,500	Upper bound of 2150 scenarios

To run more than one scenario, RiverWare has a multirun function. The RiverWare multirun function is setup as follows. Figure 51 shows the Multi Run Module configuration.

Multirun Setup Steps:

1. Create a Multi Run Module (MRM).
2. Set the mode to concurrent.
3. Check input DMIs, traces.
4. Check generate comma-separated values (CSV) file and create the output files wanted on the outputs tab.
5. Set the run parameters to run from for a 30-year period. Oct. 2459 to Sept. 2489 were used because Oct. 2459 was the previous start period of the UDWRe's Model runs. RiverWare only allows simulation for 1900 onwards. The year 2459 was used to accommodate paleoclimate periods that date back to 1400 AD.
6. Select the RiverWare ruleset.
7. Set the first trace to 1 and the number of traces to 1. The trace notation denotes each scenario.

To combine traces for the hydrology, demand, and sedimentation inputs, the RiverSmart plugin was used. RiverSmart additionally allows combinations of RiverWare inputs, rules, and the MRM.

RiverSmart Setup Steps:

1. Create RiverSmart objects: the RiverWare program, RiverWare model, RiverWare policy, RiverWare MRM, and the DMI sequence.
2. Setup the RiverWare program, RiverWare model, RiverWare ruleset, and RiverWare MRM, using the RiverSmart Documentation (CADSWES, 2020) RiverSmart.
3. Setup the DMI sequence configuration
   iv. Select the name of the DMI
   v. Select the DMI as Direct Connect
   vi. Set the DMI sequence 1 through 6, for hydrology, 1 to 6 for demands, and 1 through 3 for sedimentation
   vii. Add the Excel files to read, with the worksheet sequence set as Trace

The RiverSmart plugin is used to run the combination of hydrology, demand, and reservoir sedimentation inputs in RiverWare (Figure 52, brown DMI Seq boxes). The RiverSmart plugin inputs the Hydrology, Demand and Sedimentation traces to the RiverWare model. The different evaporation rates for the reservoirs are implemented using three separate RiverWare and RiverSmart models.

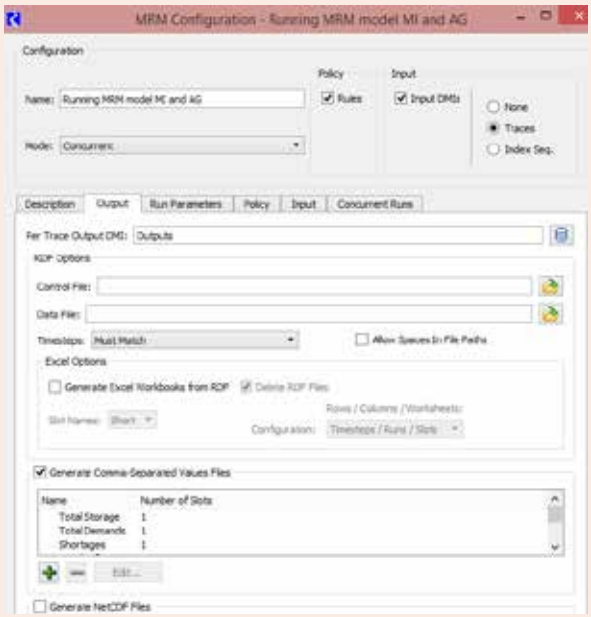

Figure 51. Screenshot of the Multi Run Module (MRM) configuration that shows set up for correct RiverWare and RiverSmart model runs.

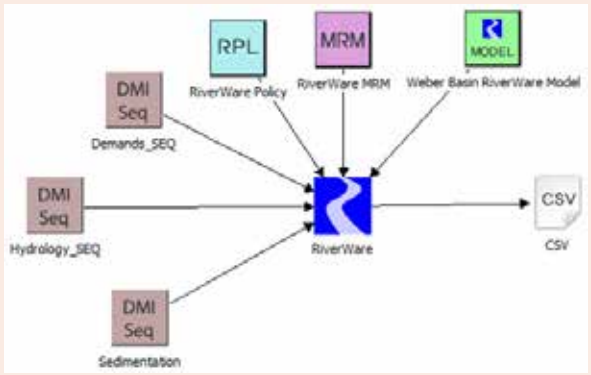

Figure 52. Snapshot of set up of RiverSmart that shows the input data objects used.

vi. RiverWare runs

Key Findings

- 324 simulations representing combinations of stream flow, demand, reservoir sedimentation, and reservoir evaporation scenarios were run in RiverWare.

This study used the RiverWare multirun function in combination with the RiverWare plugin called RiverSmart to automatically run 324 combinations of 6 inflow, 6 demand, 3 reservoir sedimentation, and 3 Willard Bay evaporation scenarios. A run is a selected combination of an inflow, demand, reservoir sedimentation, and reservoir evaporation scenario and their associated values. For example, the first run uses inflows of 796 KAF per year from the Hot Dry Scenario, the 492 KAF per year average annual demands, 0% reservoir sedimentation, and 3.2 ft/year in evaporation of Willard Bay. The three reservoir evaporation scenarios were setup as separate RiverWare models. Thus, each model (reservoir evaporation rate) had 108 combinations of 6 inflow, 6 demand, 3 reservoir sedimentation, and one reservoir evaporation scenario.

For each run, RiverWare outputs monthly total basin reservoir storage and total basin delivery shortages in each month of the simulation period. Total basin storage is the sum of all the reservoir storage in the Weber River Basin reservoirs. Total basin delivery shortage is the sum of the delivery shortages of the WBWCD demands.

RiverSmart generates model outputs as a comma separate value (csv) file in a separate folder for the run and reservoir evaporation rate model used. For example, in the *Base RiverWare Evaporation* folder, *Scenario*

subfolder, the *Trace1*,*Trace1*,*Trace1* subfolder contain results for the first run for the Base RiverWare Evaporation model (Everitt, 2020). Here *Trace1*,*Trace1*,*Trace1* indicates 362 KAF average annual demand (the first demand scenario), the 1520 to 1550 (Paleo-Flow) monthly inflows (first inflow scenario), and 0% change to reservoir storage due to sedimentation (first sedimentation scenario). The RiverWare model then outputs the shortage and storage levels for each month into a csv file into the *Trace1*,*Trace1*,*Trace1* folder. R scripts (R a free statistical analysis software) are then used to gather the output files from the 324 separate folders, organize, clean, sort, filter, analyze, and show results as time series and contour plots.

vii. Performance metrics

Key Findings

- Two performance metrics were used. One, the fraction of years (reliability) when June 1st total basin reservoir storage meets the moderate, severe, and extreme (380,000, 320,000, and 280,000 acre-feet of total reservoir storage) targets defined in the Weber Basin Drought Contingency Plan. And two, shortage to users.

The performance metrics used to evaluate RiverWare results are three storage metrics and a shortage metric. First, we use the storage level metrics to quantify the fraction of years (reliability) the June 1st total reservoir storage meets moderate, severe, and extreme storage levels (380,000, 320,000, and 280,000 acre-feet) defined by the WBWCD in their drought contingency plan (JUB Engineers, 2018) (Figure 53). These targets were confirmed in an early project meeting with WBWCD staff.

	PROJECTED JUNE 1ST TOTAL BASIN STORAGE		AVERAGE NUMBER OF YEARS BETWEEN EVENTS	
Drought Level	Acre-Feet	% of Total Basin Storage Capacity	1430 - 1970	1971 - 2017
Moderate	340,000 to 380,000	64% - 72%	36	7
Severe	280,000 to 340,000	53% - 64%	60	No Events
Extreme	Less than 280,000	Less Than 53%	135	No Events

Figure 53. Storage metric levels, and their associated storage characteristics, used for this study were the same as in the WBWCD drought contingency plan (JUB Engineers, 2018).

June 1st values are used because June 1st is the end of the snowmelt runoff season and beginning of the demand season when storage typically peaks for the year. We calculate reliability as the number of years where June

$$\text{Reliability} = \frac{\textit{Number of times June 1st Storages are above the Threshold}}{\textit{Number of years}} \qquad \textbf{(Equation 2)}$$

1st total reservoir storage is above the drought level thresholds divided by the total number of years in the simulation period of 30 years (Equation 2).

Second, the UDWRe RiverWare model calculates a delivery shortage based on the difference between the amount of demand called for by each service area and the amount of water available. The thresholds for the UDWRe shortage calculation are based on the previous Weber Basin Fortran model.

D. RESULTS

System vulnerability is defined by the frequency of total reservoir storage falling below the storage level targets and by water usage shortages.

i. Reservoir storage levels

Key Findings

System strengths

- The current modeled historical conditions with about 960,000 acre-feet per year of inflow, 550,000 acre-feet of demand, no sedimentation, and 3.2 feet per year of evaporation from Willard Bay are able to consistently maintain total reservoir storage above the 380,000 acre-feet moderate (yellow) target defined in the drought contingency plan (Figure 54).
- Demands will need to increase by about 160,000 acre-feet per year and/or inflow decrease by about 80,000 acre-feet per year from the modeled historical conditions for total reservoir storage to drop below the 380,000 acre-feet target in 10 to 20% of modeled years.
- For the 10% reservoir sedimentation rate, the yellow, orange, and red reservoir storage targets of 380,000, 320,000, and 280,000 acre-feet are met the same fraction of years for the same inflows and demands as with 0% sedimentation (Figure 55).

System vulnerabilities

- When reservoir sedimentation rates increase to 30%, the yellow, orange, and red reservoir storage targets are violated much more frequently (Figure 55).
- A unit volume reduction in inflow leads to more violations in storage targets than the same unit volume increase in demand (Figure 55).
- In the hot-dry future climate scenario that has average inflows of 800,000 acre-feet per year, total reservoir storage will fall below the 380,000 acre-feet moderate target in 50% or more of simulated years regardless of the annual demand (Figure 55).
- Several droughts within the tested scenarios last four years and longer. During these droughts, total reservoir storage stays below the red 280,000 acre-feet threshold for multiple years (Figure 56).

We use contour plots to show how storage reliability changes in response to different combinations of inflow (y-axis) and demands (x-axis) (Figure 54). For example, there are 36 inflow-demand combinations shown as black circles that represent RiverWare model runs. The blue square shows the historical (base) values of approximately 550 KAF/year (thousands of acre-feet/year) average annual demand and approximately 960 KAF average inflow. Axis labels on the top and right label the demand and inflow scenarios. For Figure 54, the reservoir sedimentation scenario is 0%, and the Willard Bay evaporation rate scenarios used is the RiverWare base case 3.2 feet/year.

There is no yellow contour on or near the historical blue marker of 550 KAF per year of demand and 960 KAF per year of inflow, meaning that at these demands, inflows, 0% sedimentation, and 3.2 feet/year evaporation levels, June 1st total reservoir storage *always* stays above 380 KAF for each year of the 30-year simulation period.

However, move right from the historical point and increase annual demands by approximately 160,000 acre-feet per year. Additionally, move down and decrease inflows 80,000 acre-feet per year by to 880 KAF on the y-axis.

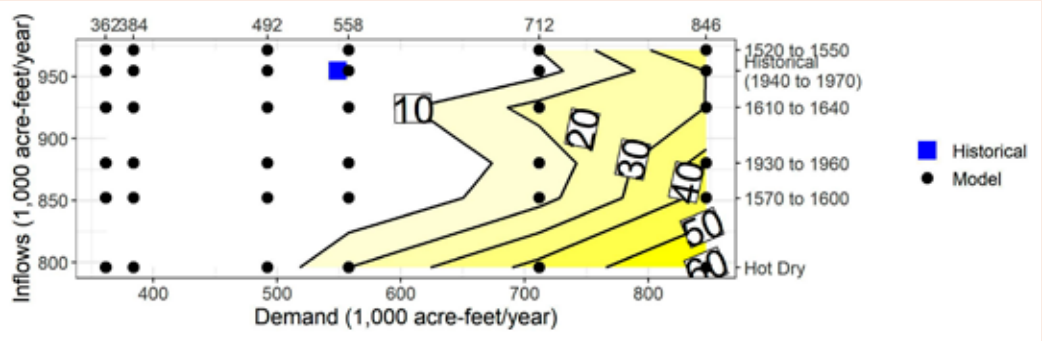

Figure 54. Percent of time (contours) Weber Basin June 1st system storage will fall below the moderate drought criteria of 380,000 acre-feet total system storage for different demands (x-axis) and inflows (y-axis) with 0% reservoir sedimentation and 3.2 feet/year reservoir evaporation. Top and right axis label the demand and inflow scenarios.

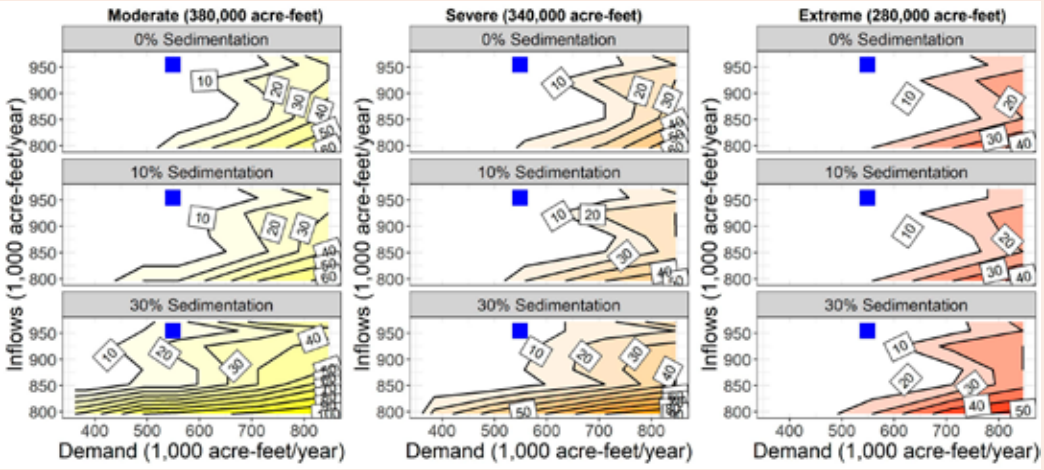

Figure 55. Storage reliability expressed as percent of years (contours) Weber Basin June 1st system storage does not meet different reservoir storage targets of 380,000, 340,000, and 280,000 acre-feet (yellow, orange, and red columns) for different demands (x-axis), inflows (y-axis), and reservoir sedimentation rates of 0%, 10%, and 30% (rows). The historical blue marker shows the annual average demand of 550 KAF and the average annual inflow of 960 KAF.

The new point with 712 KAF per year of demand and 880 KAF per year of inflow (scenario of 1930-1960 inflows) is located between the 10 and 20 percent contour lines. For these changes in inflows and demands, the system will see total June 1 reservoir storage fall below the 380 KAF level in 10-20% of years.

Figure 54 shows that WBWCD storage is vulnerable to increases in demand of 100 KAF per year or reductions in inflow of 100 KAF per year relative to historical conditions. Further, when demands exceed approximately 700 KAF per year, total June 1st reservoir storage will always fall below the 380-KAF threshold at some point during the 30-year simulation period no matter what inflows are. Additionally, the frequency of June 1st total reservoir storage falling below the 380,000 acre-feet threshold will increase as demands increase and inflows decrease.

Figure 55 compares storage reliability for the three different reservoir storage targets (yellow, orange, and red columns of subplots) and three different sedimentation rates (rows of subplots). To give context, the top left subplot is Figure 53. The contours of storage reliability in each column of Figure 54 subplots interpolate a fraction of years the storage target will not be met among the 108 runs of varied demands, inflows, and sedimentation rates. In all subplots, the reservoir evaporation rate for Willard Bay is still 3.2 feet/year.

Figure 55 shows that the June 1st storage is only mildly sensitive to a 10% storage loss from sedimentation. However, at 30% storage loss, storage targets are violated for many more combinations of inflow and demand.

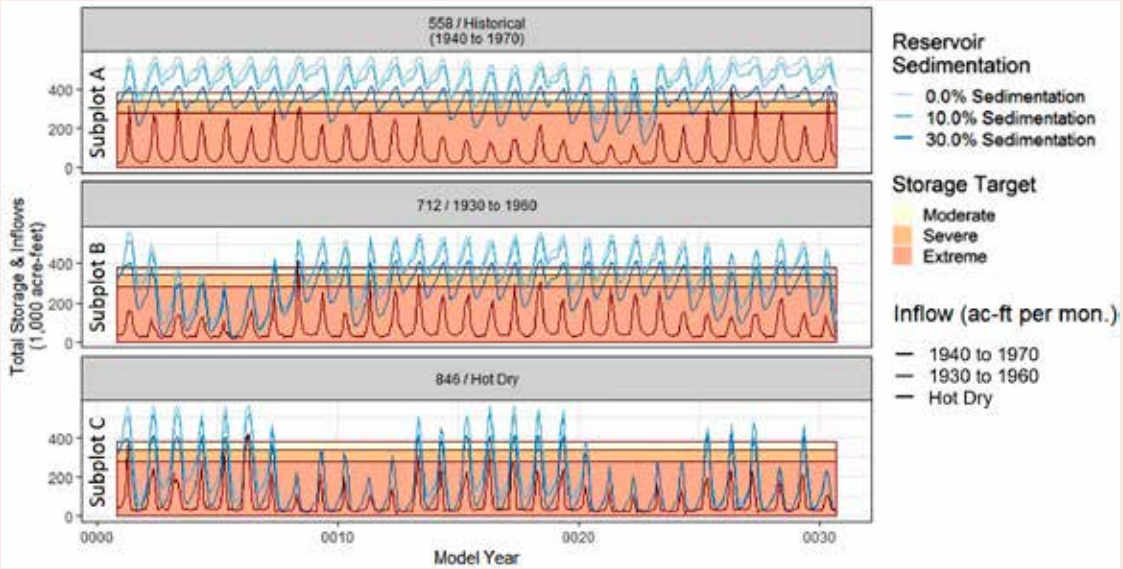

Figure 56. Comparison of inflows (black lines) to total reservoir storage for different sedimentation rates (blue lines) and scenarios of increasing demand and decrease inflows (subplots). Yellow, orange, and red shaded regions show the moderate, severe, and extreme reservoir storage targets.

Figure 14 also shows that a reduction to the inflow leads to more violations of the storage targets than an increase in demand of the same annual volume, especially when inflows fall below 850 KAF. For the 30% sedimentation scenario and inflows below 850 KAF per year, total reservoir storage will fall below the 380 KAF threshold in 10% or more of simulated years regardless of the annual demand. For inflows of 800 KAF/year such as estimated for the Hot-Dry future climate scenario, total reservoir storage will fall below the 380 KAF threshold in 50% or more of simulated years regardless of the annual demand. In contrast, a 50 KAF increase in demand to 600 KAF/year will only see total reservoir storage fall below the 380 KAF threshold in 20% or more of simulated years.

Figure 56 compares total time-series of storage to inflows for three reservoir sedimentation rates (0%, 10%, 30%, blue lines) and three scenarios of increasing demands/declining flows (upper to lower subplots). In subplot A, Model Years 14 and 19 mark the beginning of four years of sustained low inflows. In Model Year 19, reservoir storage immediately falls below the extreme reservoir level of 280 KAF for the scenario with a reservoir sedimentation rate of 30%. But storage also recovers to 380 KAF that same year. Reservoir storage for Model Years 20-22 falls below the 280 KAF extreme level for all reservoir sedimentation rates during the summer of each year. But storage also rebounds to at least the moderate target of 380 KAF every year. In Subplot B, one critical 6-year drought occurs in Model Years 1-6. A second 7-year drought occurs in Model Years 24-30. The second drought has one intermediate year of increased flow (Model Year 28). At the end of the first two years of the first drought, reservoir storage falls to about 120 KAF with 0% reservoir sedimentation and near 0 KAF for the 30% reservoir sedimentation scenario. Storage for all the sedimentation scenarios rebound in the same year to at least 280 KAF. In subsequent years of the drought, minimum storage for the year is consistently below 100 KAF and near 25 KAF in Model Year 5 for each reservoir sedimentation scenario. By Model Year 5, storages are the same regardless of the reservoir sedimentation rate. This pattern of the same reservoir storage for the different reservoir sedimentation rates persists into Model Years 7 and 8 – the first two years of the post-drought recovery. During the second drought, reservoir storage falls below the 280 KAF extreme target then recovers to 320 KAF or higher. Model Year 30 shows very low storages that are comparable to Model Years 2 and 3. Subplot C has the highest demands and lowest inflows and shows that the total system storage goes below the extreme storage level of 280 KAF every year regardless of the sedimentation rate. Extreme droughts in Model Years 8-12 and 20-24 with sustained inflows of less than 200 KAF per year show reservoir storage stays below the extreme level of 280 KAF for most of each year and storage is the same regardless of the reservoir sedimentation rate. For reference, this last high demand-low supply scenario appears in the bottom right black circle in Figure 54.

ii. Shortages

Key Findings

System strengths

- During the modeled historical conditions, delivery requests are met nearly all the time with few shortages (Figures 57 and 58).
- Deliveries are met and shortage are small across all three reservoir sedimentation rates (Figure 57).

System vulnerabilities

- The historical system is very close to seeing a total basin shortage of 40,000 acre-feet per year or more in at least 1 of 30 years (Figure 58).
- If demand increases by 100,000 acre-feet per year, the worst shortage would increase to about 160,000 acre-feet per year and some shortage would occur in 50% of years (Figure 58).
- As expected, shortages increase substantially as inflows decrease and demands increase. (Figure 57).

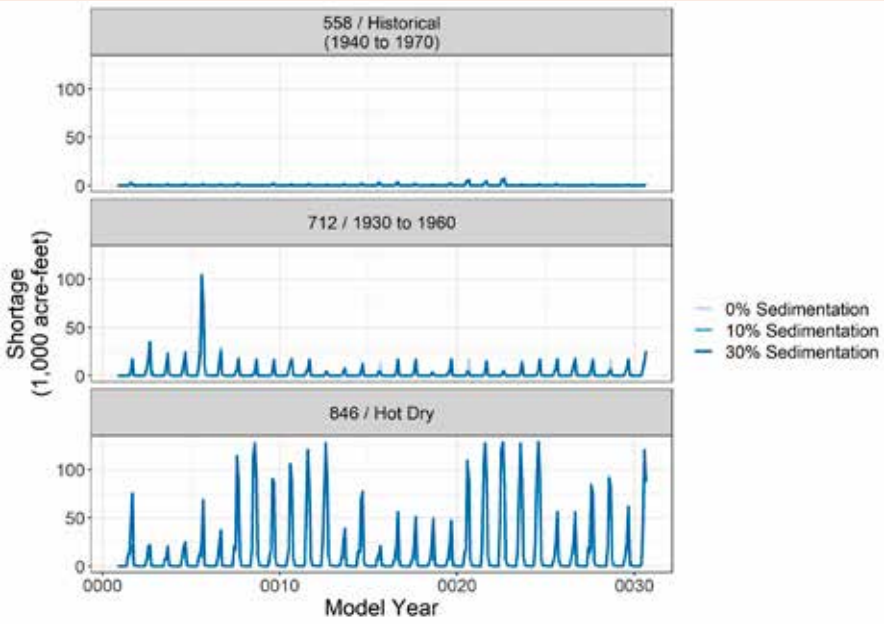

Figure 57. Time series of total shortage to service areas for different sedimentation rates (blue lines) and scenarios of demand/inflows (panels).

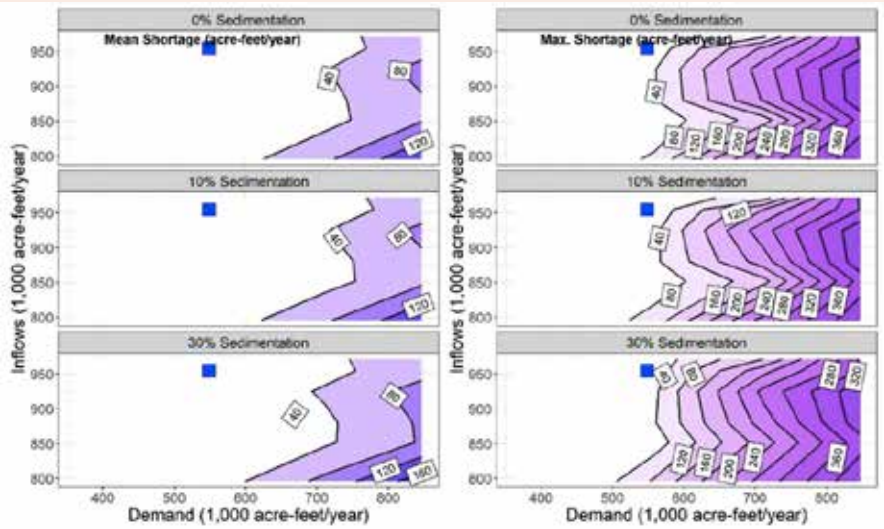

Figure 58. Mean and maximum annual shortage in acre-feet to service areas (contours) for each sedimentation scenario (row), annual demand (x-axis), and inflows (axis). Shortages increase with increased demand and reduce inflows.

Plots of time series of total shortages to all service areas for the three reservoir sedimentation rates and demand/inflow scenarios show shortages are largely the same across the three sedimentation rate scenarios (Figure 57). As expected, shortages increase as demand increases and inflows decrease. In the largest 846 KAF/year demand/Hot-Dry scenario, shortages over 100 KAF/month are seen in many of the drought years. Contour plots of the mean annual shortages for different demand and inflow scenarios show annual demand would have to increase 150 KAF/year to incur average annual shortage of 40 KAF (Figure 58). However, demand would only need to increase by 25 KAF/year to incur a shortage of 40 KAF in at least one of the 30 modeled years. The near vertical slopes of the contour lines show annual shortages are much more sensitive to demand than inflows. Additionally, the Figure 58 subplots in each column are near identical and show that shortages are nearly insensitive to reservoir sedimentation.

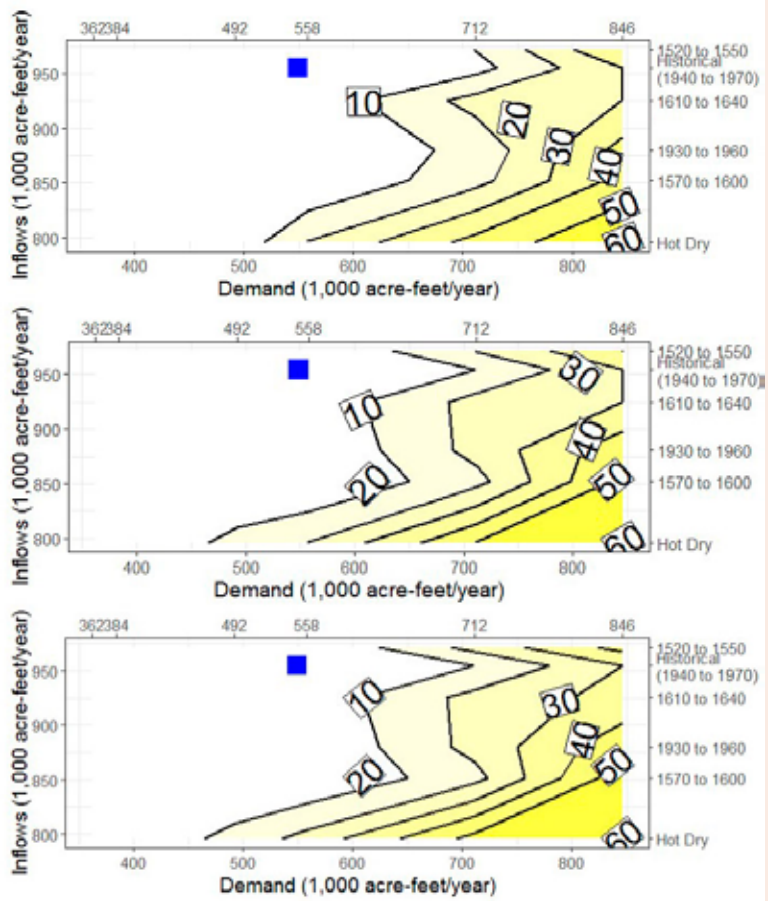

Figure 59. Percent of years (contours) Weber Basin June 1st system storage falls below 380,000 acre-feet for evaporation rates of 3.2 (Subplot A), 3.7 (Subplot B), and 4.0 feet/year (Subplot C) at different annual demands (x axis), inflows (y-axis) and a base case reservoir sedimentation rate of 0%.

iii. Evaporation

Key Findings

System strengths

- The Weber Basin system storage is insensitive to Willard Bay evaporation rates between 3.2 and 4.0 feet per year (Figure 59).

System vulnerabilities

- None identified.

Contour plots show the percent of years that the June 1st reservoir storage level is below the moderate threshold storage level of 380 KAF for different combinations of inflow, demand, the base case reservoir sedimentation rate, and base case, historical, and late century reservoir evaporation rates of 3.2, 3.7, and 4.0 feet per year (Figure 59). To give context, subplot A is Figure 13. The three subplots for the three reservoir evaporation rates are very similar and show that the Weber River water system is not very sensitive to the evaporation rate. Because the system is not sensitive to evaporation with 0% sedimentation, we do not show results for the other combinations of reservoir sedimentation and evaporation.

E. CONCLUSION

Key Findings

- A bottom-up vulnerability analysis showed the combinations of uncertain future demands, inflows, reservoir sedimentation rates, and reservoir evaporation rates where the Weber Basin water system will meet delivery requests and keep June 1 total reservoir storage above targets.
- The bottom-up vulnerability analysis also showed the conditions where reservoir storage will fall below targets and there will be shortage. Work remains to test the existing drought contingency plan cutback operations under a wide range of uncertain future inflows, demands, and reservoir sedimentation rates.
- Work remains to identify reservoir release, diversion, and sharing operations that can improve system performance and reduce vulnerability across the uncertain future streamflow, demand, reservoir sedimentation, and reservoir evaporation conditions.
- Work also remains to identify impacts on service areas in the Riverware model that are the direct responsibility of the WBWCD.
- Future work can use data, models, code, and resources posted at https://github.com/jacobeveritt/WeberBasinVulnerability.

Water system managers want to know the future conditions to which their water system is vulnerable. Here we use a bottom-up vulnerability analysis to show the combinations of uncertain future demands, inflows, reservoir sedimentation rates, and reservoir evaporation rates that the Weber Basin water system will not be able to deliver requested water or sustain reservoir storage above target levels. Six 30-year inflow scenarios included 3 paleo droughts, two droughts from the recent historical record, and an extreme hot-dry future climate scenario for the basin developed by the Western Water Assessment. 324 runs representing different combinations of the uncertain future factors -- inflows, demand, reservoir sedimentation, and reservoir evaporation -- were simulated in the UDWRe RiverWare model for the Weber basin using the RiverSmart plugin. Total reservoir storage levels and total shortages were outputted and compiled for each run.

Visualization of the results show several areas where the system can tolerate changes in conditions. First, the Weber River Basin system can presently sustain June 1st total reservoir storage at or above 380 KAF across all years for existing demands of up to 600 KAF/year and inflows at or above 825 KAF/year. Under these conditions, there are no shortages. Second, reservoir storage is only mildly sensitive to 10% reservoir storage lost due to sedimentation. Third, system demands would need to increase by 150 KAF/year before average annual shortages would rise to 40 KAF/year. And fourth, reservoir storage is only mildly sensitive to increases of reservoir evaporation rates up to 4.0 feet/year.

The results also identify several key system vulnerabilities. First, if demand increases by 100 KAF per year or inflows decrease by 100 KAF per year relative to historical conditions, managers will see June 1st reservoir storage fall below the moderate storage threshold of 380,000 acre-feet in at least 10% of years. The percent of years storage falls below 280 KAF will increase to 50% if demands increase to 850 KAF/year. Second, sustained low inflows of three years and longer will drop the June 1st reservoir level into the extreme storage level below 280 KAF regardless of the reservoir sedimentation rate. For several simulated drought events, June 1st reservoir storage will fall below 100 KAF and persist for multiple years. In the later years of these drought events, reservoir storage will persist below the 280 KAF extreme target for the entire year. Third, as reservoir sedimentation rates rise, reservoir storage is more sensitive to inflows than to demands. Fourth, demand need only increase by 25 KAF/year over historical conditions to see at least one year with an annual shortage of at least 40 KAF/year.

WBWCD managers can use these vulnerability results in at least four ways. First, identify the future streamflow,

demand, reservoir sedimentation, and reservoir evaporation conditions that pose future problems. Second, start planning for how to cope with those conditions should they materialize. Third, track conditions over time and identify the signposts or tipping points when conditions deteriorate to necessitate enacting plans. And fourth, communicate to member agencies and users that many uncertainties lie ahead due to future climate and additional factors. Communicating can include encouraging member agencies and users to plan for a multitude of uncertainties.

There are several limitations to this vulnerability assessment. We selected a limited number of model inflows, demands, sedimentation rates, and evaporation rates that do not necessarily span all possible future values for these inputs. For example, there could be even more extreme, low inflows such as with the streamflow projections in Section 4a of low precipitation and moderate or high emissions. If simulated, these inflow scenarios would likely yield even lower reservoir storages and higher shortages. Different intermediate demand scenarios could be used that represent different combinations of population growth, per capita water use, agricultural to urban conversion rates, and potential evapotranspiration. There was very limited reservoir sedimentation data and thus a wide range of sedimentation rates spanning 0% to 30% were simulated. Model outputs and vulnerability criteria of June 1st reservoir storage targets and total annual shortages reflect current WBWCD operations. Use of other targets like higher June 1st storage levels, October storage levels, or service areas specifically served by the WBWCD would give basin managers a different, possibly better image of how basin storage responds to individual and combinations of future inflows, demands, reservoir sedimentation, and reservoir evaporation conditions. An October storage level criterion would represent an end-of-the irrigation season condition and the yearly low point in timeseries plots of reservoir storage. If we could identify the modeled service areas or portions of them that are managed by the WBWCD, further work could identify WBWCD-specific output.

Lastly, the study only considers existing modeled reservoir operations where service areas call on water from one or more reservoirs in a priority order. Further work could identify how existing reservoir operations and deliveries could be adapted to increase reservoir storage and reduce shortages across uncertain future inflow, demand, and reservoir sedimentation conditions. Together, the bottom-up vulnerability analysis identifies future inflow, demand, reservoir sedimentation, and reservoir evaporation conditions for which the Weber Basin system can likely cope and future conditions where the system will see low reservoir storage and high shortages.

Future Work

- Work remains to test the existing drought contingency plan cut back operations across deep uncertainties future stream flows, demands, and reservoir sedimentation rates.
- Work remains to better characterize tradeoffs between total reservoir storage and shortages to users under deeply uncertain future conditions.
- Work remains to identify reservoir storage, diversion, and sharing operations that can improve system performance and reduce vulnerability across deep uncertainties in future stream flows, demands, and reservoir sedimentation rates.
- Work can use data, models, code, and resources posted at https://github.com/jacobeveritt/WeberBasinVulnerability.

Data Availability

The input data, model, code, and directions for this study are available on GitHub at, https://github.com/jacobeveritt/WeberBasinVulnerability (Everitt, 2020).

7. APPENDICES

A. APPENDIX 1

Site details for the subcatchments of the Weber River Basin (section 2.b)

i. Site details

When looking at the streamflow response to climate in the watershed, it is important to narrow our sites to those that contain a more natural hydrologic signal. Man-made diversions significantly affect how streamflow is partitioned by diverting water into canals and other waterways. Stream gauges that are located below diversions are important for management decisions, but they will not be an accurate representation of the natural streamflow signal. For this reason, we have selected five catchments from the original nine that are either above all dams/diversions or are below storage dams but above diversions. OSF and WO are major headwaters while ECJ, CC, and LC are headwaters that will be important for looking at the role of climate-landscape interaction (Table 19).

Table 19. Site details for the five subcatchments of the Weber River basin that were used to develop statistical streamflow models.

LOCATION RELATIVE TO DAMS/ DIVERSIONS	ABOVE DAM/ DIVERSION		BELOW DAM FOR STORAGE ONLY			BELOW DIVERSION			
Catchment Name	East Canyon at Jeremy Ranch	Chalk Creek	Lost Creek	Ogden South Fork	Weber at Oakley	East Canyon at Morgan	Ogden at Pineview	Weber at Coalville	Weber at Gateway
Catchment Abbreviation	ECJ	CC	LC	OSF	WO	ECM	OP	WC	WG
Area (km2)	148.8	642.7	325.3	356.4	420.2	373.4	822.6	1123.8	4212.4
Mean Elevation (m)	2234	2298	2230	2200	2759	2144	2051	2407	2189

ii. Unit conversions

When computing statistics on catchments of different sizes, it is useful to normalize streamflow over catchment area. This yields a one-dimensional value (inches) that can then be more easily compared with other catchments as well as precipitation values. To convert to acre-ft:

$$annual\ streamflow\ (in)\ x\ \frac{1m}{39.37in}\ x\ catchment\ area\ (m^2)\ x\ \frac{1\ acre-ft}{1233\ m^3}$$

Photo: Echo Reservoir in Utah. Credit: Daniel/Adobe Stock.

iii. Multiple linear regression statistics for predicting streamflow

Table 20. Regression statistics of the precipitation-streamflow relationship in subcatchments of the Weber River basin. The slope represents the incremental increase in streamflow for each increase in precipitation, and is analogous to water yield. The R^2 value represents the fraction of variance in streamflow explained by precipitation.

	ECJ	CC	LC	OSF	WO
Slope	0.701	0.389	0.220	0.569	0.663
Intercept	-10.86	-4.77	-2.21	-6.76	-6.69
R^2	0.80	0.63	0.34	0.68	072
p-value	3E-06	1E-20	9E-06	9E-25	3E-32

Table 21. Multiple Linear Regression statistics of streamflow variability of subcatchments. The coefficient and predictability added (R^2) of each metric are shown.

		INTERCEPT	PRECIPITATION	BASEFLOW	MELT RATE	REMAINING ERROR
ECJ	Coefficient	-0.511	0.087	67.176	128.027	
	R^2		0.80	0.02	0.15	0.03
CC	Coefficient	-1.830	0.095	372.843	92.446	
	R^2		0.63	0.20	0.14	0.04
LC	Coefficient	-0.247	0.028	216.416	98.374	
	R^2		0.34	0.37	0.27	0.02
OSF	Coefficient	-1.383	0.109	163.831	111.225	
	R^2		0.68	0.09	0.18	0.05
WO	Coefficient	-6.420	0.243	452.054	73.188	
	R^2		0.72	0.07	0.13	0.08

iv. Cumulative discharge functions for estimating streamflow timing

Timing of streamflow within the year is estimated using cumulative discharge functions (CDFs) based on the historical record. For each site-year we construct a CDF that shows what fraction of the total streamflow has occurred on each day of the water year. Typical CDFs are created for different climate scenarios (warm/dry, warm/wet, cool/dry, etc.) in each catchment by averaging all CDFs from years that fall into the specified range of climate conditions (Table 22).

Table 22. Percentile range of climatic conditions used to develop each typical CDF. Each typical CDF is developed by taking the mean of all CDFs that fall within the specific range of precipitation and temperature. The overlap within ranges allows for a more conservative calculation of CDFs. Since projected future temperatures are in the high-very high range, the temperature scale is different than that used for precipitation values.

	LOW P	MED P	HIGH P	HIGH T	VERY HIGH T
Percentile	P<40%	20<P<80%	P>60%	T>85%	T>85% (from warmer neighbor)

Each CDF can then be used, along with a total estimated streamflow value, to create a hydrograph. The daily change in fractional amount given by the CDF is multiplied by the annual streamflow to yield a streamflow value for each day, which is then plotted as a hydrograph (Figure 60 and Figure 61)..

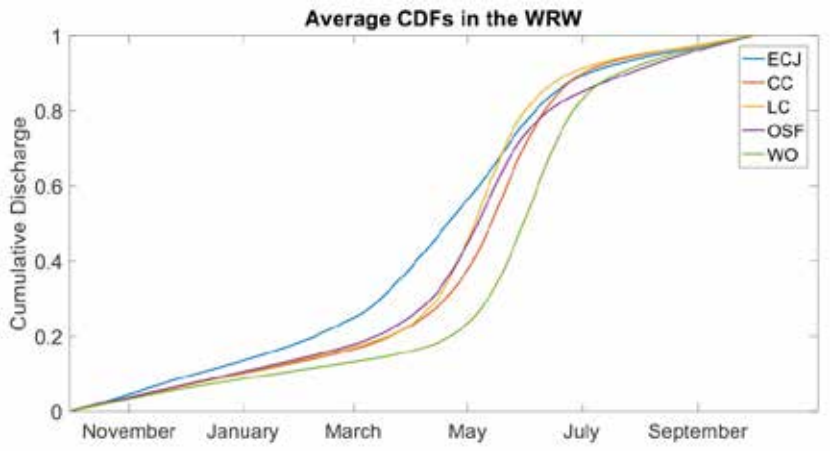

Figure 60. Average Cumulative Discharge Functions of the Weber River basin. The point where the CDF starts to increase more rapidly corresponds to snowmelt induced flow on the hydrograph. Similarly, the point where the CDF starts to level out corresponds to a return to baseflow conditions on the hydrograph.

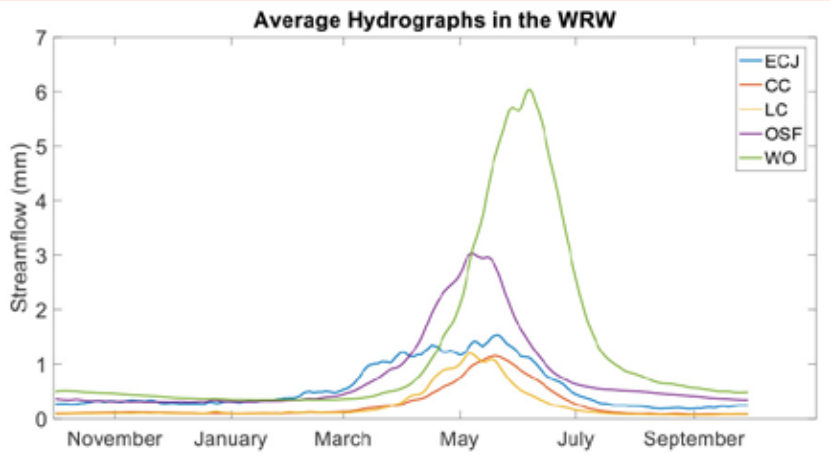

Figure 61. Average hydrographs of the Weber River basin as derived from the average CDFs for each subcatchment.

B. APPENDIX 2

Site-specific climate change values (Sections 3b, 3c, and 5b)

Table 23. Climate change at specific sites based on dynamical downscaling. In the column headings, mid indicates the change for mid-century (2035-2044) relative to historical (1995-2005) and late indicates the change for late-century (2085-2094) relative to historical. T indicates the temperature change in degrees Fahrenheit, P indicates the precipitation change as a percent, and S indicates the snowfall change in inches of snow water equivalent (SWE).

LOCATION	MID T	LATE T	MID P	LATE P	MID S	LATE S
Ben Lomond Peak	2.7	5.3	4.1	7.0	-1.9	-6.5
Chalk Creek #2	2.4	4.7	9.2	14.0	1.3	0.4
Horse Ridge	2.5	5.1	7.1	10.6	0.6	-2.1
Lost Creek-Croyden	2.7	5.4	8.4	12.5	-0.6	-2.9
Smith Morehouse	2.4	4.7	8.6	12.2	1.2	-0.1
Thaynes Canyon	2.4	4.8	8.4	13.1	1.2	-0.4
Trial Lake	2.3	4.6	9.2	16.5	2.3	3.0
Weber-Echo	2.7	5.5	11.6	15.0	-0.5	-1.9
Weber-Oakley	2.4	4.9	9.4	11.6	0.5	-1.5
Weber-Plain City	2.8	5.5	5.7	8.7	-1.2	-3.1

C. APPENDIX 3

Weber Basin Water Conservancy District Shortages, David E. Rosenberg

i. Introduction

This appendix presents RiverWare model shortage results from the bottom-up vulnerability analysis that are specific to the Weber Basin Water Conservancy District (WBWCD). The WBWCD staff requested these results during a late February 2020 presentation of preliminary results.

ii. Analysis Methods

A first task was to identify which of the 20 service areas in the RiverWare model for the Weber Basin (McGettigan and Melchner, 2018) that were the responsibility of WBWCD. After discussion, consultation with the Utah Division of Resources, and examination of spreadsheet summaries of some Utah Division of Water Rights records, it was determined that WBWCD is fully responsible for 3 service areas -- Ogden Valley, Park City, and Gateway Canal (Table 2-1). The WBWCD is also responsible for 59,800 of the 102,500 acre-feet per year maximum diversion to Slaterville. The other 42,700 acre-feet per year of the Slaterville diversion goes to Hooper Irrigation, Wilson Canal, South Slaterville Canal, and Plain City Irrigation and is not WBWCD responsibility.

District staff surmised that in 2020 there were approximately 23,000 acre-feet in replacement contracts. These replacement contracts are releases from reservoirs to replace groundwater withdrawals along the Wasatch Back (Eastern Summit and Morgan County) minus consumptive use for second homes and other uses. Thus, the total RiverWare modeled WBWCD responsibility of 199,100 acre-feet per year of maximum demand in Table 2-1 plus 23,000 acre-feet of replacement water gives approximately the 227,000 acre-feet per year WBWCD contracted for in 2020. The slight difference is due to inexactness of the maximum demand amounts in the Riverware model that include observed deliveries up until about May 2018.

As a second task, a new demand management interface (DMI) configuration was written in RiverWare to output a Comma Separated Value (csv) file of shortages in each month of each model year for each service area. Previously, the DMI output total basin shortage (sum of all service areas). Shortage in RiverWare is the difference between the delivery request (max demand in Table 2-1) and model delivered water. The RiverSMART tool was reconfigured to run the new DMI. Then each model scenario was rerun to generate monthly shortage values for each service area in each scenario.

Third, the service area specific shortages were post processed in R (a statistical program) to calculate the total demand for the service areas for which WBWCD is responsible. Total shortages for the Slaterville service area were prorated by the factor 0.58 = (59,800 acre-feet per year for WBWCD)/(102,500 acre-feet per year for service area) to estimate the WBWCD shortage for the Slaterville service area. For example, a total shortage of 1,000 acre-feet per month to Slaterville was assigned 580 acre-feet to WBWCD and 420 acre-feet to the other users.

iii. Results

Time series and contour plots were generated to show the effects of uncertain inflows, demands, and reservoir sedimentation rates on shortages to WBWCD service areas (Figures 2-1 to 2-2). These figures correspond to Figures 56 and 57 in the main report that show basin total shortage. The WBWCD modeled shortages were also compared to the WBWCD Drought Contingency Plan annual demand reduction targets (hereafter, cutbacks) specified in the rightmost column of Table 6-3 (JUB Engineers, 2018)(Figure 2-3). The cutbacks increase as total June 1 reservoir storage drops below 380,000, 340,000 and 280,000 acre-feet (Table 2-2). Drought

Table 24. Weber River model maximum demands and service areas for which WBWCD is responsible (acre-feet per year) (adapted from McGettigan and Melchner, 2018)

SERVICE AREA	MAX DEMAND	PORTION TO WBWCD	PORTION NOT WBWCD
Eastern Summit			
SA1 - Weber Provo Diversion Canal	67,700		
SA2 - Oakley to Wanship	40,600		
SA3 - Wanship to Echo	12,700		
SA4 - Echo to Devils Slide	9,800		
Morgan County			
SA5 - Lost Creek	8,600		
SA6 - Devils Slide to Stoddard	24,900		
SA8 - East Canyon	13,000		
SA9 - Stoddard to Gateway	1,800		
Ogden Valley and Ogden River to Confluence			
SA12 - Ogden Valley	31,700	31,700	-
SA13 - Ogden Brigham & S. Ogden Highline canals	34,400		
SA14 - Ogden River Below Pineview	26,700		
Snyderville Basin			
SA7 - Park City	6,600	6,600	-
Wasatch Front			
SA10 - Gateway Canal	101,000	101,000	-
SA11 - Davis Weber Canal	82,500	-	-
SA15 - Slaterville	102,500	59,800	42,700
SA16 - Warren Canal	23,200	-	
SA17 - Ogden Bay Bird Refuge	60,500	-	
SA18 - G.S.L. Minerals	17,100	-	
SA19 - Gateway to Slatterville	24,300	-	
SA20 - Additional Weber Basin Demand		-	
TOTAL	**689,600**	**199,100**	**42,700**

Contingency Plan cutbacks were *not* modeled in RiverWare; instead modeled shortages were compared to the cutbacks required by the Drought Contingency Plan if reservoir storage on June 1 was below target levels. Results were only generated by the base case reservoir evaporation rate of 3.2 feet per year because prior results were insensitive to the other rates of 3.7 and 4.0 feet per year. Results are briefly discussed within the figure captions.

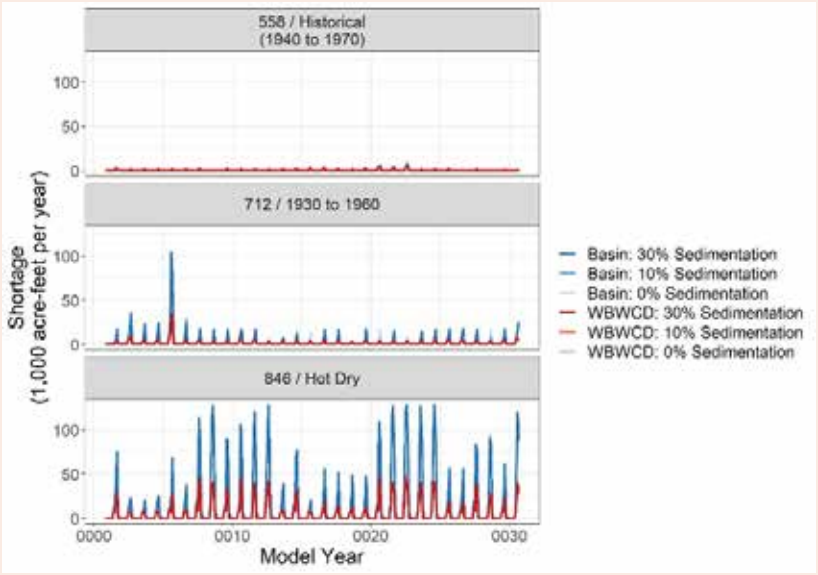

Figure 62. Comparison of time series of shortages to WBWCD service areas (red lines) and the total basin (blue lines) for different reservoir sedimentation rates (color intensity) and scenarios of increasing demand / decreasing inflows (panels). In the top panel with 558,000 acre-feet of demand per year and inflows from 1940 to 1970, shortages are small and nearly all born by WBWCD when shortages occur. In the middle and lower panels with higher demands and lower inflows, shortages are more regular, larger, and also born by non WBWCD users. Across all three scenarios, WBWCD shortages are largely unaffected by the reservoir sedimentation rate (red intensity), same as for basin total shortages (blue intensity).

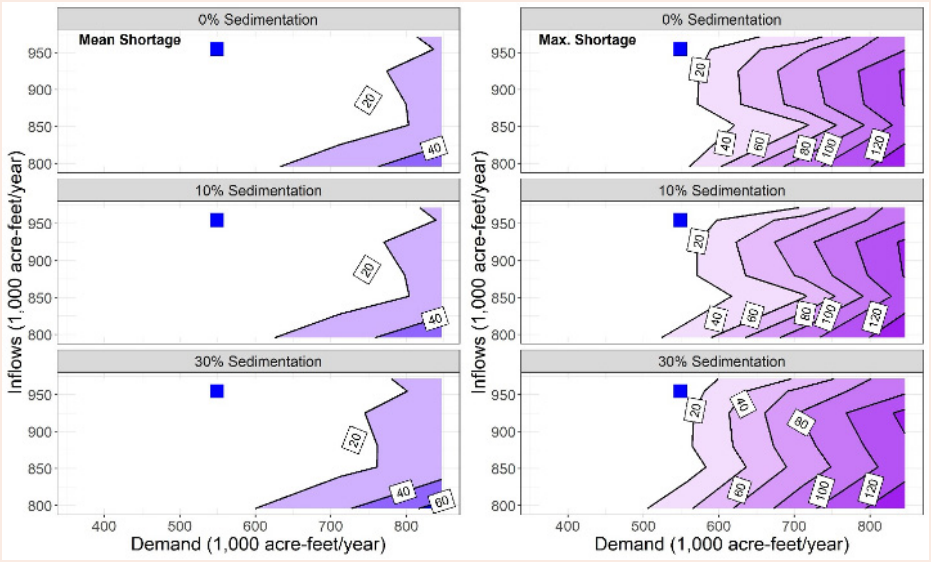

Figure 63. Mean (left panels) and maximum (right panels) annual shortage in thousands of acre-feet per year (contours) over the 30-year simulation period to Weber Basin Water Conservancy District service areas for each sedimentation (row), annual demand (x-axis), and inflow (axis) scenario. With current demands and base case inflows from 1940 to 1970 (blue squares), Weber Basin Water Conservancy District service areas receive full deliveries in nearly all simulation years. Shortages increase with increasing demand and reduced inflows similar to the pattern for total basin shortages in Figure 57. The reservoir sedimentation rate minimally influences shortages, same as Figure 2-1. WBWCD annual shortages (contours) are about 33% of basin total shortage contours in Figure 57.

Table 25. Drought Contingency Plan Cutbacks by Response Level

RESPONSE LEVEL	BASIN TOTAL STORAGE (acre-feet)	CUTBACK (acre-feet per year)
1. Normal	Above 380,000	0
2. Advisory	Above 380,000	0 to 43,000
3. Moderate	340,000 to 380,000	43,000
4. Severe	280,000 to 340,000	123,000
5. Extreme	Less than 280,000	206,000

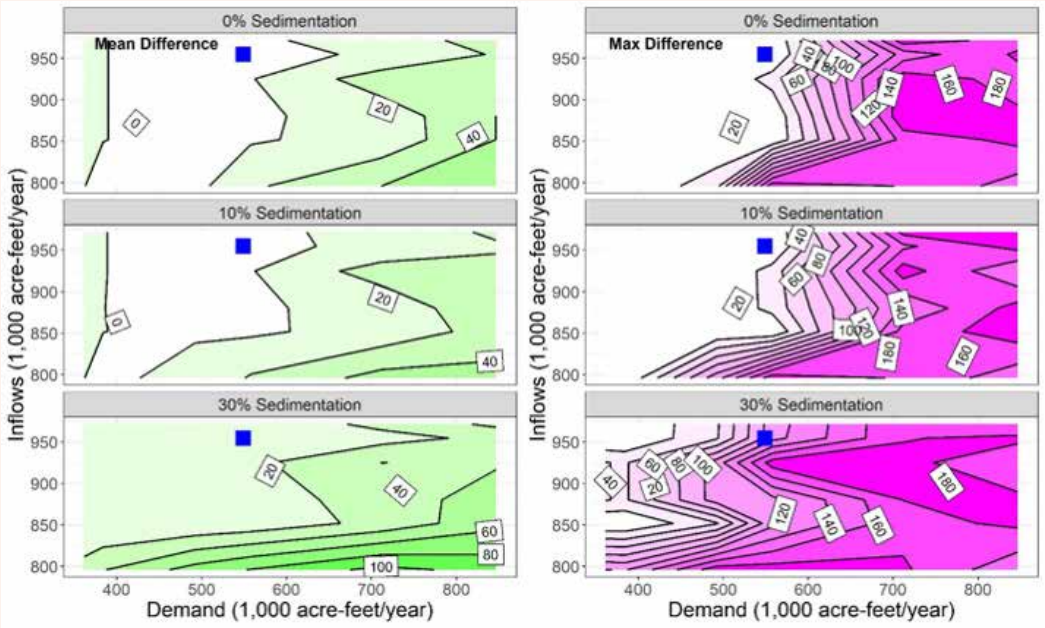

Figure 64. Amount by which WBWCD Drought Contingency Plan cutbacks exceed RiverWare modeled shortage (contours of thousands of acre-feet per year) for each reservoir sedimentation (row), annual demand (x-axis), and inflow (axis) scenario. Left panels (green) show contours of average annual difference over each 30-year simulation period. Right panels (magenta) show the largest annual difference from each 30-year simulation period. All contours are positive and indicate that for scenarios of increasing demands and decreasing inflows (bottom-right of panels), Drought Contingency Plan mandated shortages would be larger than RiverWare modeled shortages. Differences between the Drought Contingency Plan cutbacks and RiverWare modeled shortages also grow as the reservoir sedimentation rate increases. That is, shortages by the Drought Contingency Plan will be larger than the RiverWare modeled shortages shown in Figures 2-1 and 2-2. By requiring larger shortages, the Drought Contingency Plan should maintain higher reservoir storages than the RiverWare model results shown in Figures 52-54 and 57. This comparison highlights an important system tradeoff between shorting users and maintaining reservoir levels.

iv. Concluding Notes

Uncertain inflows, demands, and reservoir sedimentation effect annual shortages to WBWCD service areas in ways similar to shortages for the entire Weber basin. The analysis also highlights an important tradeoff between shorting users and maintaining reservoir levels. Drought Contingency Plan operations will most likely produce larger shortages and higher total reservoir storage levels than the RiverWare model. This tradeoff could be further explored through additional RiverWare modeling of Drought Contingency Plan operations and alternative operations that seek to identify reservoir storage and diversion operations that bolster storage, increase deliveries to users, and adapt over time as new information becomes available about future river flows, demands, and reservoir sedimentation.

v. References

JUB Engineers. (2018). "Drought Contingency Plan." Weber Basin Water Conservancy District, Layton, UT. https://github.com/jacobeveritt/WeberBasinVulnerability/blob/master/5%20-%20BackgroundInfo/WBWCD-DroughtContingencyPlanReport-Final.pdf.

McGettigan, S., and Melchner, T. (2018). "Weber River RiverWare Model: A Brief Description of the Utah Division of Water Resources Weber River RiverWare Model." Weber Basin Water Conservancy District Drought Contingency Plan, Appendix II-B. https://github.com/jacobeveritt/WeberBasinVulnerability/blob/master/5%20-%20BackgroundInfo/WBWCD-DroughtContingencyPlanReport-Final.pdf.

8. REFERENCES

Abatzoglou, J.T., and T.J. Brown, 2012. "A Comparison of Statistical Downscaling Methods Suited for Wildfire Applications." *International Journal of Climatology* 32 (5): 772–80. https://doi.org/10.1002/joc.2312.

Ajami, H., P.A. Troch, T. Maddock, T. Meixner, and C. Eastoe, 2011. "Quantifying Mountain Block Recharge by Means of Catchment-Scale Storage-Discharge Relationships." *Water Resources Research*. https://doi.org/10.1029/2010WR009598.

Alexander, E., 2018. "Searching for a Robust Operation of Lake Mead," University of Colorado, Boulder, Department of Civil, Environmental, and Architectural Engineering. https://www.colorado.edu/cadswes/sites/default/files/attached-files/searching_for_a_robust_operation_of_lake_mead_2018.pdf.

Ault, T.R., J.E. Cole, J.T. Overpeck, G.T. Pederson, and D.M. Meko, 2014. "Assessing the Risk of Persistent Drought Using Climate Model Simulations and Paleoclimate Data." *Journal of Climate*, no. Preview article: 140122102410007. https://doi.org/10.1175/JCLI-D-12-00282.1.

Ault, T.R., M.D. Schwartz, R. Zurita-Milla, J.F. Weltzin, and J.L. Betancourt, 2015. "Trends and Natural Variability of Spring Onset in the Coterminous United States as Evaluated by a New Gridded Dataset of Spring Indices." *Journal of Climate* 28 (21): 8363–78. https://doi.org/10.1175/JCLI-D-14-00736.1.

Bales, R.C, N.P Molotch, T.H Painter, M.D Dettinger, R.Rice, and J. Dozier, 2006. "Mountain Hydrology of the Western United States." *Water Resources Research* 42 (8): 1–13. https://doi.org/10.1029/2005WR004387.

Bardsley, T., A. Wood, M. Hobbins, T. Kirkham, L. Briefer, J. Niermeyer, and S. Burian, 2013. "Planning for an Uncertain Future: Climate Change Sensitivity Assessment toward Adaptation Planning for Public Water Supply." *Earth Interactions* 17 (23): 1–26. https://doi.org/10.1175/2012EI000501.1.

Barnhart, T.B, N.P Molotch, B. Livneh, A.A. Harpold, J.F. Knowles, and D. Schneider, 2016. "Snowmelt Rate Dictates Streamflow." *Geophysical Research Letters* 43 (15): 8006–16. https://doi.org/10.1002/2016GL069690.

Bekker, M.F., R.J. DeRose, B.M. Buckley, R.K. Kjelgren, and N.S. Gill, 2014. "A 576-Year Weber River Streamflow Reconstruction from Tree Rings for Water Resource Risk Assessment in the Wasatch Front, Utah." *JAWRA Journal of the American Water Resources Association*, 50(5), 1338-1348. http://dx.doi.org/10.1111/jawr.12191.

Bekker, M.F., R.J. DeRose, B.M. Buckley, R.K. Kjelgren, N.S. Gill, S.Y. Wang, et al., 2014. "Added Value from 576 Years of Tree-Ring Records in the Prediction of the Great Salt Lake Level." *The Holocene Advance* (AUGUST): 0959683614530441–0959683614530441. https://doi.org/10.1016/j.jhydrol.2015.08.058.

Belmont, P. and B. Murphy. (2019). "Assessing Vulnerability of Reservoirs to Post Wildfire Sedimentation in the Wasatch Front."

Ben-Haim, Y. (2019). "Info-Gap Decision Theory (IG)." Decision Making under Deep Uncertainty: From Theory to Practice, V. A. W. J. Marchau, W. E. Walker, P. J. T. M. Bloemen, and S. W. Popper, eds., *Springer International Publishing, Cham*, 93-115. https://doi.org/10.1007/978-3-030-05252-2_5.

Birkel, C., C. Soulsby, and D. Tetzlaff, 2011. "Modelling Catchment-Scale Water Storage Dynamics: Reconciling Dynamic Storage with Tracer-Inferred Passive Storage." *Hydrological Processes* 25 (25): 3924–36. https://doi.org/10.1002/hyp.8201. http://dx.doi.org/10.1029/2012EO410001.

Brooks, P.D, J. Chorover, Y. Fan, S.E. Godsey, R.M. Maxwell, J.P. McNamara, and C. Tague, 2015. "Hydrological Partitioning in the Critical Zone: Recent Advances and Opportunities for Developing Transferable Understanding of Water Cycle Dynamics." *Water Resources Research*. Blackwell Publishing Ltd. https://doi.org/10.1002/2015WR017039.

Brooks, P., M. Litvak, A. Harpold, N. Molotch, J. Mcintosh, P. Troch, and X Zapata, 2011. "Non-Linear Feedbacks between Climate Change, Hydrologic Partitioning, Plant Available Water, and Carbon Cycling in Montane Forests." AGU Fall Meeting Abstracts, 8.

Brown, C., Y. Ghile, M. Laverty, and K. Li, 2012. "Decision scaling: Linking bottom-up vulnerability analysis with climate projections in the water sector." *Water Resources Research*, 48(9), n/a-n/a. http://dx.doi.org/10.1029/2011WR011212.

Brown, C., S. Steinschneider, P. Ray, S. Wi, L. Basdekas, D. and Yates, 2019. "Decision Scaling (DS): Decision Support for Climate Change." Decision Making under Deep Uncertainty: From Theory to Practice, V. A. W. J. Marchau, W. E. Walker, P. J. T. M. Bloemen, and S. W. Popper, eds., *Springer International Publishing*, Cham, 255-287. https://doi.org/10.1007/978-3-030-05252-2_12.

Brown, C. and R.L. Wilby, 2012. "An alternate approach to assessing climate risks." Eos, *Transactions American Geophysical Union*, 93(41), 401-402.

CADSWES, 2020. "RiverWare Version Documentation 8.0." Center for Advanced Decision Support for Water and Environmental Systems. https://riverware.org/HelpSystem/index.html. [Accessed on: June 15, 2020].

Clow, D.W., 2010. "Changes in the Timing of Snowmelt and Streamflow in Colorado: A Response to Recent Warming." *Journal of Climate* 23 (9): 2293–2306. https://doi.org/10.1175/2009JCLI2951.1.

Daly, C., M. Halbleib, J.I. Smith, W.P. Gibson, M.K. Doggett, G.H. Taylor, J. Curtis, and P.P. Pasteris, 2008. "Physiographically Sensitive Mapping of Climatological Temperature and Precipitation across the Conterminous United States." *International Journal of Climatology* 28 (15): 2031–64. https://doi.org/10.1002/joc.1688.

DeWalle, D.R. and A. Rango, 2008. *Principles of Snow Hydrology*. Cambridge University Press.

Everitt, J. (2020). "Weber Basin Vulnerability." https://github.com/jacobeveritt/WeberBasinVulnerability.

Fan, Y., M. Clark, D.M. Lawrence, S. Swenson, L.E. Band, S.L. Brantley, P.D. Brooks, et al., 2019. "Hillslope Hydrology in Global Change Research and Earth System Modeling." *Water Resources Research* 55. https://doi.org/10.1029/2018WR023903.

Gelderloos, A., 2018. "Quantifying the Interaction between Climate and Landscape on Water Resources." University of Utah.

Gnann, S.J., R.A. Woods, and N.J.K. Howden, 2019. "Is There a Baseflow Budyko Curve?" *Water Resources Research* 55 (4): 2838–55. https://doi.org/10.1029/2018WR024464.

Godsey, S.E., J.W. Kirchner, and D.W. Clow, 2009. "Concentration-Discharge Relationships Reflect Chemostatic Characteristics of US Catchments." *Hydrological Processes* 23 (13): 1844–64. https://doi.org/10.1002/hyp.7315.

Gutmann, E.D., R.M. Rasmussen, C. Liu, K. Ikeda, D.J. Gochis, M.P. Clark, J. Dudhia, and G. Thompson, 2012. "A Comparison of Statistical and Dynamical Downscaling of Winter Precipitation over Complex Terrain." *Journal of Climate* 25 (1): 262–81. https://doi.org/10.1175/2011jcli4109.1.

Haasnoot, M., A. Warren, and J.H. Kwakkel, 2019. "Dynamic Adaptive Policy Pathways (DAPP)." Decision Making under Deep Uncertainty: From Theory to Practice, V. A. W. J. Marchau, W. E. Walker, P. J. T. M. Bloemen, and S. W. Popper, eds., *Springer International Publishing*, Cham, 71-92. https://doi.org/10.1007/978-3-030-05252-2_4.

Hansen Allen & Luce, and Bowen Collins & Associates, 2019. "Utah's Regional M&I Water Conservation Goals." *Utah Division of Water Resources*. https://water.utah.gov/wp-content/uploads/2019/11/Regional-Water-Conservation-Goals-Report-Final.pdf.

Hornberger, G.M., P.L. Wiberg, J.P. Raffensperger, and P. D'Odorico, 2014. *Elements of Physical Hydrology*. 2nd ed. Johns Hopkins University Press.

Huntington, J.L and R.G. Niswonger, 2012. "Role of Surface-Water and Groundwater Interactions on Projected Summertime Streamflow in Snow Dominated Regions: An Integrated Modeling Approach." *Water Resources Research* 48 (11): 1–20. https://doi.org/10.1029/2012WR012319.

Information, NOAA National Centers for Environmental. 2019. "Glacial-Interglacial Cycles." 2019. https://www.ncdc.noaa.gov/abrupt-climate-change/Glacial-Interglacial Cycles.

IPCC, 2018. Global Warming of 1.5C. *An IPCC Special Report on the Impacts of Global Warming of 1.5C above Pre-Industrial Levels and Related Global Greenhouse Gas Emission Pathways in the Context of Strengthening Global Response to the Threat of Climate Change, Sustai*. Edited by V. Masson-Delmott, P. Zhai, H.O. Portner, D. Roberts, J. Skea, P.R. Shukla, A. Pirani, et al.

JUB Engineers. (2018). "Drought Contingency Plan." Weber Basin Water Conservancy District, Layton, UT.

Kirchner, J.W., 2006. "Getting the Right Answers for the Right Reasons: Linking Measurements, Analyses, and Models to Advance the Science of Hydrology." *Water Resources Research* 42 (W03S04). https://doi.org/doi:10.1029/2005WR004362.

Kirchner, J.W., 2003. "A Double Paradox in Catchment Hydrology and Geochemistry." *Hydrological Processes* 17 (4): 871–74. https://doi.org/10.1002/hyp.5108.

Knowles, N., M.D. Dettinger, and D. Cayan, 2006. "Trends in Snowfall Versus Rainfall for the Western United States, 1949-2001." *Journal of Climate* 19 (April 2007): 4545–59.

Kulkarni, S. and H. Huang, 2014. "Changes in Surface Wind Speed over North America from CMIP5 Model Projections and Implications for Wind Energy." *Advances in Meteorology* 2014. https://doi.org/http://dx.doi.org/10.1155/2014/292768.

Li, E., J. Endter-Wada, and S. Li, 2019. "Dynamics of Utah's agricultural landscapes in response to urbanization: A comparison between irrigated and non-irrigated agricultural lands." *Applied Geography*, 105, 58-72. http://www.sciencedirect.com/science/article/pii/S0143622818304211.

Lukas, J., J. Barsugli, N. Doeksen, I. Rangwala, and K. Wolter, 2014. "Climate Change in Colorado." University of Colorado Boulder.

Luthi, D., M. Le Floch, B. Bereiter, T. Blunier, J. Barnola, U. Siegenthaler, D. Raynaud, et al., 2008. "High-Resolution Carbon Dioxide Concentration Record 650,000 - 800,000 Years before Present." *Nature* 453: 379–82. https://doi.org/10.1038/nature06949.

Mann, C.C., 2006. 1491: *New Revealtions of the Americas before Columbus*. NewYork: Vintage Books.

Masson-Delmotte, V., P. Zhai, H-O. Pörtner, D. Roberts, J. Skea, P.R. Shukla, A. Pirani, et al., 2018. "Global Warming of 1.5°C An IPCC Special Report: Summary for Policymakers." https://doi.org/10.1017/CBO9781107415324.

Maxwell, J.D., A. Call, and S.B. St. Clair, 2019. "Wildfire and Topography Impacts on Snow Accumulation and Retention in Montane Forests." *Forest Ecology and Management* 432 (May 2018): 256–63. https://doi.org/10.1016/j.foreco.2018.09.021.

McCabe, G.J. and D.M. Wolock, 2002. "Trends and Temperature Sensitivity of Moisture Conditions in the Conterminous United States." *Clim. Res.* 20 (1): 19–29.

McCabe, G.J. and M.D. Dettinger, 1999. "Decadal Variations in the Strength of ENSO Teleconnections with Precipitation in the Western United States." *International Journal of Climatology* 19 (13): 1399–1410.

Milly, P.C.D., J. Betancourt, M. Falkenmark, R.M. Hirsch, Z.W. Kundzewicz, D.P. Lettenmaier, and R.J. Stouffer, 2008. "Climate Change: Stationarity Is Dead: Whither Water Management?" *Science* 319 (5863): 573–74. https://doi.org/10.1126/science.1151915.

NOAA Earth Systems Research Lab, 2019. "Trends in Atmospheric Carbon Dioxide." 2019. http://www.esrl.noaa.gov/cmd/ccgg/trends/.

NRCS National Water and Climate Center, 2019a. "Reservoir Storage Summary for the End of September 2019." 2019. https://www.wcc.nrcs.usda.gov/ftpref/support/water/westwide/reservoir/resv_data_current.pdf.

NRCS National Water and Climate Center, 2019b. "Utah Snotel Data." 2019. https://www.nrcs.usda.gov/wps/portal/wcc/.

Pierce, D., 2014. "LOCA Statistical Downscaling." 2014. http://loca.ucsd.edu.

Pierce, D.W., D.R. Cayan, and B.L. Thrasher, 2014. "Statistical Downscaling Using Localized Constructed Analogs (LOCA)." *Journal of Hydrometeorology* 15 (6): 2558–85. https://doi.org/10.1175/jhm-d-14-0082.1.

Prein, A.F., R.M. Rasmussen, K. Ikeda, C. Liu, M.P. Clark, and G.J. Holland, 2016. "The Future Intensification of Hourly Precipitation Extremes." *Nature Climate Change* 1 (December): 1–6. https://doi.org/10.1038/nclimate3168.

Reneau, S.L., D. Katzman, G.A. Kuyumjian, A. Lavine, and D.V. Malmon, 2007. "Sediment Delivery after a Wildfire." *Geology* 35 (2): 151–54. https://doi.org/10.1130/G23288A.1.

Resources, Utah Division of Water. 2009. "Weber River Basin," 90.

Rhoades, A.M., P.A. Ullrich, and C.M. Zarzycki, 2018. "Projecting 21st Century Snowpack Trends in Western USA Mountains Using Variable-Resolution CESM." *Climate Dynamics* 50 (1–2): 261–88. https://doi.org/10.1007/s00382-017-3606-0.

Rupp, D.E., J.T. Abatzoglou, K.C. Hegewisch, and P.W. Mote, 2013. "Evaluation of CMIP5 20th Century Climate Simulations for the Pacific Northwest USA." *Journal of Geophysical Research* 118 (April 2013): 1–23. https://doi.org/10.1002/jgrd.50843.

Scalzitti, J., C. Strong, and A. Kochanski, 2016a. "Climate Change Impact on the Roles of Temperature and Precipitation in Western U.S. Snowpack Variability." *Geophysical Research Letters* 43 (10): 5361–69. https://doi.org/10.1002/2016GL068798.

Scalzitti, J., C. Strong, and A.K. Kochanski, 2016b. "A 26 Year High-Resolution Dynamical Downscaling over the Wasatch Mountains: Synoptic Effects on Winter Precipitation Performance." *Journal of Geophysical Research: Atmospheres* 121 (7): 3224–40. https://doi.org/10.1002/2015JD024497.

Skamarock, W.C, J.B. Klemp, J. Dudhia, D.O. Gill, D.M. Barker, W. Wang, and J.G. Powers, 2005. "A Description of the Advanced Research WRF Version 2. NCAR Tech. Note TN-468 STR, 88pp." Available from NCAR; P.O. BOX 3000; BOULDER, CO, 7–25.

Smith, H.G., G.J. Sheridan, P.N.J. Lane, P. Nyman, and S. Haydon, 2011. "Wildfire Effects on Water Quality in Forest Catchments: A Review with Implications for Water Supply." *Journal of Hydrology* 396 (1–2): 170–92. https://doi.org/10.1016/j.jhydrol.2010.10.043.

Smith, K., C. Strong, and S. Wang, 2015. "Connectivity between Historical Great Basin Precipitation and Pacific Ocean Variability: A CMIP5 Model Evaluation." *Journal of Climate* 28 (15): 6096–6112. https://doi.org/10.1175/JCLI-D-14-00488.1.

Stagge, J.H., D.E. Rosenberg, R.J. DeRose, and T.M. Rittenour, 2018. "Monthly paleostreamflow reconstruction from annual tree-ring chronologies." *Journal of Hydrology*, 557, 791-804. https://www.sciencedirect.com/science/article/pii/S0022169417308855.

Stoelzle, M., K. Stahl, and M. Weiler, 2013. "Are Streamflow Recession Characteristics Really Characteristic?" *Hydrology and Earth System Sciences* 17.

Stonely, T., K. Short, M. Sufita, R. Barrus, B. King, and G. Smith, 2010. "Managing Sediment in Utah's Reservoirs." Utah Division of Water Resources, Salt Lake City, Utah. https://water.utah.gov/wp-content/uploads/2019/03/Managing-Sediment-In-Utahs-Reservoirs1.pdf.

Strong, C., A.K. Kochanski, and E.T. Crosman, 2014. "A Slab Model of the Great Salt Lake for Regional Climate Simulation." *Journal of Advances in Modeling Earth Systems* 6 (3): 602–15. https://doi.org/10.1002/2014MS000305.

Taylor, K.E., R.J. Stouffer, and G.A. Meehl, 2012. "An Overview of CMIP5 and the Experiment Design." *Bull. Amer. Meteor. Soc.* 93: 485–98.

Troch, P.A., G.F. Martinez, V.R.N. Pauwels, M. Durcik, M. Sivapalan, C. Harman, P.D. Brooks, H. Gupta, and T. Huxman, 2009. "Climate and Vegetation Water Use Efficiency at Catchment Scales." *Hydrological Processes*. https://doi.org/10.1002/hyp.7358.

Trujillo, E. and N.P. Molotch, 2014. "Snowpack Regimes of the Western United States." *Water Resources Research* 50 (7): 5611–23. https://doi.org/10.1002/2013WR014753.

University of Utah, 2019. "Utah Population Projections." Kem C. Gardner Policy Institute, University of Utah. https://gardner.utah.edu/demographics/population-projections/. [Accessed on: June 15, 2020].

US Bureau of Reclamation, 2013. "Downscaled CMIP3 and CMIP5 Climate and Hydrology Projections: Release of Downscaled CMIP5 Climate Projections, Comparison with Preceding Information, and Summary of User Needs."

US National Climate Assessment, 2014. *Climate Change Impacts in the United States Climate Change Impacts in the United States*. https://doi.org/10.7930/j0z31WJ2.

USGCRP, 2017. *Climate Science Special Report: Fourth National Climate Assessment, Volume I*. Edited by

D.J. Wuebbles, D.W. Fahey, K.A. Hibbard, D.J. Dokken, B.C. Stweart, and T.K. Maycock. Washington, DC. https://doi.org/10.7930/J0J964J6.

USGCRP, 2018. *Impacts, Risks and Adaptation in the United States: Fourth National Climate Assessment, Volume II*. Washington, DC. https://doi.org/10.7930/NCA4.2018.CH20.

Utah Division of Water Resources (UDWR), 2018. "2015 Municipal and Industrial Water Use Data." Utah Department of Natural Resources, Salt Lake City, UT. https://water.utah.gov/wp-content/uploads/2019/08/2015-MI-Data-2019-v2.pdf.

Voepel, H., B. Ruddell, R. Schumer, P. Troch, P. Brooks, A. Neal, M. Durcik, and M. Sivapalan, 2011. "Quantifying the Role of Climate and Landscape Characteristics on Hydrologic Partitioning and Vegetation Response." *Water Resources Research* 47. https://doi.org/10.1029/2010WR009944.

Vuuren, D.P. van, J. Edmonds, M. Kainuma, K. Riahi, A. Thomson, K. Hibbard, G.C. Hurtt, et al., 2011. "The Representative Concentration Pathways: An Overview." *Climatic Change* 109 (1): 5. https://doi.org/10.1007/s10584-011-0148-z.

Wang, J., D.E. Rosenberg, J.C. Schmidt, and K.G. Wheeler, 2020. "Managing the Colorado River for an Uncertain Future." Center for Colorado River Studies, Utah State University, Logan, Utah. http://qcnr.usu.edu/coloradoriver/files/CCRS_White_Paper_3.pdf.

Weber Basin Water Conservancy District (WBWCD), 2017. "WBWCD Supply and Demand Study."

Weber Basin Water Conservancy District (WBWCD), 2018a. "2018 Annual Summary."

Weber Basin Water Conservancy District (WBWCD), 2018b. "2018 Drought Contingency Plan."

Weber Basin Water Conservancy District (WBWCD), 2013. "Water Conservation Plan Update." Weber Basin Water Conservancy District, 52 pp. https://conservewater.utah.gov/pdf/SamplePlans/WBWCD2013.pdf.

Weber Basin Water Conservancy District (WBWCD), 2020. "District History." Weber Basin Water Conservancy District. https://weberbasin.com/AboutUs/DistrictHistory.

Westerling, A.L., 2016. "Increasing Western US Forest Wildfire Activity: Sensitivity to Changes in the Timing of Spring." Philos. Trans. Royal Soc. B 371: 2015078.

Wittenberg, H. and M. Sivapalan, 1999. "Watershed Groundwater Balance Estimation Using Streamflow Recession Analysis and Baseflow Separation." *Journal of Hydrology*. https://doi.org/10.1016/S0022-1694(99)00040-2.

Wood, A. and T. Bardsley, 2015. "Vic Model Calibration and Future Hydroclimate Analysis in Selected Utah Watersheds: Report to the Utah Division of Water Resources." Boulder, CO.

Zagona, E.A., T.J. Fulp, R. Shane, T. Magee, and H.M. Goranflo, 2001. "Riverware: A Generalized Tool for Complex Reservoir System Modeling." *JAWRA Journal of the American Water Resources Association*, 37(4), 913-929. https://onlinelibrary.wiley.com/doi/abs/10.1111/j.1752-1688.2001.tb05522.x.